p. 145

Material Property for Designing, Analyzing, and Fabricating Space Structures

FINAL REPORT

GRANTOR-NASA AMES RESEARCH CENTER

GRANTEE-CALIFORNIA POLYTECHNIC STATE UNIVERSITY

GRANT NUMBER NAG2-637

November 15, 1989 - December 31, 1991

Principal Investigator

Faysal A. Kolkailah, Ph.D., P.E.
Professor of Aeronautical Engineering

California Polytechnic State University
San Luis Obispo, CA 93407

ABSTRACT

Material Property for Designing, Analyzing, and Fabricating Space Structures

Faysal A. Kolkailah, Ph.D., P.E.

The objective of the first task of this study was to perform an analytical study of plasma assisted bullet projectile. The finite element analysis and the micro-macromechanic analysis was applied to an optimum design technique for the multilayered graphite/epoxy composite projectile that will achieve hypervelocity of 6-10 Km/s.

For the second task of this study, the objective was to determine the feasibility of dialectics to monitor cure of graphite/epoxies. Several panels were fabricated, cured, and tested at Cal Poly and the astronautics lab with encouraging results of monitoring the cure of graphite/epoxies.

As to the third task of this study, the objective was to determine the optimum cure process for large structures. Different orientation were used and three different curing cycles were employed. A uniaxial tensile test was performed on all specimens. The optimum orientation with the optimum cure cycle were concluded.

ACKNOWLEDGEMENTS

I would like to thank the Edwards Air Force Astronautic Laboratory for sponsorship of the research. Also, I wish to express my thanks to Ames Research Center for their directional and administrative help and support.

I would like to take this opportunity to express my deep gratitude to Mr. Gelhausen and both Mr. Jim Wanchek and Mr. Jim Koury for their technical support and help during the course of this research effort.

INTRODUCTION

Composites are the preferred materials for future high performance structures. While isotropic materials such as steel, aluminum, and titanium are useful for specific purposes, organic and metallic composites may be used for a wide range of applications. to achieve the higher performances of composites, several tedious mathematical calculations must be accomplished. Computers are ideally suited to perform these calculations.

However, the fact that engineers have little practical experience designing and building composite structures in a major concern. this problem arises from a lack of funds at universities for expansion of facilities to include composite laboratories in the curricula and an insufficient number of qualified instructors. If future engineers do not become familiar with composites in college than they will have little reason to use composites in future designs. In carrying out the tasks of this study, the participating students are given a unique opportunity for valuable hands-on experience.

OBJECTIVE

The objective of this project is to determine material properties for advanced materials applicable to space structures. The properties of these materials will be employed in designing, analyzing, and fabricating composite structures at the Astronautics Laboratory (AL) at Edwards Air Force Base.

TASK I

AN OPTIMUM DESIGN ANALYSIS OF COMPOSITE PROJECTILE

An Optimum Design of Composite Projectile

A Thesis
Presented to the Faculty of
California Polytechnic State University
San Luis Obispo

In Partial Fulfillment
of the Requirements for the Degree of
Master of Science in Aeronautical Engineering

by
Thomas D. Kim
October 1990

APPROVAL PAGE

TITLE : An Optimum Design of Composite Projectile

AUTHOR : Thomas Dong-Hyup Kim

DATE SUBMITTED : October 1990

Faysal A. Kolkailah
Thesis Advisor

Signature

Lawrence H. Nelson
Committee Member

Signature 10-24-90

James L. Koury
Committee Member

Signature

Doral R. Sandlin
Department Head

Signature

ABSTRACT

AN OPTIMUM DESIGN OF COMPOSITE PROJECTILE

Thomas Dong-Hyup Kim

October 1990

The subject of this study is to apply the finite element analysis and the micro-macromechanic analysis to an optimum design technique for the mutilayered graphite/epoxy composite projectile that will achieve hypervelocity of 6-10 km/s.

The optimum design technique used in this study depends on the internal pressure, external body force induced on the projectile, the angle of the lay ups, and the materials. These dependent relations are used to calculate the optimum radii, the required minimum thickness of the projectile, and the minimum number of lay ups.

The micro-macromechanic (Mic-Mac) analysis enables designer to calculate readily the stresses, strains, and displacements in each layers during the firing of the projectiles. In Mic-Mac analysis, laminated plate theory is used and the projectile is designed as a pressure vessel. The Mic-Mac analysis did not provide an accurate stress/strain values. However, this technique is useful in preliminary design process, since the analysis determines the approximated values.

The finite element analysis (FEA) code TEXGAP2D was employed for the analysis of two dimensional projectile model. The FEA code translated the loads, boundary conditions, and material specifications from the finite element pre- and post-processor code called the PATRAN. Combined use of PATRAN and TEXGAP2D obtained an accurate structural analysis of a projectile. Assumptions were made to simplify both the projectile model and the loads. Analysis of the type and degree of complexity described in this study is continued in the research community and no experimental data are present at this time. Results from an analyses are presented which illustrate the method.

ACKNOWLEDGEMENTS

This author sincerely thanks professor Faysal A. Kolkailah and Mr. James L. Koury for their assistance and guidance throughout the course of his undergraduate/graduate studies and through the completion of this thesis.

The author would like to acknowledge the efforts and appreciation of the staff of the Composite Materials Laboratory and the Design Evaluations Group at the Air Force Astronautics Laboratory for assisting the development of the projectiles.

The author would like to thank the Aeronautical Engineering Department at California Polytechnic State University, San Luis Obispo for the support and making him a better person. The author would like to thank anyone whom he didn't mentioned here.

This work is dedicated to my family and my girlfriend Tamlyn. Without their understanding and support this opportunity could never have occurred.

TABLE OF CONTENTS

TABLES

FIGURES

Figure		page

CHAPTER 1

INTRODUCTION

Background

The goal of a research on electromagnetic launchers (railgun) is to develop an electromagnetic means of accelerating substantial masses or perhaps tightly bound group of particles to the hypervelocity regime. The definition of hypervelocity is understood as a velocity substantially greater than that achievable with conventional propellants (> 2 km/s).

The principle of the railgun is shown in Figure-1.

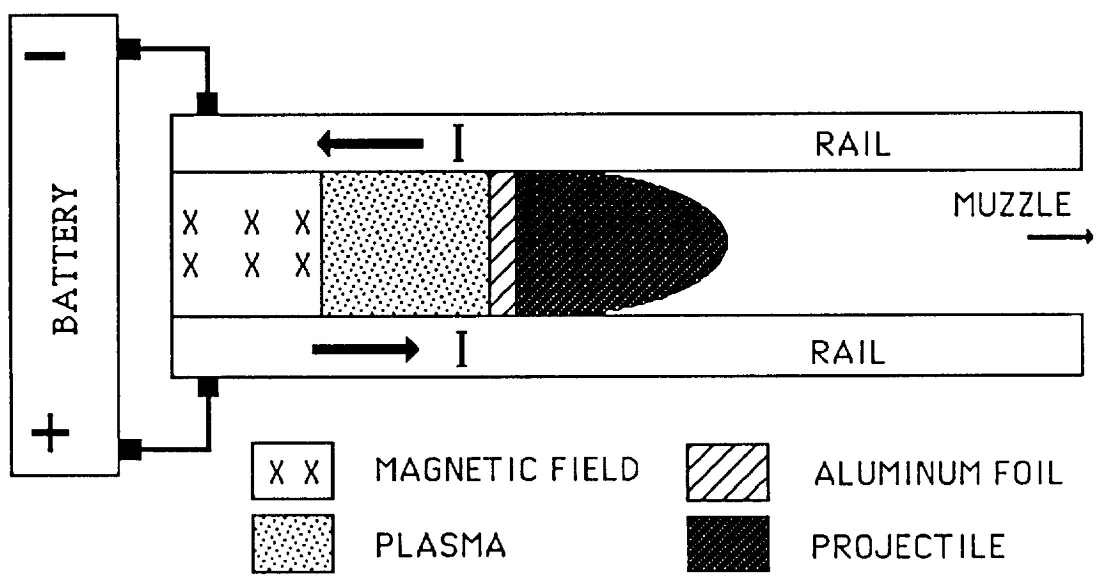

FIGURE 1 THE RAILGUN CONFIGURATION

The current flowing in the rails produce a magnetic flux density between the rails and this magnetic field interacts with the current flowing in the foil attached back of the projectile. Then high amount of current (0.5-2.0 mega-amps) causes a deflagration of an electrically heated aluminum foil which turns into plasma causing rapidly expanding hot gases giving initial driving force.

Rashleigh and Marshall's pioneering paper on the railgun in 1978 reported a velocity of 5.7 km/s for 2.5-g projectile. The reliable operation of a plasma-armature railgun today is limited to about 6.5 km/s. Two experiments have reported achieving 8 km/s with gram size projectile, but this performance is generally erratic for reasons which are not well understood. The projectile used in those experiments consist of polycarbonate (Lexan). The current record velocity for a railgun is about 10 km/s achieved in one test with an expendable launcher using a gram size particle.

The emerging high modulus, high strength composite materials are proposed by Air Force for the construction of projectile. It is known that the use of composite materials improves performance and offers a significant amount of material savings up to 25% over that of metal (isotropic) materials such as the aluminum. However, to take full advantage in the use of orthotropic properties of the composite materials, a reliable design method based on accurate stress analysis with the use of an appropriate failure criterion is required.

Current research being done at the Eglin Air Force Base, Florida and Sparta Inc. of San Diego, California emphasizes the need for the lightweight projectile that can withstand enormous loads and pressures. The understanding of the plasma conditions inside the barrel and the material characteristics are some of the critical area that needs to be better understood.

Objective

The objective of this study is to perform an optimum design analysis of a projectile that will survive the initial given pressures and loads. This design will assist in the construction of a composite projectile that will achieve hypervelocity of 6-10 km/s.

This is first time that composite material is considered for the use as a projectile. The design will be based on micro-macromechanic analysis, modeling and pre/post processing by PATRAN code, and the finite element analysis code of TEXGAP2D. The finite element method is a proven technique for using computers to predict a wide variety of structural behaviors.

The assumptions used for this analysis include the following:

- Uniform base pressure distribution
- Axisymmetric loading
- Perfectly constrained at rails during launch
- Friction effects neglected
- No tumbling after exit from barrel

The Problem

In 1989, a group of researchers at the Eglin Air Force Base, Florida and the Air Force Astronautics Laboratory, California designed and fabricated composite projectile that was experimented. The figure describing the projectile is shown below. The projectile was 130 mm long and had diameter of 82 mm. The material used was T300 Graphite/ Epoxy. The railgun used for this experiment had 5 meter long barrel with in bore diameter of 56 mm. The electrical current used for the firing of the projectile was 750,000-1.0 million amperes, creating the base pressure of 30-40 ksi and the external body force of 500,000 - 600,000 g's..

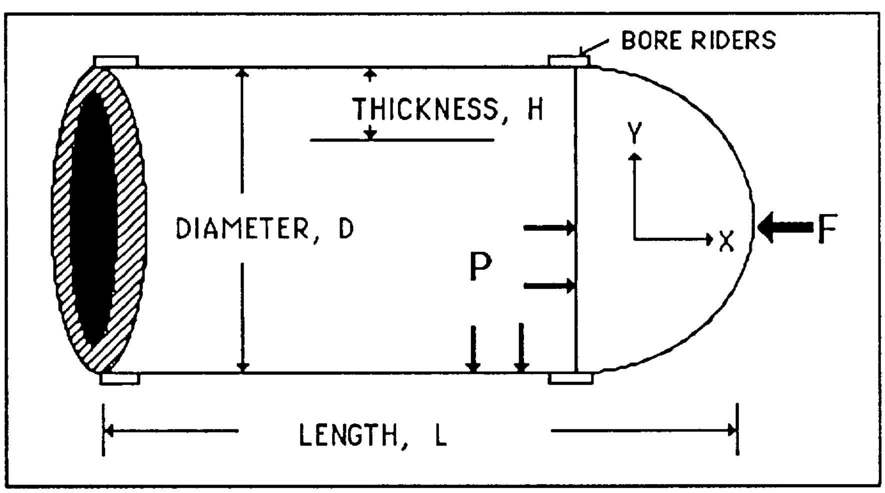

FIGURE 2 PROJECTILE CONFIGURATION

The projectile was preaccelerated with gaseous helium at velocity of 1.0 km/s before the current was switched on. At that instant time of the given current, the deflagration of the aluminum foil behind the projectile created a massive pressure which the dome section of the projectile was assumed to be blown off. Initially, the body section of the projectile reached velocity of approximately 4.7 km/s inside the railgun barrel. As the projectile reached the exit muzzle, the velocity declined to zero. Later it was concluded that the barrel and the projectile was fluctuating causing the velocity to decrease rapidly.

This study is to analyze the structure of the projectile that had the failure and proceed to design projectile that will survive the next firing coming up in 1991.

Finite Element Analysis

Modeling of the projectile was performed using PATRAN computer applications. A projectile model is generated using grids, lines, arcs, and patches. The type of element employed is a two dimensional quadrilateral elements. The finite element analysis parameters such as forces, loads, and boundary conditions are inserted at any stages of modelling process. Once the model has been completed, it is transferred to decoder module of any finite element analysis code such as TEXGAP, NASTRAN, ABAQUS,...etc. The decoder takes graphical information produced by PATRAN and creates the input neutral file that will be used by the analysis module. The geometry of the model is checked while enabling the user to define material and element properties associated with the projectile model.

After creating and decoding the neutral file by PATRAN, the model is ready to be processed by employing TEXGAP2D or any other finite element analysis processors. TEXGAP2D FEA processor calculates stresses and displacements of the loaded model. Completed error free analysis of the model is then translated back to PATRAN for the visualization. The effects of the stresses on a model can be displayed graphically using many different stress criteria and visual display options. More detailed description of PATRAN and TEXGAP codes are listed in Chapter 2.

CHAPTER 2

METHOD OF ANALYSIS

Introduction

Analysis performed in this study was first obtained by the laminated plate theory with the use of computer program called GENLAM and spreadsheet analysis of micro-macromechanics.

In order to determine the accurate stress concentration of the projectile structure and find the possible failure sites, the finite element code TEXGAP2D was used for the analysis. The mesh generation of finite element model was performed by the use of PATRAN modelling code. The finite element code CS/NASTRAN was initially used with only few successes due to the difficulty of interfacing and translating with PATRAN code. The details of the computer codes are described below.

GENLAM Program

The GENLAM computer program was developed by the Think Composites of Dayton, Ohio. In GENLAM, the coefficients in the governing differential equations are calculated using the laminated plate theory (LPT) listed in Appendix B. After the boundary value problem has been solved the LPT is used to calculate the strain and the stress state in the plate. However, in many instances the in-plane loads and the moments are known in statically determinant problems. The LPT can then be used directly to calculate the stress in the plate. Therefore, GENLAM calculates the stress values at the top and bottom of each ply.

Micro-Macromechanic Analysis (Mic-Mac)

The integrated micro-macromechanics analysis was performed using spreadsheet based on Microsoft Excel. This program was also developed by Think Composites of Dayton, Ohio. Input of the ply angle, thickness, pressure, axial force, and safety factor determines the stresses and strains. The analysis employed in this analysis does not consider buckling, or the interlaminar failures. The assumption such as uniform pressure distribution and drag is neglected in this analysis.

In this analysis, filament wound pressure vessel (projectile) is assumed to have adjacent (±ß) angle lay ups and that adjacent (±ß) lay ups act as an orthotropic unit. Projectile can be made up with several of such orthotropic units wound one over another as in Figure-3 below. It is assumed that the length (L) of the projectile is such that the longitudinal bending deformation due to the end closures of the vessel is limited to only small end portions of the projectile compared to the overall length. The projectile is subject to axisymmetric internal pressure and external body force.

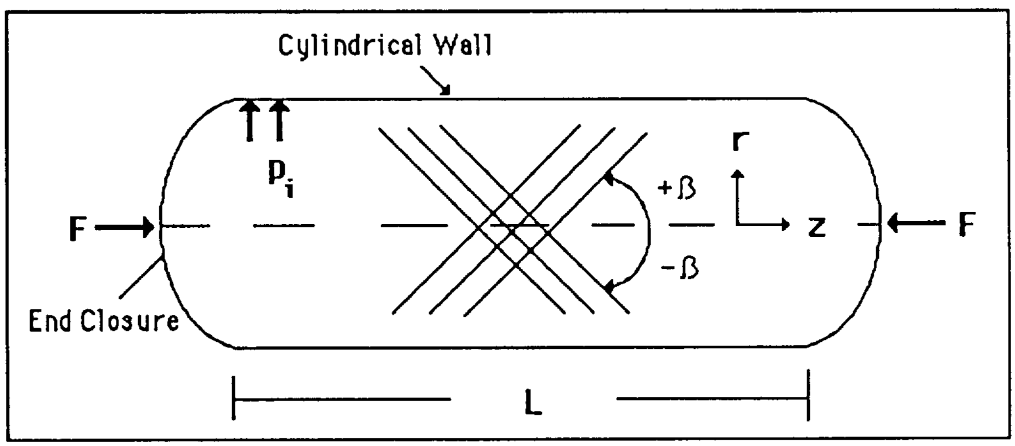

FIGURE 3 CONFIGURATION OF THE CLOSED END CYLINDER

The Mic-Mac program is then applied to the problem solving. The program is divided into four distinguishing parts.

- Lamination module
- Strength analysis module
- Stress analysis module
- Micromechanics module

In lamination module Table 1 next page, the ply material is identified and up to four ply angles of any value can be selected in any order.

TABLE 1 THE LAMINATION MODULE

A	B	C	D	E	F	G	H	I
READ ME	Theta 1	Theta 2	Theta 3	Theta 4				
[ply angle]	**0.0**	**90.0**	**54.5**	**-54.5**	[repeat]	h, #	h, E-3	[Rotate]
[ply#]	**0**	**0**	**1**	**1**	**67.0**	134.0	660.0	**0.00**

The number of plies in each ply group is arbitrary. Being limited to symmetric laminates, the total number of plies is twice the sum of the ply group. In choosing the ply angle for this analysis, trial and error was performed in order to find the desired ply angles.

The strength analysis module Table 2, computes both intact and degraded plies. This calculates the in-plane strength with and without considering residual stress resulting from the lamination of a multidirectional composite. Quadratic failure criterion is used.

TABLE 2 THE STRENGTH ANALYSIS MODULE

A	B	C	D	E	F	G	H	I
R/intact	#####	#####	0.99	0.99	R/FPF	0.99	safety	**1.50**
R/degraded	#####	#####	2.59	2.59	R/LPF	2.59	R/lim*	1.73
					R/ult	2.59	R/lim	0.99

The maximum laminate stress and strain at first-ply-failure (FPF) or last-ply-failure (LPF) is simply the resulting laminate stress or strain multiplied by the strength ratio. The lowest strength ratio determines the ply group that would fail first, which is the FPF of the laminate. The ultimate of the laminate is the higher of the FPF and LPF. This is valid if we limit loading to the monotonic, proportional type only; i.e., no unloading and reloading. Safety margin of 1.5 is used in the analysis.

A design limit is defined as the lower FPF and LPF divided by safety margin. With this definition, limit is always equal to or lower than FPF. Defining another limit called limit*, which equals ultimate divided by safety margin. At limit* matrix cracking is tolerated.

The stress analysis module of Table 3 on next page, the length and diameter of the cylinder is plotted. There are three possible loads: an axial force in tension or compression, internal or external pressure, and a torque applied along the cylinder axis. For this analysis, an axial force was assumed to be that of an impact force caused by the exploding foil behind the projectile.

TABLE 3 THE STRESS ANALYSIS MODULE

A	B	C	D	E	F	G	H	I
	size, m or in	∂L,∂D,E-3		<sg>	<sg>lim	<sg>lim*	<sg>ult	{E°}lim
[Length]	**5.00**	19.51	1	65.	65.	113.	169.	2.8
[Diameter]	**3.60**	25.79	2	128.	127.	221.	332.	7.5
Angle of twist,deg		0.00	6	0.	0.	0.	0.	6.9
	[Load]	[Load] lim		<ep>E-3	<ep>lim	<ep>lim*	<ep>ult	E^u/E^
Axial load F	**10.00**	9.94	1	3.90	3.88	6.73	10.10	0.33
Pressure P	**47.00**	46.71	2	7.16	7.12	12.36	18.54	0.41
Torque	**0.00**	0.00	6	0.00	0.00	0.00	0.00	0.98

This axial force is calculated from the Lorentz Force equation.

$$F = \frac{1}{2} L \times I^2 \qquad \text{--(1)}$$

where L is the inductance and the I is the current. All loads can be applied simultaneously.

The laminate stress induced from the combined loads can be calculated using the in-plane stress equations below.

$$\sigma_1^o = \frac{PD}{4h} + \frac{F}{\pi D h} \qquad \text{--(2)}$$

$$\sigma_2^o = \frac{PD}{2h} \qquad \text{--(3)}$$

where P is the pressure, D is the diameter of the cylinder, h is the thickness, and the F is the axial force.

The resulting strains are calculated from the in-plane stress-strain relation

$$\{\epsilon^o\} = [a^*]\{\sigma^o\} \qquad \text{--(4)}$$

where a* is the normalized compliance matrices and it is obtained as follows:

$$[A] = \int_{-\frac{h}{2}}^{\frac{h}{2}} [Q]\, dz \qquad \text{--(5)}$$

and

$$[A^*] = \frac{[A]}{h} \qquad \text{--(6)}$$

obtaining,

$$[a^*] = [A^*]^{-1} \qquad \text{---(7)}$$

where $[A]$ is the In-plane stiffness and A* is the normalized in-plane stiffness. $[Q]$ is the on-axis plane stress stiffness which can be computed from the engineering constants as follows:

$$[Q] = \begin{bmatrix} \frac{E_X}{1 - \gamma_X\gamma_Y} & \gamma_X Q_{YY} & 0 \\ \gamma_Y Q_{YY} & \frac{E_Y}{1 - \gamma_X\gamma_Y} & 0 \\ 0 & 0 & E_S \end{bmatrix} \qquad \text{--------------(8)}$$

where Q12 = Q21, Q16 = Q61 = 0, Q26 = Q62 = 0 and E is the Young's Modulus and γ is the Poission's ratio. The growths in length due to the applied loads can be found using the displacement equation below.

$$\partial L = L \in_1^o$$

where L is the length. Finally the stresses and strains at limit, limit* and ultimate are the resulting stress and strain multiplied by the corresponding strength ratios.

The micromechanics module Table 4 lists the principal laminate stiffness component and the loss of each component due to matrix degradation.

TABLE 4 THE MICROMECHANICS MODULE

A	B	C	D	E	F	G	H	I
	T opr	c,moist	vol/f	Em	Efx	Xm	Xfx	Em/Em°
Baseline	71.6	0.005	0.66	0.49	45	8.1	770	0.30
[Modified]	**71.6**	**0.005**	**0.66**	**0.49**	**45**	**8.1**	**770**	**0.30**
Mod/Base	1.000	1.000	1.000	1.000	1.000	1.000	1.000	1.000
Mod-Base	0.0	0.000	Hot/Wet	0.49	45	8.1	770	

If the degradation factor is lower than 0.3, the loss of laminate stiffness is expected to be lowered. Also listed are the thermal and moisture expansion coefficients of the laminate. This could be an important factor when the material is exposed to slowly changing environments for long period of time, or if it is subjected to suddenly changing environments for short time period such as in plasma conditions.

PATRAN Analysis

Mesh generation of finite element analysis was performed by PATRAN code developed by the PDA Engineering of Costa Mesa, California. PATRAN function is the ability to construct, view, analyze, and understand the nature and behavior of an object. The result is to optimize the design. PATRAN is split into four major areas or phases of concern:

- Geometric Modeling
- Analysis Modeling
- Analysis
- Postprocessing

In Geometric Modeling involves creation of an accurate solid or generation of a continuous geometry surface model of a structure. This is the development of a set of mathematically defined regions which closely approximate the physical object. Grids, lines, and patches are used to create the model.

The Analysis Modeling is the creation of finite elements and their loading environments based upon this geometric model. This is where the model can be subdivided into any required density for finite element model generation. This phase is analysis dependent and there may be several finite element models generated from one geometry model. The loads and material properties are assigned in this phase. Boundary conditions are inserted in this phase as well. Model is constrained in radial direction and the external body force (acceleration of gravity) is simply obtained from the equation below.

$$\text{Gee} = \frac{\text{Total applied force}}{\text{Mass of projectile}} = \frac{P\,A}{M_P}$$

For isotropic material properties the PATRAN command is as follows:

PMAT, mat, ISO, ym, , n, r, a

where "mat" is the material identification, "ym" is the Young's modulus, "n" is the Poisson's ratio, "r" is the mass density, and "a" is the coefficient of thermal expansion. The shear modulus field and all additional fields are ignored by the translator.

The PATRAN command for generating nodes is as follows:

GFEG, id-LPH, Gtype, mesh,,,,spc-list

where "id-LPH" is the identification number of nodes, "Gtype" is defined as structural node, "spc-list" is the single point constraint number.

The PATRAN command for generating elements is as follows:

CFEG, id-LPH, QUAD/8/7,,prop-id

where"QUAD/8/7" element type produces an axisymmetrical 8-node quadratic element, and "prop-id" is the property identification.

The PATRAN command to set boundary condition is as follows:

DFEG, id-LPH, option,load, set-id

where "option" is the either Pressure, Force, or Displacement, "load" is the amount of load applied on the model.

An analysis of its behaviors can be performed, once a completely described finite element model has been developed in conjunction with its properties and loads. PATRAN reads finite element analysis code performed by the TEXGAP2D and converts analysis results output from analysis program into files which can be read and translated by PATRAN.

In Postprocessing phase, the graphics oriented interpretation of the analysis results are displayed. The stress concentration, displacements, and the deformed geometry is colored and displayed visually. Many plot options are listed in this phase such as contour , fringe , and deformed or undeformed model is plotted. Figure 4 is the representation of the finite element generated by the PATRAN.

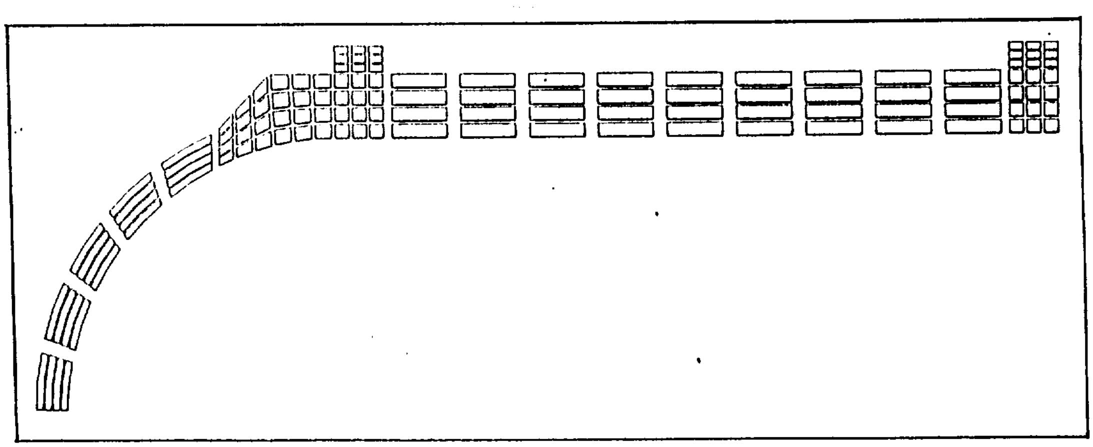

FIGURE 4 FINITE ELEMENT MODEL

TEXGAP2D Finite Element Analysis

The finite element analysis code TEXGAP2D developed by ANATECH International Corporation was used to analyze the model. The Air Force Astronautics Laboratory, California has funded the development of the TEXGAP program over the last decade in order to provide for the accurate determination of stresses and deformation fields in various areas.

TEXGAP2D is a finite element program for the analysis of static, two-dimensional, linear elastic plane or axisymmetric bodies. The TEXGAP FEA was performed using the VAX/VMS on a Ethernet network system. Computer terminals Tektronix model 4109A and model 4207 was used to input and analyze the data..

TEXGAP2D contains the provision for calculating, along user prescribed sets of element boundaries, displacement and traction data files. These files can be used to calculate boundary data used in a subsequent solution of a portion of the original model. TEXGAP uses many built in subroutines. After displacements have been calculated in one of the routines, the strains and the stresses are calculated in routine called STRESS.

TEXGAP employ solution of simultaneous equations by elimination. A brief review of the basic technique used in programming equation solver is discussed below.

Let the simultaneous equations be represented as:

$$\sum_{j=1}^{n} a_{ij}x_j = b_i \quad \text{for } i = 1,2,\ldots n \qquad \text{----------------------------(9)}$$

where a_{ij} are the stiffness coefficients, b_i the nodal point forces and x_j the unknown, and n is the total number of degree of freedoms (DOF). The standard elimination procedure is to solve for x_1 in terms of x_2, x_3, ...x_n from the first equation. It is important to use the first equation to eliminate the first unknown because no re-ordering (pivoting) is necessary. Solving the first equation for x_1 gives

$$x_1 = \frac{1}{a_{11}} \left(b_1 - \sum_{j=2}^{n} a_{1j}\, x_j \right) \qquad \text{----------------------------------(10)}$$

This equation (10) is now substituted for j=2 through j=n

$$b_i = \frac{a_{i1}}{a_{11}} (b_1 - \sum_{j=2}^{n} a_{1j}\, x_j) + \sum_{j=2}^{n} a_{ij}\, x_j \qquad \text{-----------------------(11)}$$

and collecting

$$\sum_{j=2}^{n} (a_{ij} - \frac{a_{i1}a_{1j}}{a_{11}})\, x_j = b_i - \frac{a_{i1}}{a_{11}}\, b_1 \quad \text{for } i = 2, 3, \ldots n \qquad \text{-------(12)}$$

Thus, the order of the system of equations is reduced from size n to n-1. After n-1 such eliminations, the equations are reduced to an upper triangular from that permits solution for the unknowns by backsubstitution. This direct Gaussian elimination is straight forward code in Fortran language. The code does not take advantage of either the symmetry or the banded nature of the equilibrium equations generated by finite element methods.

The following is the TEXGAP2D input deck that is to calculate the stresses and strains.

```
$ PROJECTILE
AXISYMMETRIC
SETUP, 311, DEF, 20
*EXTERNAL
BODY, FORCE, 32000
SOLVE
STRESS, 2
TRANSLATE
STOP
```

As can be seen the input deck is quiet short, but this can be representative of a very complex problem. It is assumed that all the setup information is contained in the external file including the material properties.

CHAPTER 3

ANALYSIS RESULTS

Introduction

The four different axisymmetrical projectile models with various thicknesses were analyzed by PATRAN and TEXGAP2D. The first model investigated was made and fired in 1989 without much successful results. The next three models are proposed design concept that are analyzed and one of the model is to be constructed for the firing in 1991.

The material used for these investigations were an isotropic carbon fibers with the Young's Modulus of 25 x 10^6 psi, Possion's ratio of 0.3, and the density of 0.064 lb/in^3. The effects of stress concentration and failure analysis of the projectile is evaluated.

As mentioned earlier, Mic-Mac analysis was used to get approximated values. The material considered in this analysis was the IM6/Epoxy (Carbon fiber). This material has high axial ply stiffness and axial ply strength when compared with other composite materials as listed in Table 5 next page. With this material and the axial force, internal pressure, length, and diameter are inserted into Mic-Mac program to be analyzed. The program then calculates the stresses, strains, and the strength ratios at various thicknesses. Various Mic-Mac analysis are shown in Table 9 in Appendix C.

Mic-Mac Results

With a given data of outside diameter (≤ 3.66 inches) and pressure (47 ksi), Mic-Mac analysis demonstrated that the optimum design of a projectile is accomplished by choosing an optimum lay up angles of ±54.5 degrees and a thickness of 0.6600 inches. This resulted in highest ultimate stress (burst pressure) of 169 ksi and in-plane stress limit was 65 ksi. A comparison of the various lay up angles with the stress is shown in Figure 5 and Figure 6 in Page 15 thru 16.

TABLE 5 COMPARISON OF VARIOUS COMPOSITE MATERIALS

TYPE	CFRP	CFRP	KPRP	GFRP	CFRTP
FIBER	IM6	T300	KEV 49	E-GLASS	AS4
MATRIX	EPOXY	EPOXY	EPOXY	EPOXY	PEEK
ENGINEERING CONSTANTS, MSI OR DIMENSIONLESS					
Ex	29.46	26.27	11.03	5.6	19.45
Ey	1.626	1.49	0.08	1.2	1.27
Es	1.22	1.04	0.33	0.6	0.74
nu/x	0.32	0.28	0.34	0.26	0.28
V/f	0.66	0.7	0.6	0.45	0.66
rho	1.6	1.6	1.46	1.8	1.6
ho, E-6 in	4925	4925	4925	4925	4925
PLY STIFFNESS, KSI					
Qxx	29.63	26.39	11.12	5.68	19.55
Qyy	1.63	1.5	0.8	1.22	1.3
Qxy	0.52	0.42	0.27	0.32	0.36
Qss	1.22	1.04	0.33	0.6	0.74
PLY STRENGTH, KSI					
X	507.98	218	203	154	309
X'	223.51	218	34	89	160
Y	8.13	6	2	4	12
Y'	21.77	36	8	17	29
S	14.22	10	5	10	23

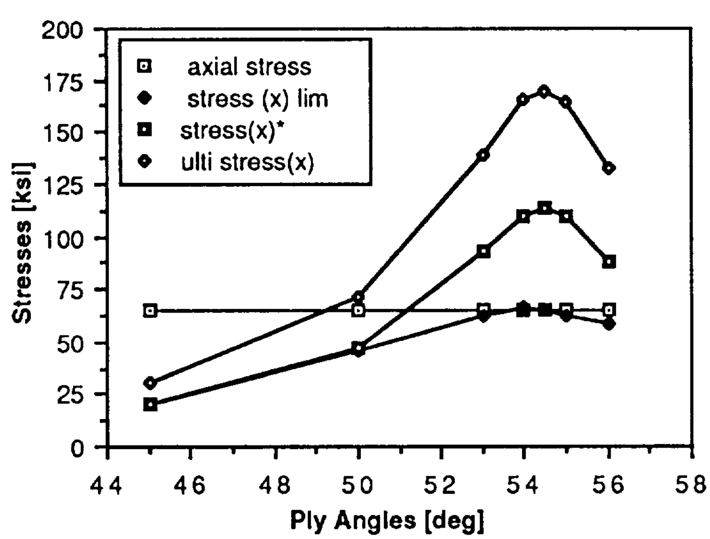

FIGURE 5 STRESS VS. PLY ANGLES

From the Figure 7 shows a minimum thickness of 0.6600 inches, the in-plane stress was 65 ksi which was equal to the in-plane stress limit. This resulted in strength/ stress ratio of R = 1.0. This ratio determines that possible failure will occur in the first ply. If R value falls below R ≤ 1.0, the applied stress has exceeded the strength. But, if R > 1.0, then applied stress can be increased. This figure is illustrated in page 17.

Figure 8 shown in page 17 is the Strength Ratio versus the Thickness. At thickness of 0.3448 inches, the strength/stress ratio (R) value was R/FPF = 0.52. This determines that the applied stress has exceeded the strength by a factor of 1.92 and the first-ply-failure (FPF) is most likely to occur.

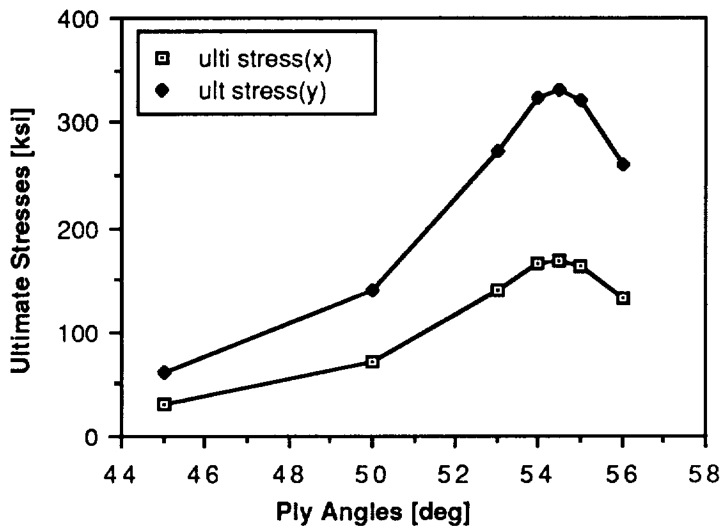

FIGURE 6 ULTIMATE STRESSES VS. PLY ANGLES

The last-ply-failure (LPF) is not likely even at this load due to the strength ratio for the last-ply-failure is R/LPF = 1.35. If the R/LPF = 1.0, the total destruction of the projectile is evident. At thickness of 0.7880 inches, the strength ratio was R/FPF = 1.19 and the applied stress can increase by a factor of 1.19 before the first ply-failure occurs. Analyzing the data and the figures, it was determined that at the thickness of 0.6600 inches, the in-plane longitudinal (axial) stress based on the strength of material was calculated to be 65 ksi which equals to the in-plane longitudinal stress at the design limit. At this stress limit of 65 ksi,

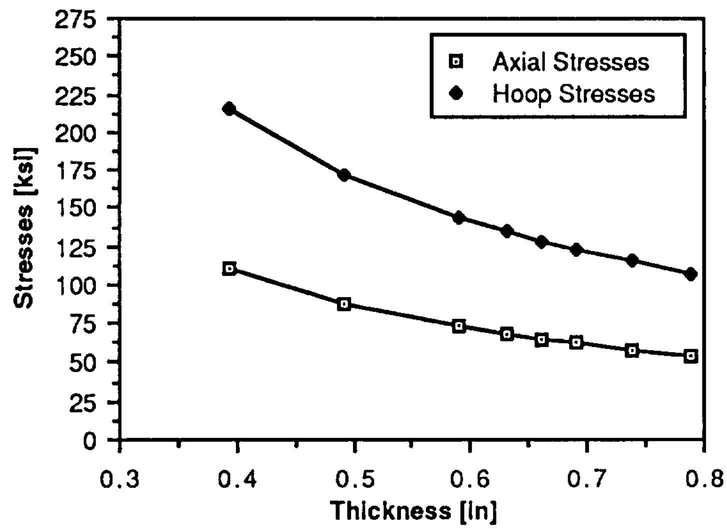

FIGURE 7 STRESS VS. THICKNESS AT PLY ANGLES OF ± 54.5 DEGREES

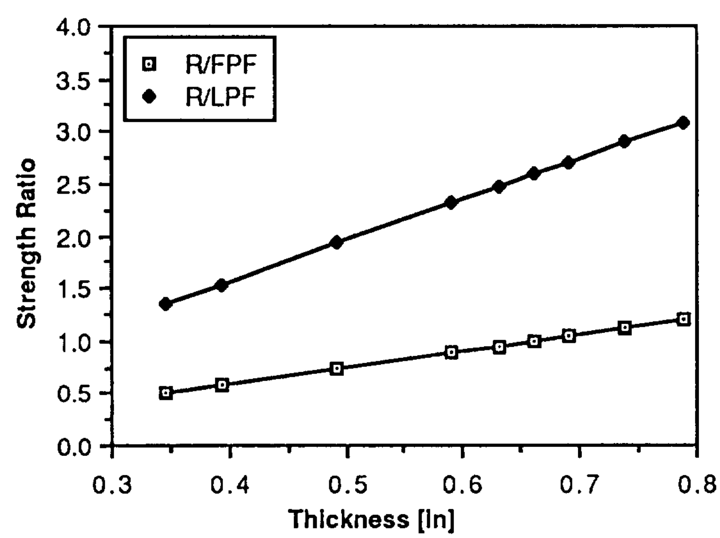

FIGURE 8 STRENGTH RATIO VS. THICKNESS AT ± 54.5 DEGREES

the strength ratio was R/LPF = 1.0. This is where the first-ply-failure is starting to occur. If this value becomes R < 1.0, the applied load should be decreased. The length value had no effective changes in either the stresses or the strains. This is due to the fact that the length effects only angle of twist under torque. Since no torque was applied to the vessel, all the values stayed constant. The stresses and strains discussed at limit, limit* and ultimate are the resulting stress and strain multiplied by the corresponding strength ratios. From this analysis, recommends that the thickness should not be less than 0.6600 inches which is considered an optimum thickness for the given conditions. However, the values obtained were averaged over the entire pressure vessel. These results should be used as an approximated values for the initial design process. In this analysis, the stress concentration and the exact failure regions were not available to be determined.

PATRAN and TEXGAP Results

All of the results of TEXGAP2D are given in Tables 6 thru 8 at the end of the Chapter 3 and and in Appendix E. Figure 9 shows the internal body force of 50 ksi and external body force (G loading) of 1 x10^6 gees and radially constrained projectile model generated by the PATRAN. Figures 10 thru 14 represent analyzed results of axisymmetrically loaded projectile performed by TEXGAP. The dimension of the projectile has 79 mm length, 2.6 mm dome thickness and 5 mm body thickness.

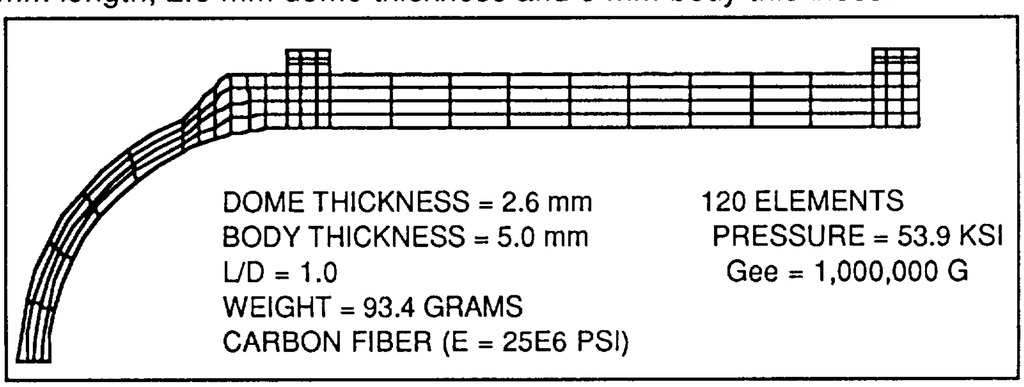

FIGURE 10 PROJECTILE WITH 2.6 mm DOME THICKNESS

Results shows the highest stress concentrations and bending moments at the regions of the dome section. The maximum stress of 2198 ksi was located at the middle section of the dome as indicated by the spectrum analyzer. The minimum stress (compressive) of -309 ksi did cause the buckling and bending of the projectiles body and the dome section. These stresses shown by the figure are results of the internal pressure loading and the external body force. Thus, as noted in the test firing in 1989, the dome section of the projectile is most likely to have failed causing the destruction of the dome.

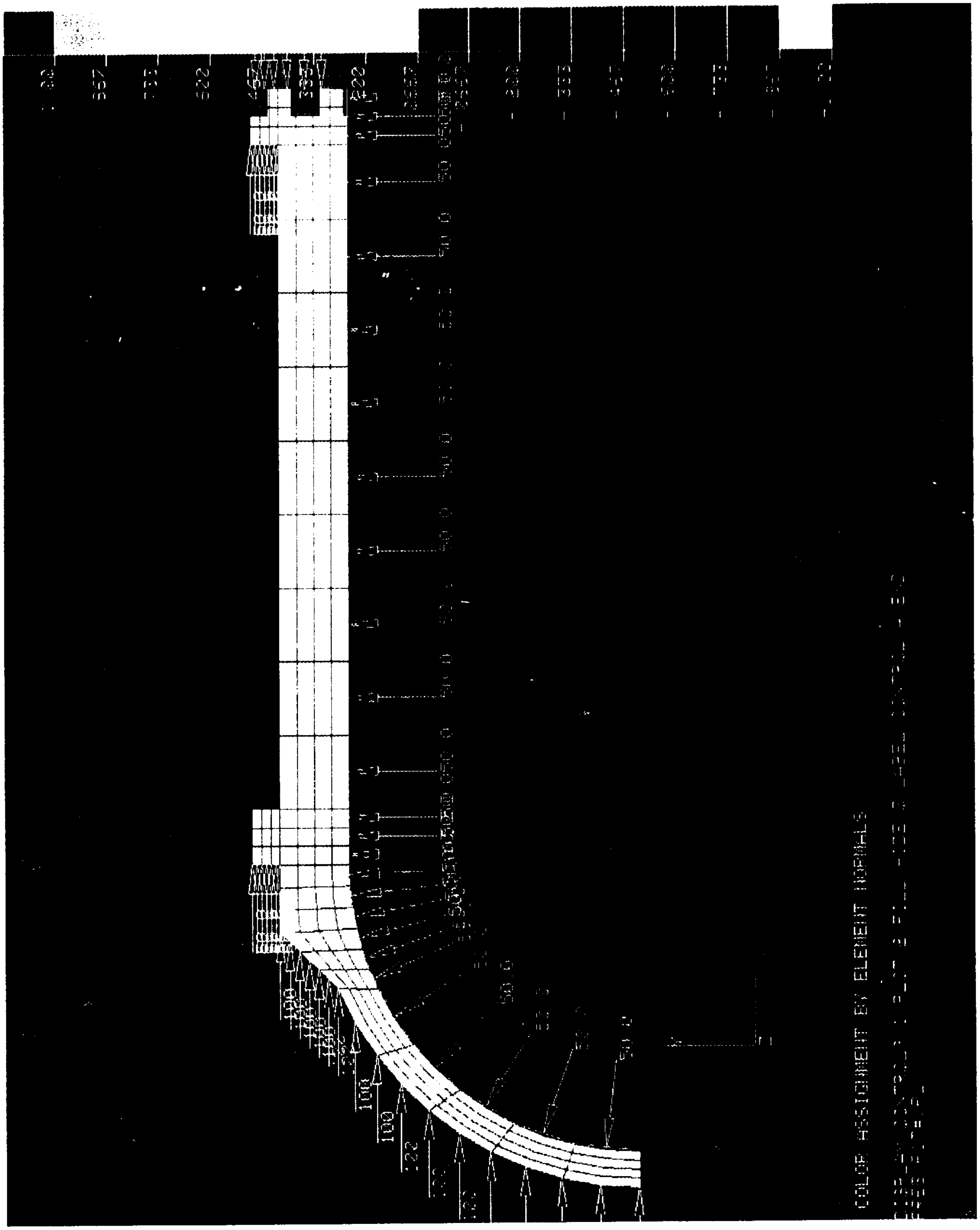

FIGURE 9 MODEL WITH BOUNDARY CONDITIONS

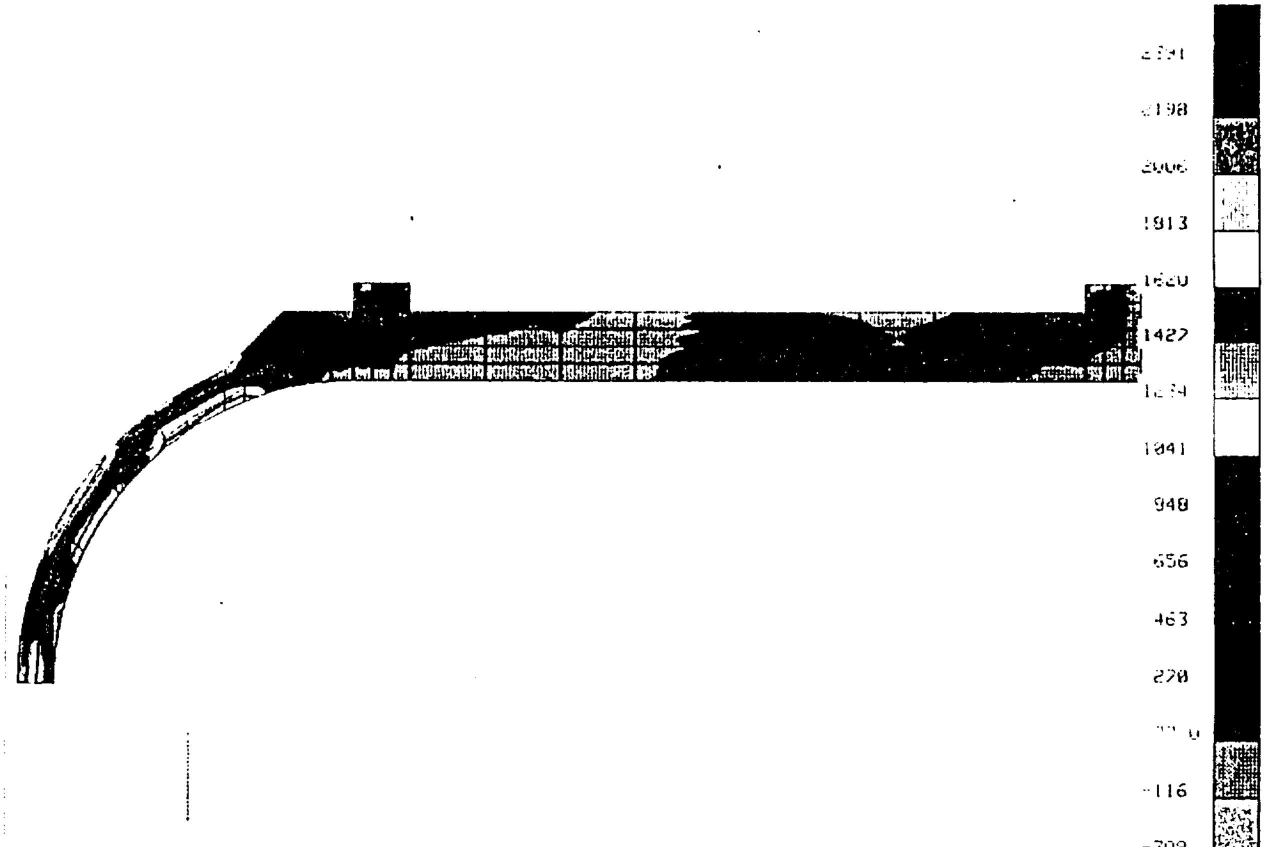

FIGURE 11 STRESS ANALYSIS OF 2.6 mm DOME PROJECTILE

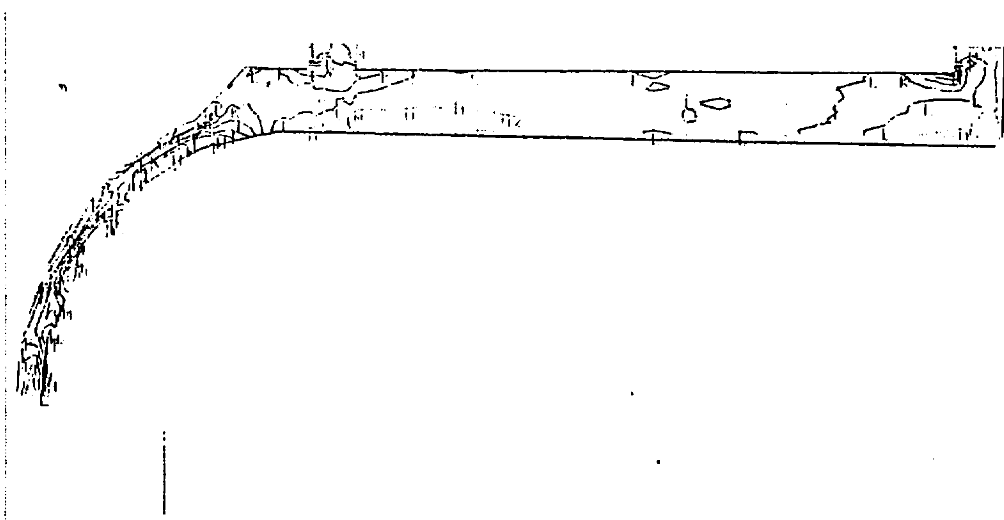

FIGURE 12 CONTOUR PLOT OF 2.6 mm DOME PROJECTILE

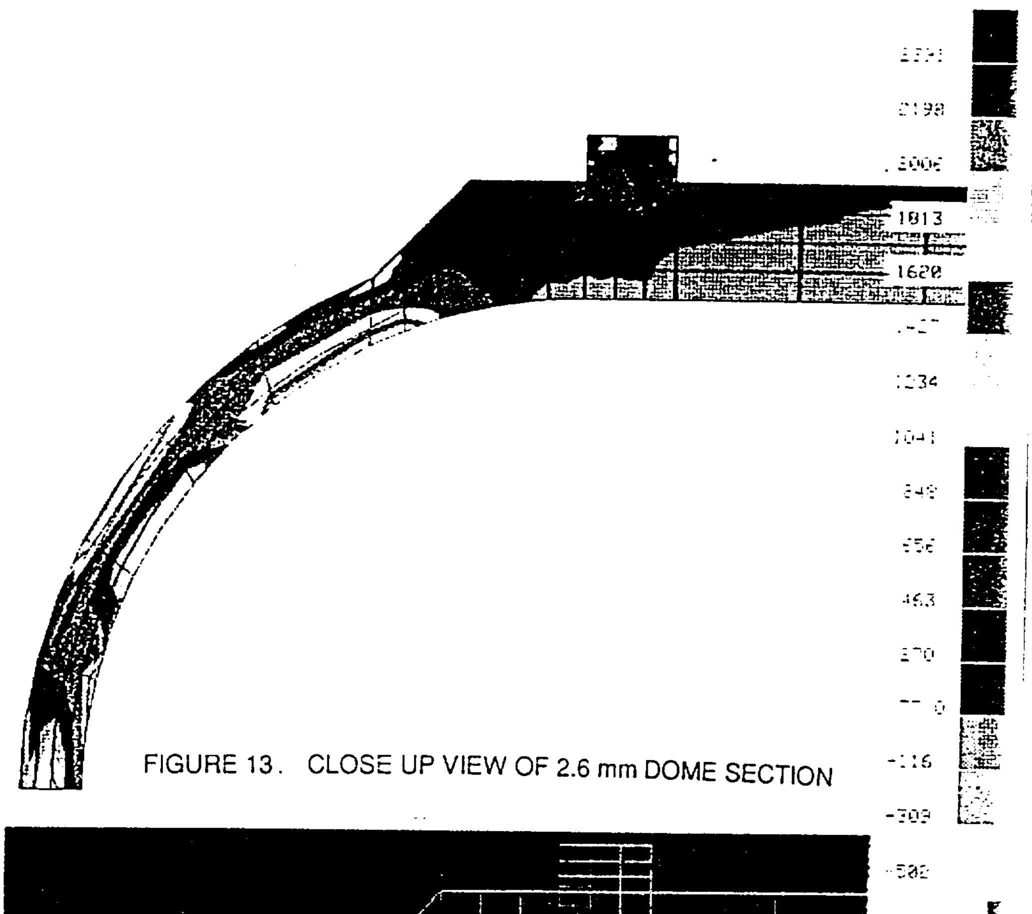

FIGURE 13. CLOSE UP VIEW OF 2.6 mm DOME SECTION

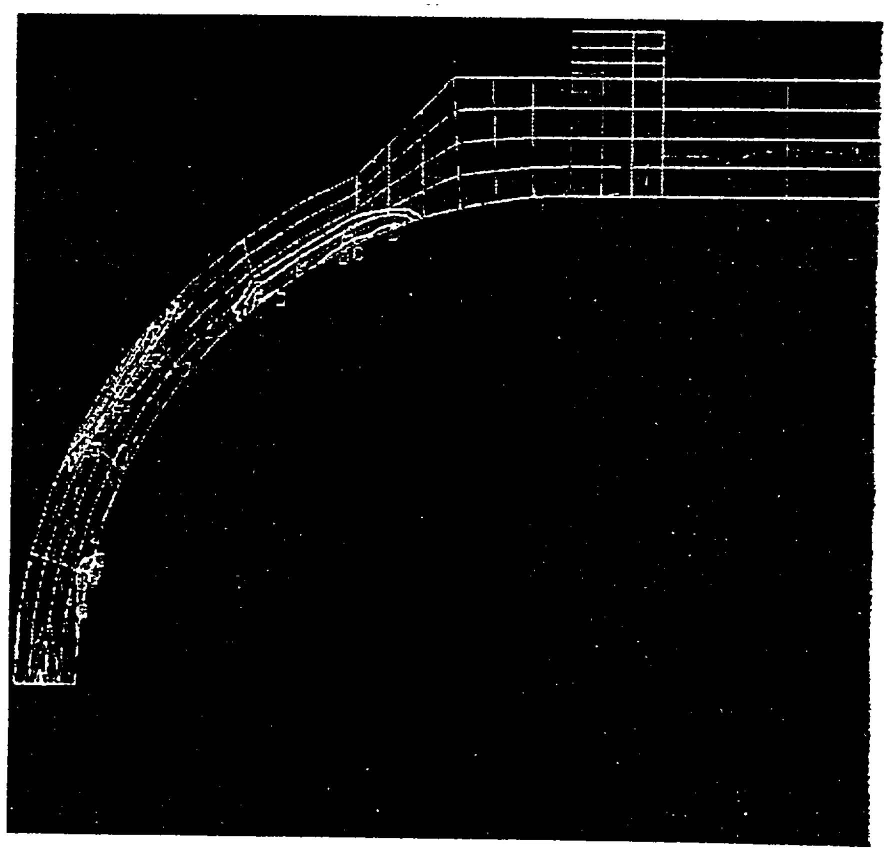

FIGURE 14 CLOSE UP VIEW OF THE CONTOUR PLOT AT THE DOME

ORIGINAL PAGE IS
OF POOR QUALITY

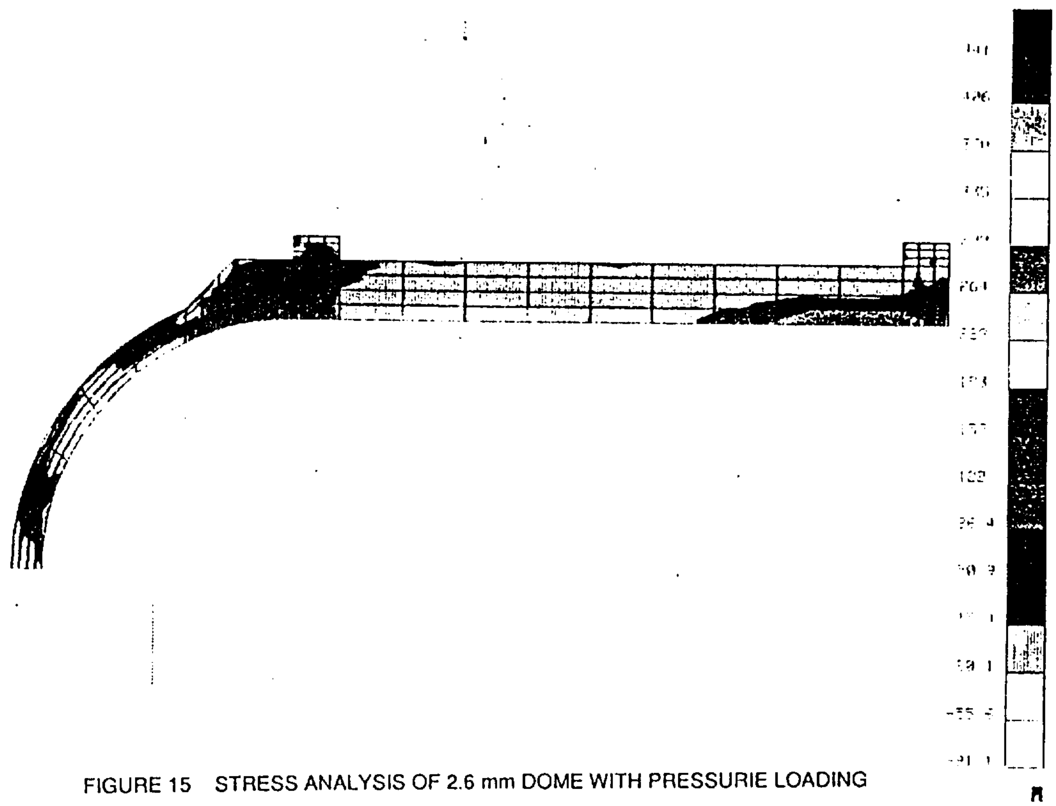

FIGURE 15 STRESS ANALYSIS OF 2.6 mm DOME WITH PRESSURIE LOADING

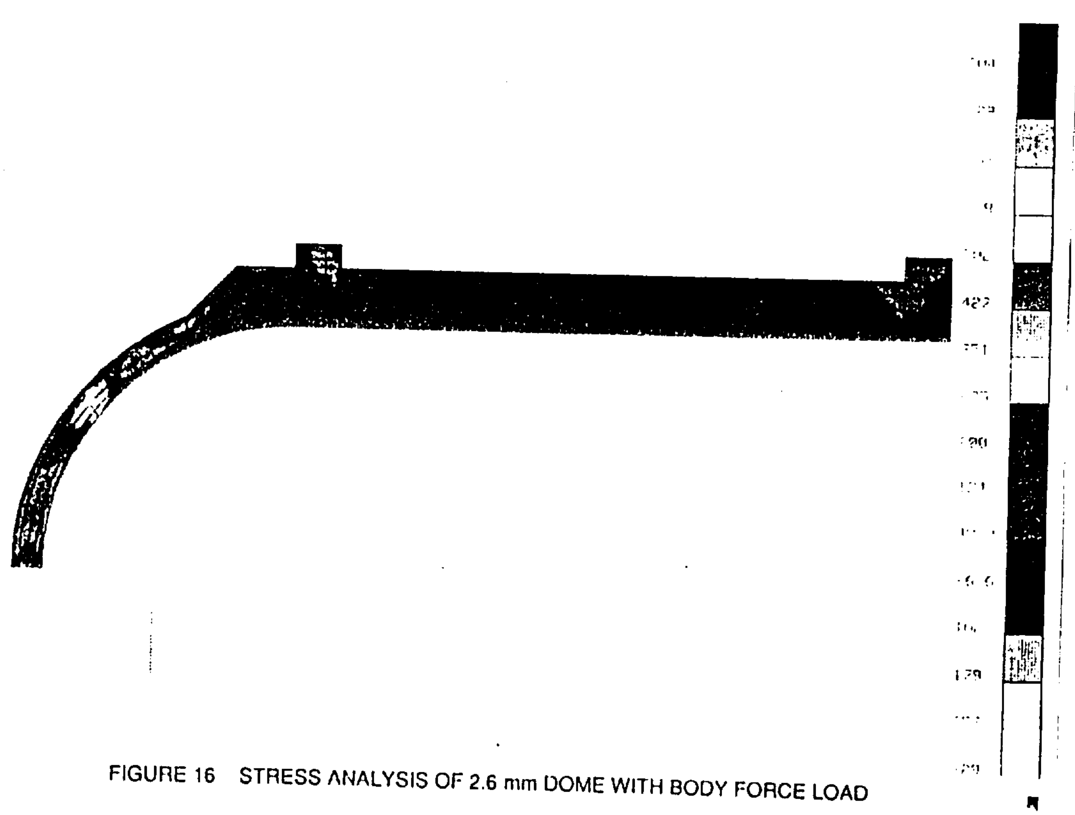

FIGURE 16 STRESS ANALYSIS OF 2.6 mm DOME WITH BODY FORCE LOAD

Analyzing individual loads on the projectile, Figure 15 shows only the pressure loading of 50 ksi acting on the projectile. The maximum stress of 406 ksi and minimum stress of -91.1 ksi was located at the dome. It is noted that pressure loading caused most of its stress concentration at the bottom end of the projectile with average stress of 157 ksi. Also at the location of the dome/body interface had large amount of stresses (50.9) ksi resulting the buckling of the mid body section of the model.

Figure 16 shows the results obtained only by the external body force of $1.x10^6$ gees. The maximum stress of 729 ksi was located in small portion of the dome and the minimum stress of -329 ksi was also at the dome section. Large stress concentration was located at the dome and the end section of the projectile. External body force resulted in higher stress than the pressure loading. Combine loading of the forces yield almost three fold increase in stresses. It was noted that by decreasing the both loads on the projectile by half of the original value also decreased the stress by half.

Figure 17 below shows the projectile with dome thickness of 5.0 mm.

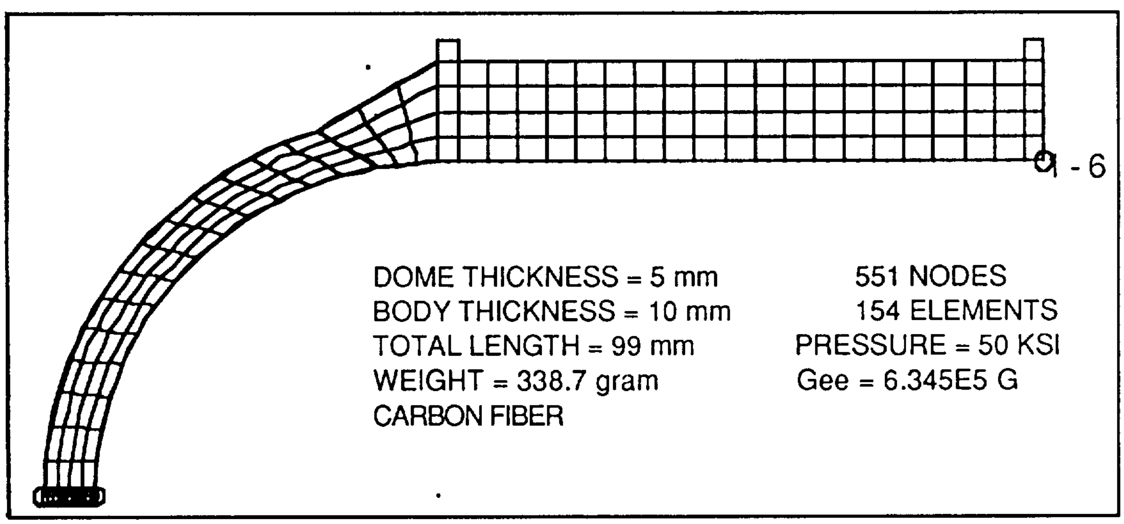

FIGURE 17 PROJECTILE WITH 5.0 mm DOME THICKNESS

Figure 18 and Figure 19 shows the results of the TEXGAP plotted by the PATRAN. Most of the stress concentrations was located at the dome

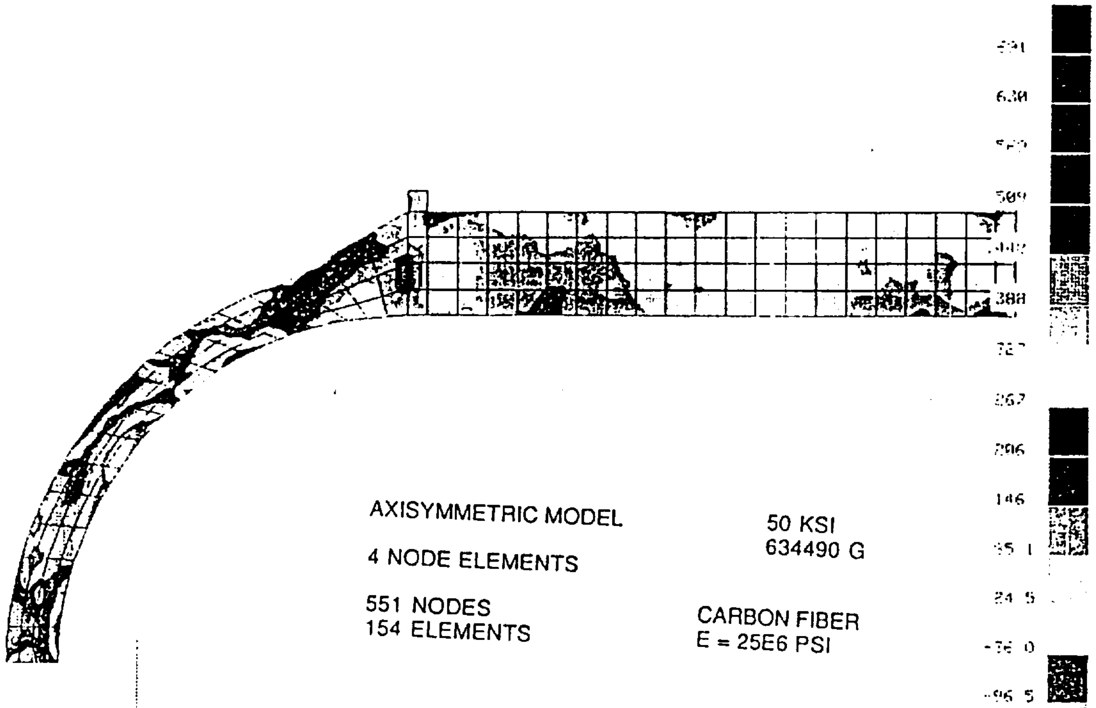

FIGURE 18 STRESS ANALYSIS OF 5.0 mm DOME PROJECTILE

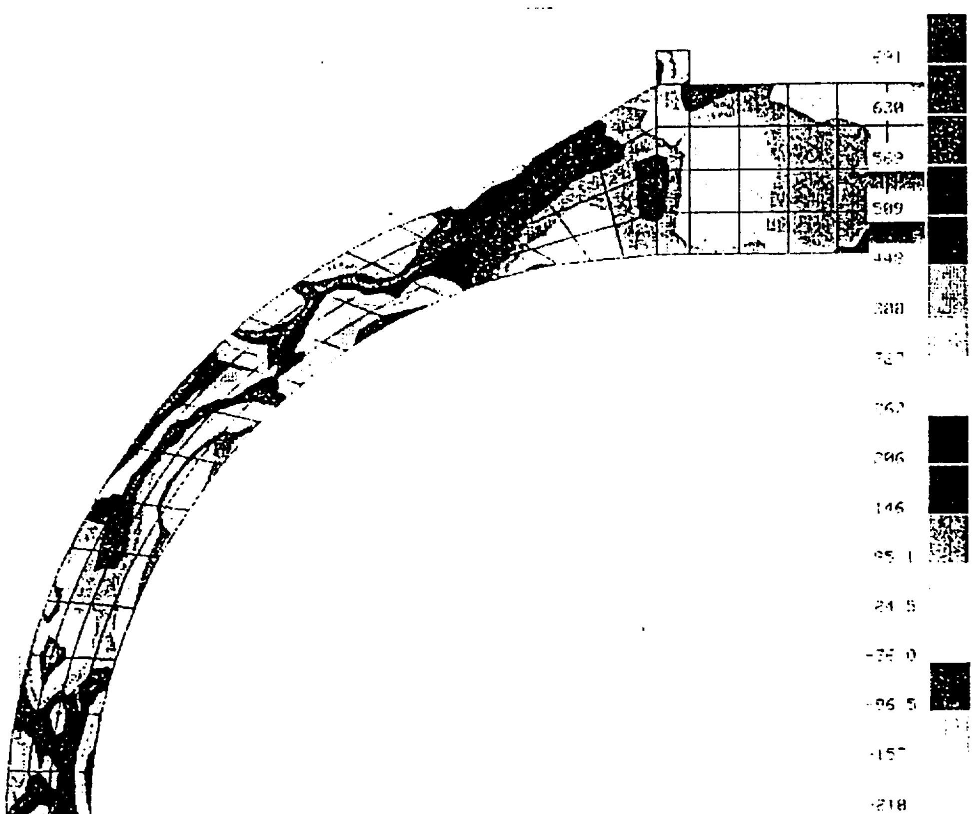

FIGURE 19 CLOSE UP VIEW OF 5.0 mm DOME SECTION

ORIGINAL PAGE IS
OF POOR QUALITY

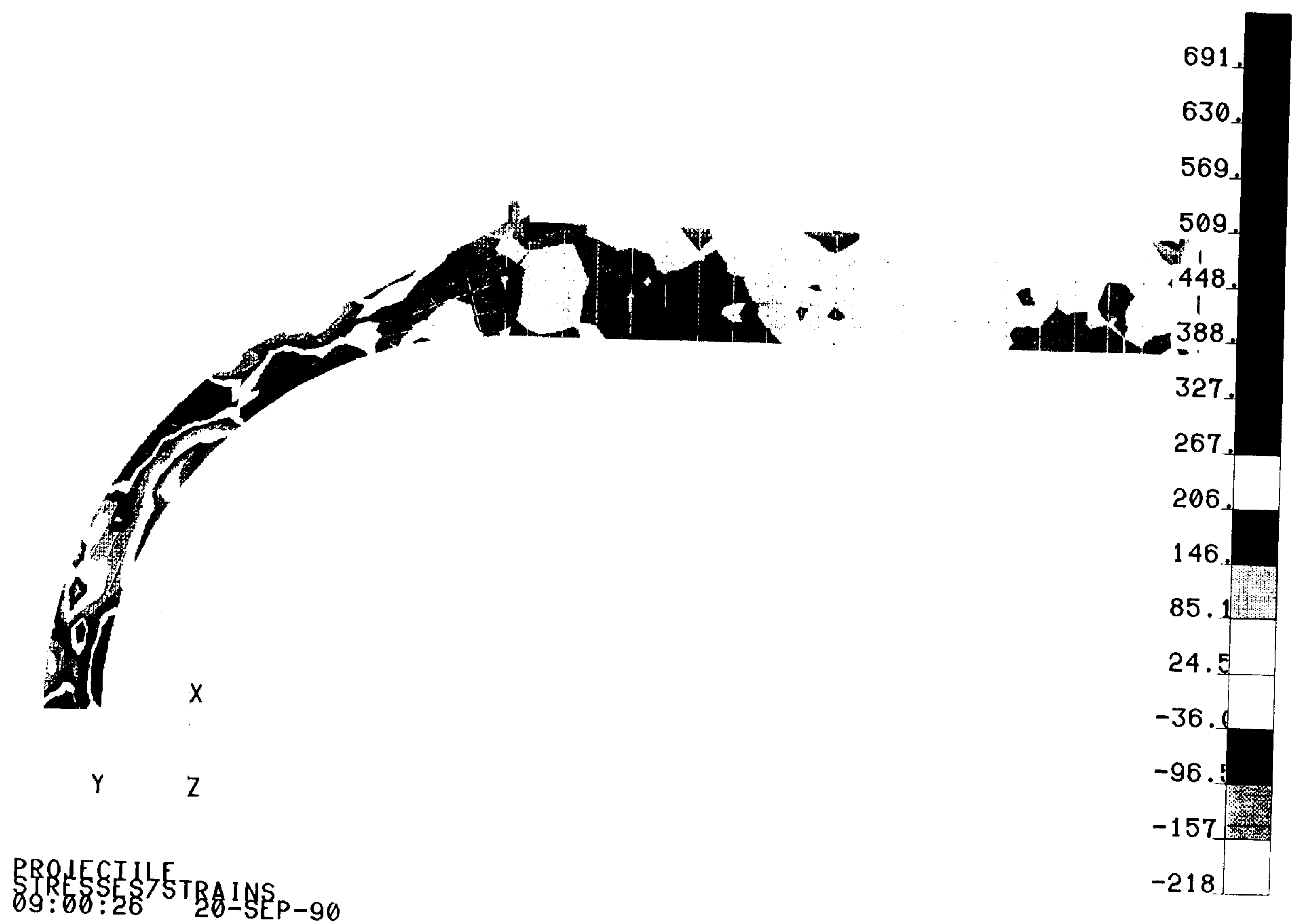
691.
630.
569.
509.
448.
388.
327.
267.
206.
146.
85.1
24.5
-36.0
-96.5
-157
-218
X
Y
Z
PROJECTILE
STRESSES/STRAINS
09:00:26 20-SEP-90

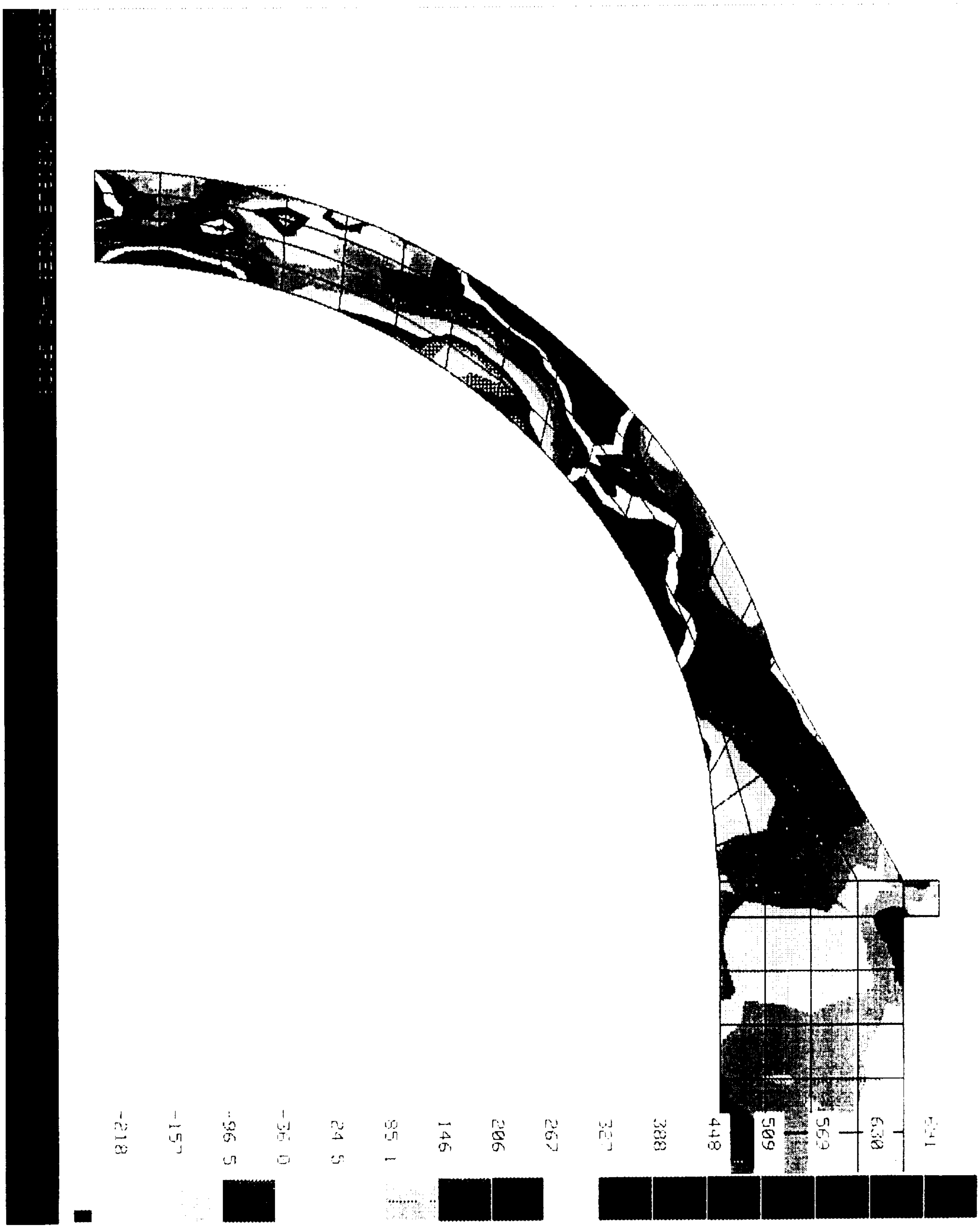

ORIGINAL PAGE IS
OF POOR QUALITY

with the maximum stress of 715 ksi and minimum stress of -238 ksi. The possible failure sites are easily viewed by the figures. Even at the thickness of 10 mm, the mid-body section is under compressive force which will cause the buckling. The buckling of the dome and the body caused by the large bending moments closely follow previous pattern displayed by the Figure 11. Overall, stress decreased more than 60 % when compared with the Figure 11.

Figure 20 shows the projectile with the dome thickness of 8 mm.

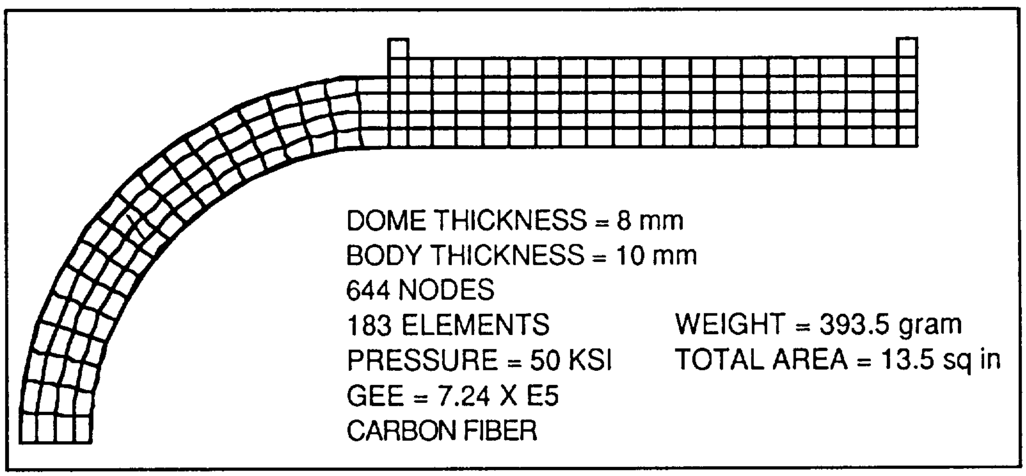

FIGURE 20 PROJECTILE WITH 8 mm DOME THICKNESS

Figure 21 is the plotted results of TEXGAP2D. It is interesting to note that the high stress concentration is located not at the dome section, but on the body section of the projectile. The highest stress of 1188 ksi was located at very small point near the body/bore rider interface. This stress migrated down well into the body section causing high stresses along the way. Although high stresses of 344 ksi was present at the front portion of the dome, the rest parts had moderate stress of 103 ksi. The lowest stress of -380 ksi was located at the dome/bore rider section. This is the part where the buckling would likely to occur. Therefore, this projectile has good chance of surviving the firing. The only major concern is the high weight of 393.5 grams which is an increase of 16.9 % compared with 5.0 mm dome projectile. However, at same time, the stress has decreased by 36 %.

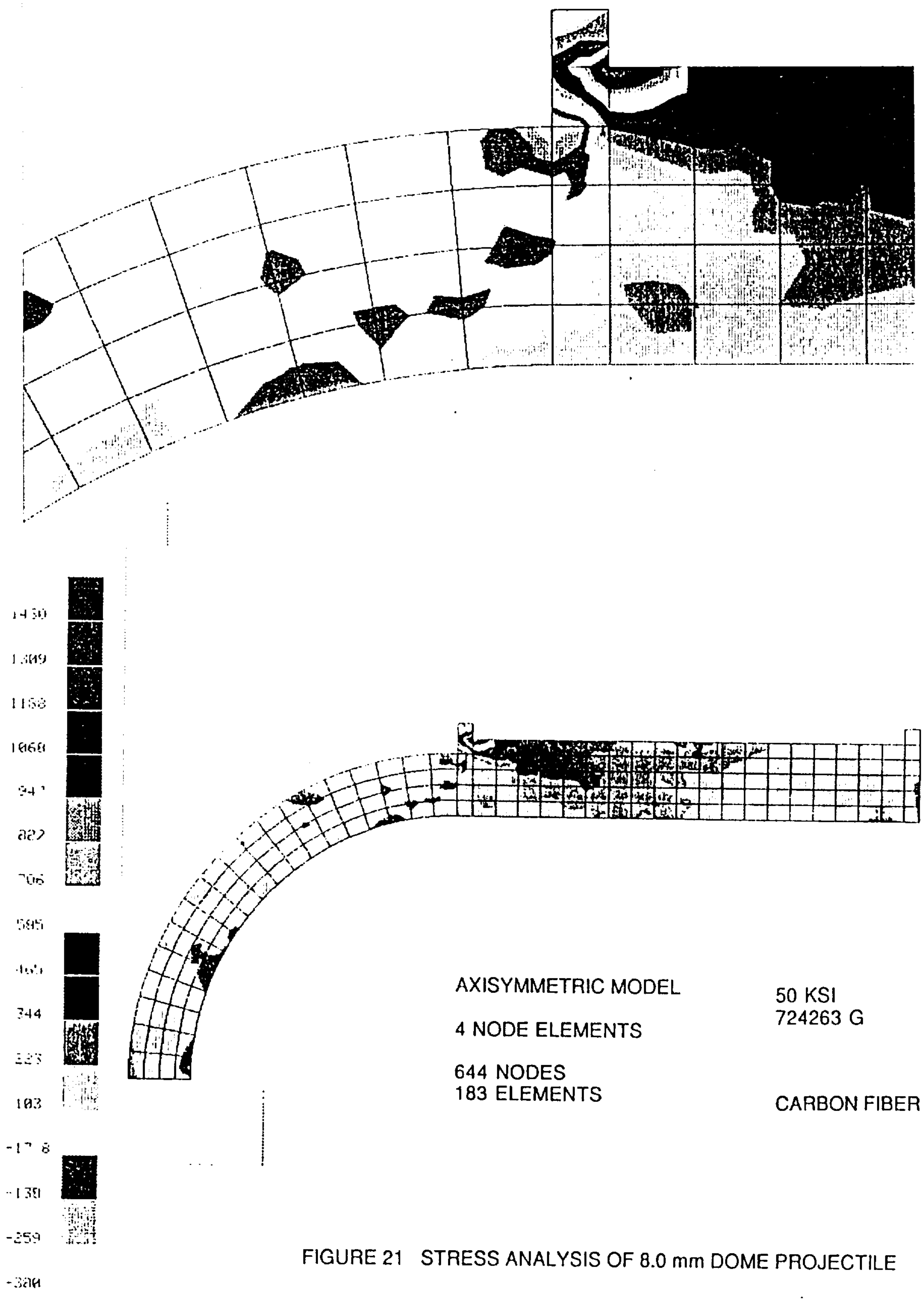

FIGURE 21 STRESS ANALYSIS OF 8.0 mm DOME PROJECTILE

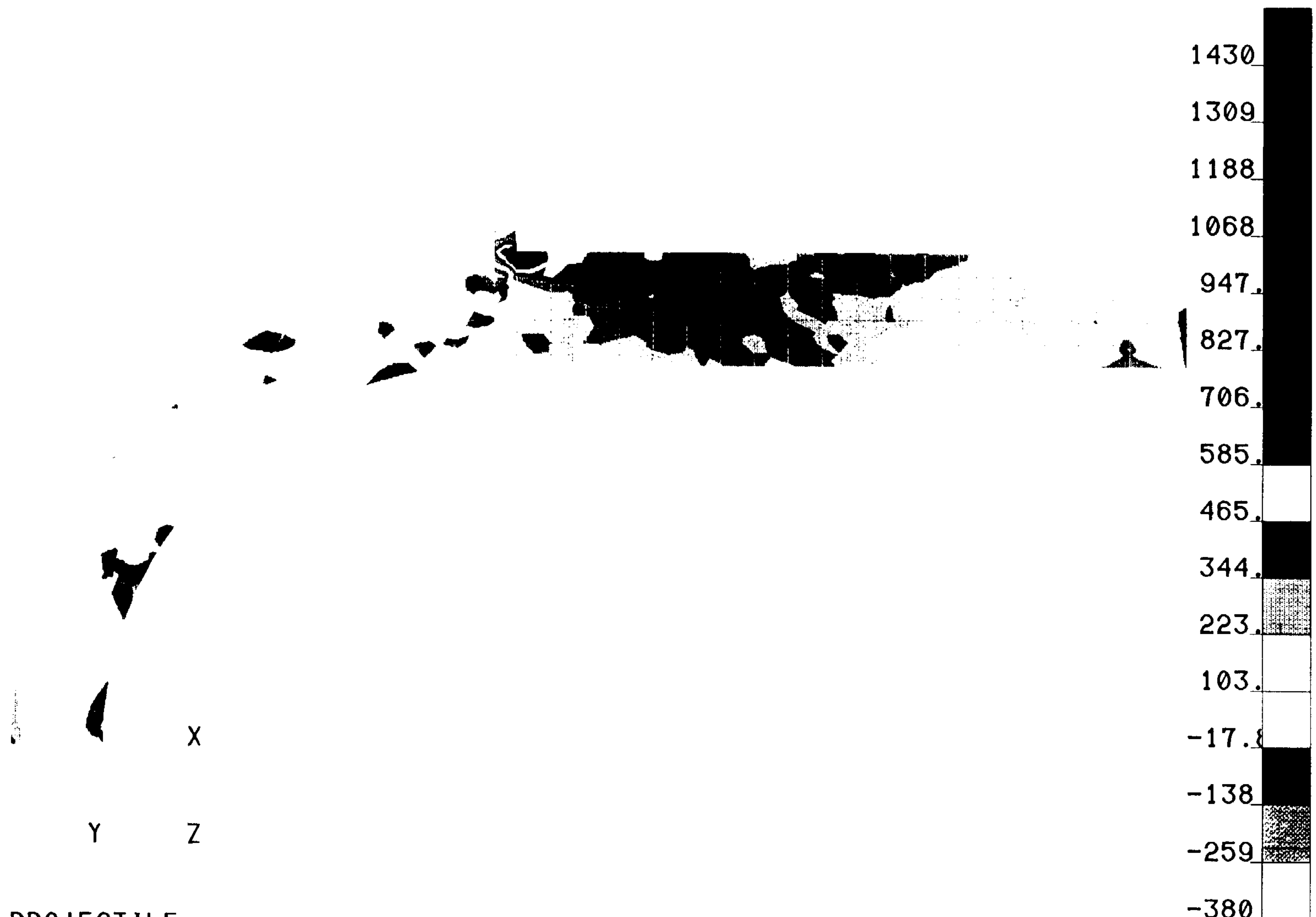

PROJECTILE
STRESSES/STRAINS
12:15:07 31-AUG-90

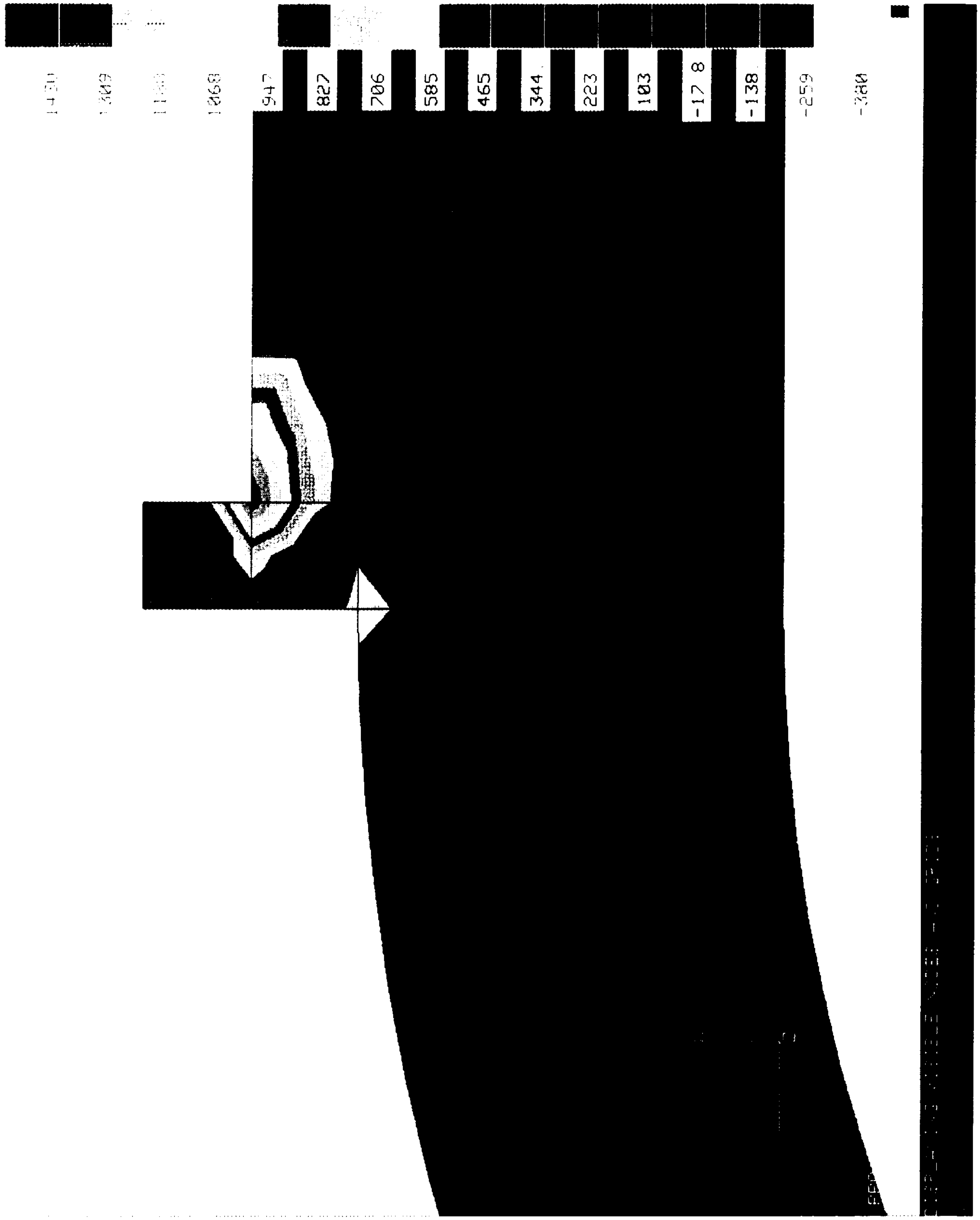
1068
947
827
706
585
465
344
223
103
-17.8
-138
-259
-380

Figure 22 shows the projectile with dome thickness of 10 mm and Figure 23 is the plotted result of the TEXGAP2D analysis. This projectile has a uniform thickness of 10 mm at the dome and the body of the projectile. The weight is increased 28.3% when compared with projectile of Figure 17. The high stress concentration was located at the bottom section of the dome/body interface. At that point, the maximum stress of 444 ksi was recorded. The minimum stress of -93.3 ksi was located at the center portion of the dome. This projectile would probably have survived the test firing. The projectile shows very little buckling at the dome and at the mid-body section. The stress has decreased by 47.1% when compared with the projectile with 5 mm dome. This is illustrated in the Figure 24 in page 29 along with the Figure 25 which describes the effects of the pressure loading. Increase of the pressure resulted in the increase of the gravity acceleration and stresses.

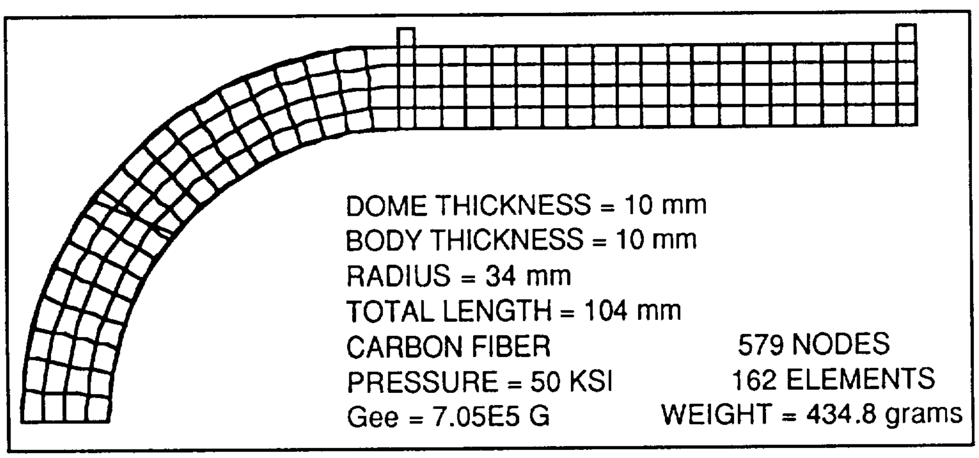

FIGURE 22 PROJECTILE WITH 10 mm DOME THICKNESS

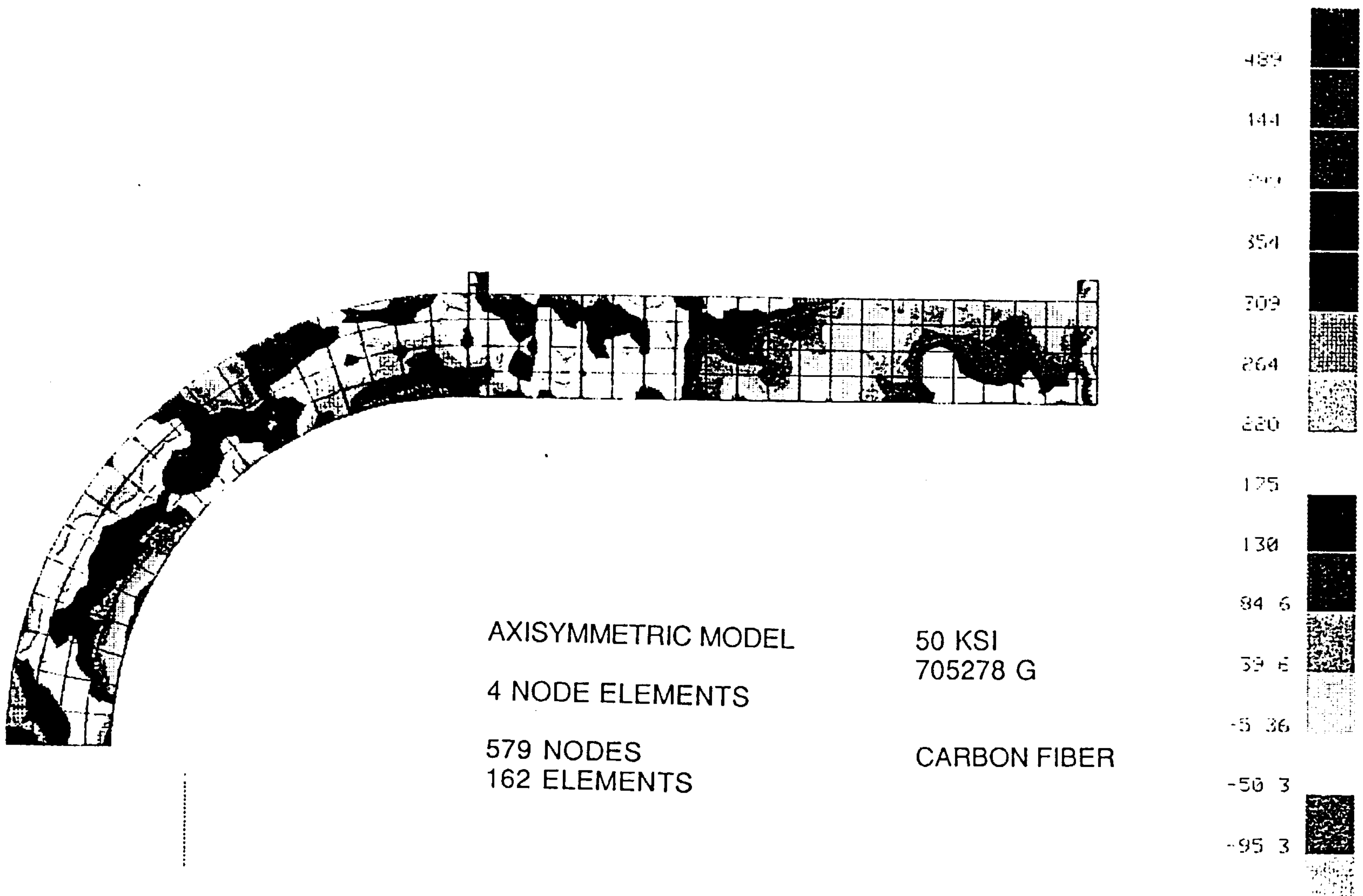

FIGURE 23 STRESS ANALYSIS OF 10.0 mm DOME PROJECTILE

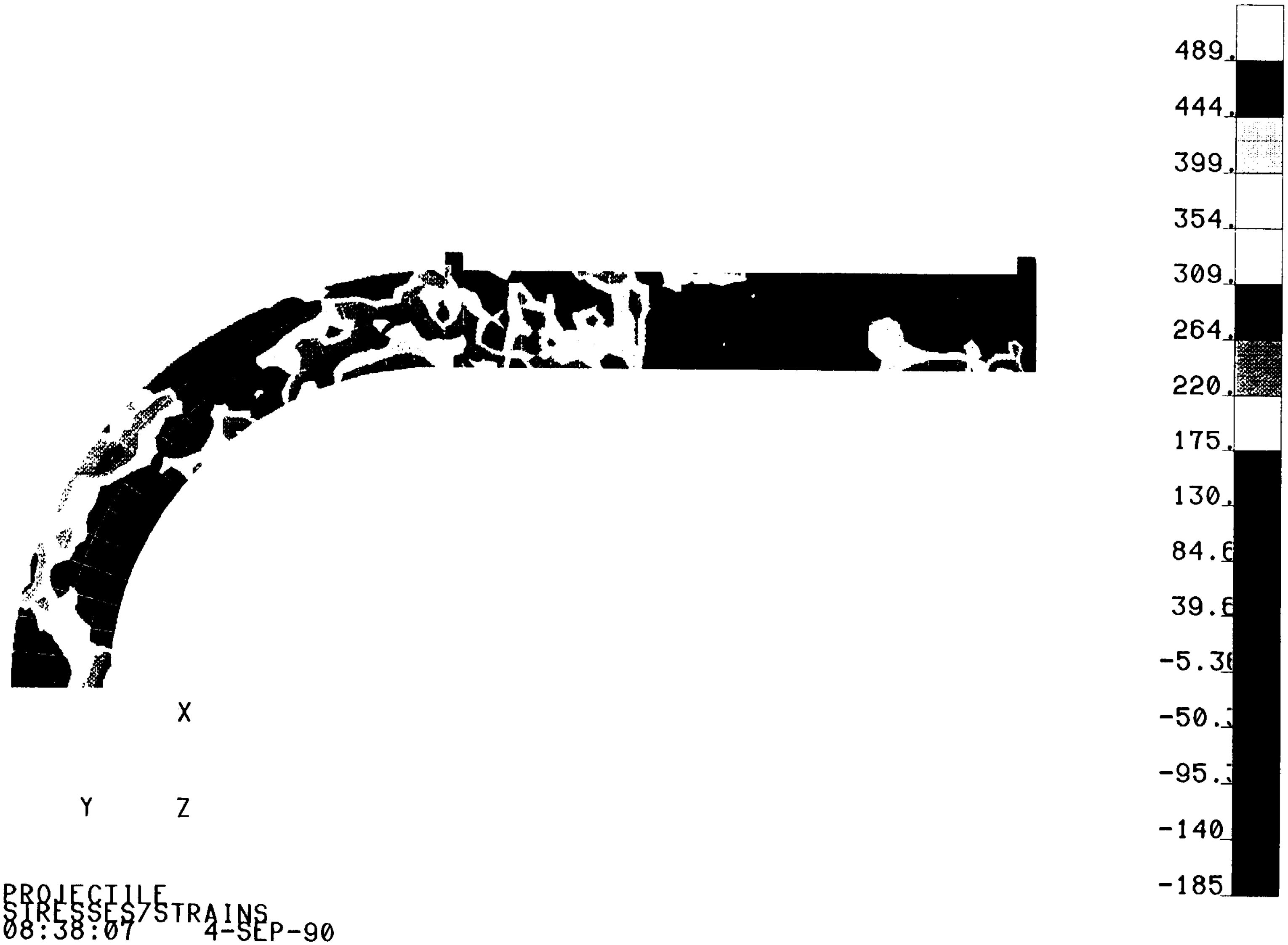

ORIGINAL PAGE IS
OF POOR QUALITY

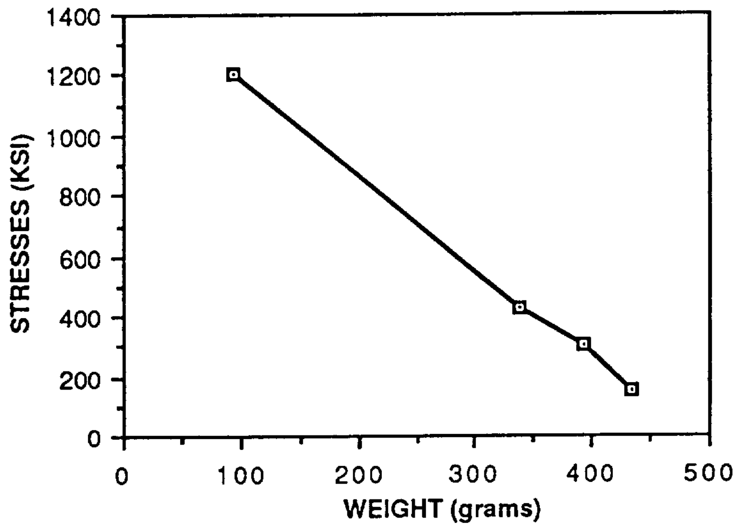

FIGURE 24 STRESSES VERSUS WEIGHT

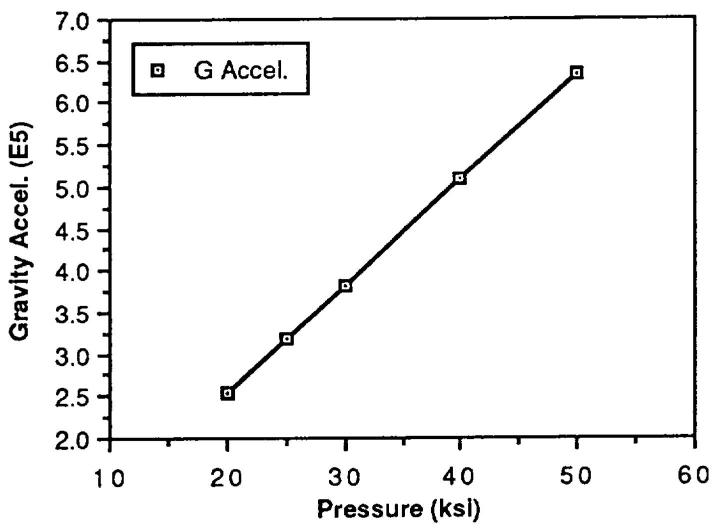

FIGURE 25 GRAVITY ACCELERATION VERSUS PRESSURE

TABLE 6 STRESS ANALYSIS DATA OF 5 mm DOME PROJECTILE

T E X G A P 8 4 - 2 D VERSION

58SEP-90 PAGE 1

AXISYMMETRIC PROBLEM

projectile

LARGEST AND SMALLEST STRESSES AND STRAINS BY MATERIAL

MATERIAL = 10

QUANTITY	R	Z	ELEM	MAXIMUM	R	Z	ELEM	MINIMUM
SIGR	3.496E+00	9.382E+01	90	8.223E+02	3.588E+00	9.884E+01	91	-1.144E+03
SIGZ	0.000E+00	9.650E+01	88	6.900E+02	1.963E+01	9.076E+01	108	-7.845E+02
SIGT	2.562E+01	8.940E+01	119	6.775E+02	3.588E+00	9.884E+01	91	-1.082E+03
TAURZ	1.920E+01	8.806E+01	110	6.439E+02	2.562E+01	8.940E+01	119	-5.297E+02
TAURT	3.615E+01	6.124E+01	154	0.000E+00	3.615E+01	6.124E+01	154	0.000E+00
TAUZT	3.615E+01	6.124E+01	154	0.000E+00	3.615E+01	6.124E+01	154	0.000E+00
SIG1	2.562E+01	8.940E+01	119	9.206E+02	1.920E+01	8.806E+01	114	-4.345E+02
SIG2	2.812E+01	8.702E+01	119	2.238E+02	1.920E+01	8.806E+01	110	-1.450E+03
SIG3	2.562E+01	8.940E+01	119	6.775E+02	3.588E+00	9.884E+01	91	-1.082E+03
TAUMAX	0.000E+00	9.900E+01	87	7.427E+02	4.025E+01	1.674E+01	27	2.196E+00
EPSR	3.496E+00	9.382E+01	90	2.790E-05	3.588E+00	9.884E+01	91	-3.333E-05
EPSZ	0.000E+00	9.775E+01	87	3.279E-05	1.963E+01	9.076E+01	108	-3.665E-05
EPST	1.636E+01	8.981E+01	110	2.821E-05	3.588E+00	9.884E+01	91	-3.007E-05
GAMRZ	1.920E+01	8.806E+01	110	6.696E-05	2.562E+01	8.940E+01	119	-5.509E-05
GAMRT	3.615E+01	6.124E+01	154	0.000E+00	3.615E+01	6.124E+01	154	0.000E+00
GAMZT	3.615E+01	6.124E+01	154	0.000E+00	3.615E+01	6.124E+01	154	0.000E+00
EPS1	0.000E+00	9.900E+01	87	3.767E-05	1.941E+01	8.941E+01	113	-1.330E-05
EPS2	1.762E+00	9.521E+01	90	-1.017E-06	1.920E+01	8.806E+01	110	-5.873E-05
EPS3	1.636E+01	8.981E+01	110	2.821E-05	3.588E+00	9.884E+01	91	-3.007E-05
GAMMAX	0.000E+00	9.900E+01	87	7.725E-05	4.025E+01	1.674E+01	27	2.284E-07

TIME IN STRESS = 7.140E+00 SECONDS

TEXGAP2D TO PATRAN TRANSLATION (RESULTS FROM STRESS OPTION)
GENERATED PATRAN STRESS/STRAIN NEUTRAL FILE
GENERATED PATRAN DISPLACEMENT NEUTRAL FILE

TIME IN TRANSLATE = 1.150E+00 SECONDS

TABLE 7 STRESS ANALYSIS DATA OF 8 mm DOME PROJECTILE

T E X G A P 8 4 - 2 D VERSION

318AUG-90

projectile

LARGEST AND SMALLEST STRESSES AND STRAINS BY MATERIAL

MATERIAL = 10

QUANTITY	R	Z	ELEM	MAXIMUM	R	Z	ELEM	MINIMUM
SIGR	4.200E+01	5.800E+01	77	4.853E+02	4.200E+01	6.000E+01	77	-1.348E+03
SIGZ	4.400E+01	5.800E+01	82	1.720E+03	4.200E+01	6.000E+01	73	-7.686E+02
SIGT	4.400E+01	5.800E+01	82	6.650E+02	4.200E+01	6.000E+01	77	-5.746E+02
TAURZ	4.400E+01	5.800E+01	82	6.685E+02	4.400E+01	6.000E+01	182	-6.891E+02
TAURT	4.600E+01	1.000E+00	183	0.000E+00	4.600E+01	1.000E+00	183	0.000E+00
TAUZT	4.600E+01	1.000E+00	183	0.000E+00	4.600E+01	1.000E+00	183	0.000E+00
SIG1	4.400E+01	5.800E+01	82	1.969E+03	4.200E+01	6.000E+01	77	-5.322E+02
SIG2	2.589E+01	9.307E+01	33	1.753E+02	4.200E+01	6.000E+01	77	-1.514E+03
SIG3	4.400E+01	5.800E+01	82	6.650E+02	4.200E+01	6.000E+01	77	-5.746E+02
TAUMAX	4.400E+01	5.800E+01	82	1.019E+03	3.797E+01	6.164E+01	74	4.177E+00
EPSR	4.200E+01	5.800E+01	77	2.167E-05	4.200E+01	6.000E+01	77	-3.867E-05
EPSZ	4.400E+01	5.800E+01	82	5.864E-05	4.200E+01	5.800E+01	77	-2.086E-05
EPST	3.400E+01	2.558E+01	141	1.684E-05	0.000E+00	9.400E+01	4	-7.414E-06
GAMRZ	4.400E+01	5.800E+01	82	6.952E-05	4.400E+01	6.000E+01	182	-7.167E-05
GAMRT	4.600E+01	1.000E+00	183	0.000E+00	4.600E+01	1.000E+00	183	0.000E+00
GAMZT	4.600E+01	1.000E+00	183	0.000E+00	4.600E+01	1.000E+00	183	0.000E+00
EPS1	4.400E+01	5.800E+01	82	7.163E-05	3.500E+01	2.263E+01	141	-5.380E-06
EPS2	2.646E+01	8.441E+01	40	2.308E-06	4.200E+01	6.000E+01	77	-4.727E-05
EPS3	3.400E+01	2.558E+01	141	1.684E-05	0.000E+00	9.400E+01	4	-7.414E-06
GAMMAX	4.400E+01	5.800E+01	82	1.060E-04	3.797E+01	6.164E+01	74	4.344E-07

TIME IN STRESS = 7.500E+00 SECONDS

TEXGAP2D TO PATRAN TRANSLATION (RESULTS FROM STRESS OPTION)
GENERATED PATRAN STRESS/STRAIN NEUTRAL FILE
GENERATED PATRAN DISPLACEMENT NEUTRAL FILE

TIME IN TRANSLATE = 9.500E-01 SECONDS

TABLE 8 STRESS ANALYSIS DATA OF 10.0 mm DOME PROJECTILE

T E X G A P 8 4 - 2 D VERSION

48SEP-90

projectile

LARGEST AND SMALLEST STRESSES AND STRAINS BY MATERIAL

MATERIAL = 10

QUANTITY	R	Z	ELEM	MAXIMUM	R	Z	ELEM	MINIMUM
SIGR	1.111E+01	1.026E+02	68	4.284E+02	3.900E+01	0.000E+00	158	-2.131E+02
SIGZ	3.388E+01	6.293E+01	1	5.590E+02	2.096E+01	8.677E+01	45	-3.475E+02
SIGT	3.650E+01	2.000E+00	157	4.652E+02	3.047E+01	8.010E+01	30	-1.461E+02
TAURZ	0.000E+00	1.015E+02	75	1.862E+02	4.150E+01	6.000E+01	3	-2.368E+02
TAURT	4.500E+01	2.000E+00	162	0.000E+00	4.500E+01	2.000E+00	162	0.000E+00
TAUZT	4.500E+01	2.000E+00	162	0.000E+00	4.500E+01	2.000E+00	162	0.000E+00
SIG1	3.388E+01	6.293E+01	1	5.678E+02	4.400E+01	2.000E+00	84	-2.009E+02
SIG2	9.845E+00	9.775E+01	62	2.054E+02	3.900E+01	0.000E+00	159	-3.859E+02
SIG3	3.650E+01	2.000E+00	157	4.652E+02	3.047E+01	8.010E+01	30	-1.461E+02
TAUMAX	3.351E+01	6.580E+01	9	2.839E+02	4.400E+01	7.895E+00	88	5.078E+00
EPSR	1.111E+01	1.026E+02	68	1.345E-05	3.400E+01	0.000E+00	157	-1.127E-05
EPSZ	3.388E+01	6.293E+01	1	2.005E-05	1.128E+01	9.208E+01	61	-1.187E-05
EPST	3.400E+01	0.000E+00	157	1.678E-05	3.533E+01	6.921E+01	9	-3.435E-06
GAMRZ	0.000E+00	1.015E+02	75	1.937E-05	4.150E+01	6.000E+01	3	-2.462E-05
GAMRT	4.500E+01	2.000E+00	162	0.000E+00	4.500E+01	2.000E+00	162	0.000E+00
GAMZT	4.500E+01	2.000E+00	162	0.000E+00	4.500E+01	2.000E+00	162	0.000E+00
EPS1	3.388E+01	6.293E+01	1	2.051E-05	4.400E+01	2.000E+00	84	-6.539E-06
EPS2	2.683E+01	8.475E+01	37	2.771E-06	3.900E+01	0.000E+00	159	-1.721E-05
EPS3	3.400E+01	0.000E+00	157	1.678E-05	3.533E+01	6.921E+01	9	-3.435E-06
GAMMAX	3.351E+01	6.580E+01	9	2.952E-05	4.400E+01	7.895E+00	88	5.281E-07

TIME IN STRESS = 7.270E+00 SECONDS

TEXGAP2D TO PATRAN TRANSLATION (RESULTS FROM STRESS OPTION)
GENERATED PATRAN STRESS/STRAIN NEUTRAL FILE
GENERATED PATRAN DISPLACEMENT NEUTRAL FILE

TIME IN TRANSLATE = 1.180E+00 SECONDS

CHAPTER 4

CONCLUSION AND RECOMMENDATION

In this study, the finite element analysis approach to modeling was successfully employed to produce an optimum design of a composite projectile. The computer programs Micro/Macromechanic analysis and GENLAM were useful for preliminary design calculations since these programs gave approximated values. The uses of modeling code PATRAN and finite element analysis code of TEXGAP2D could be valuable tools for any designer to have. This analysis verified the failure of the projectile that was fired in 1989 testing. The cause was the failure of the dome section due to the presence of high stress concentrations and buckling due to large bending moments.

From the three new design analyses presented in this study, the projectile with 8 mm dome thickness would be adequate enough to survive the firing conditions. The analysis showed that the stress was evenly distributed throughout the dome section where the main concern of the failure is located.

The projectile with 5.0 mm dome thickness had 60 % decrease in the stress concentration when compared with the projectile with 2.6 mm dome thickness. Even with this decrease in stress, the analysis still showed high stresses at the dome and followed similar patterns of buckling. However, the projectile has fairly good chance of surviving the firing. The projectile with 10 mm dome thickness would definitely survive the firing. This projectile showed small stress concentrations when compared with all of the other designs. The only disadvantage is the high weight it possesses.

The results shown illustrate that the complete loading environment produces a stress field that are easily understood. Another benefit from the analyses of this study is the visualization of the stress concentrations.

The various effective boundary constraints resulted in different stresses in addition to bending moments. This presented difficulties choosing the placement of the constraints. The best results were obtained when the projectile was constrained radial direction at the bottom edges of the dome and one other point at the bottom end of the projectile body.

The present code has some limitations such as it is good for the linear static analysis for the elastic regions and high loading conditions are not possible. In the future analysis, it is strongly recommended that 3-dimensional nonlinear analysis should be performed using orthotropic property conditions. One possible code that is recommended is the "DYNA 3-D" code. Finally, a better understanding of the plasma reaction, drag and the hypervelocity effects of the projectile inside the railgun is needed.

APPENDIX A

METHOD OF PROJECTILE FABRICATION

The mandrel for the projectile was designed to be used for the layup of the projectile. Figure 26 shows the configuration.

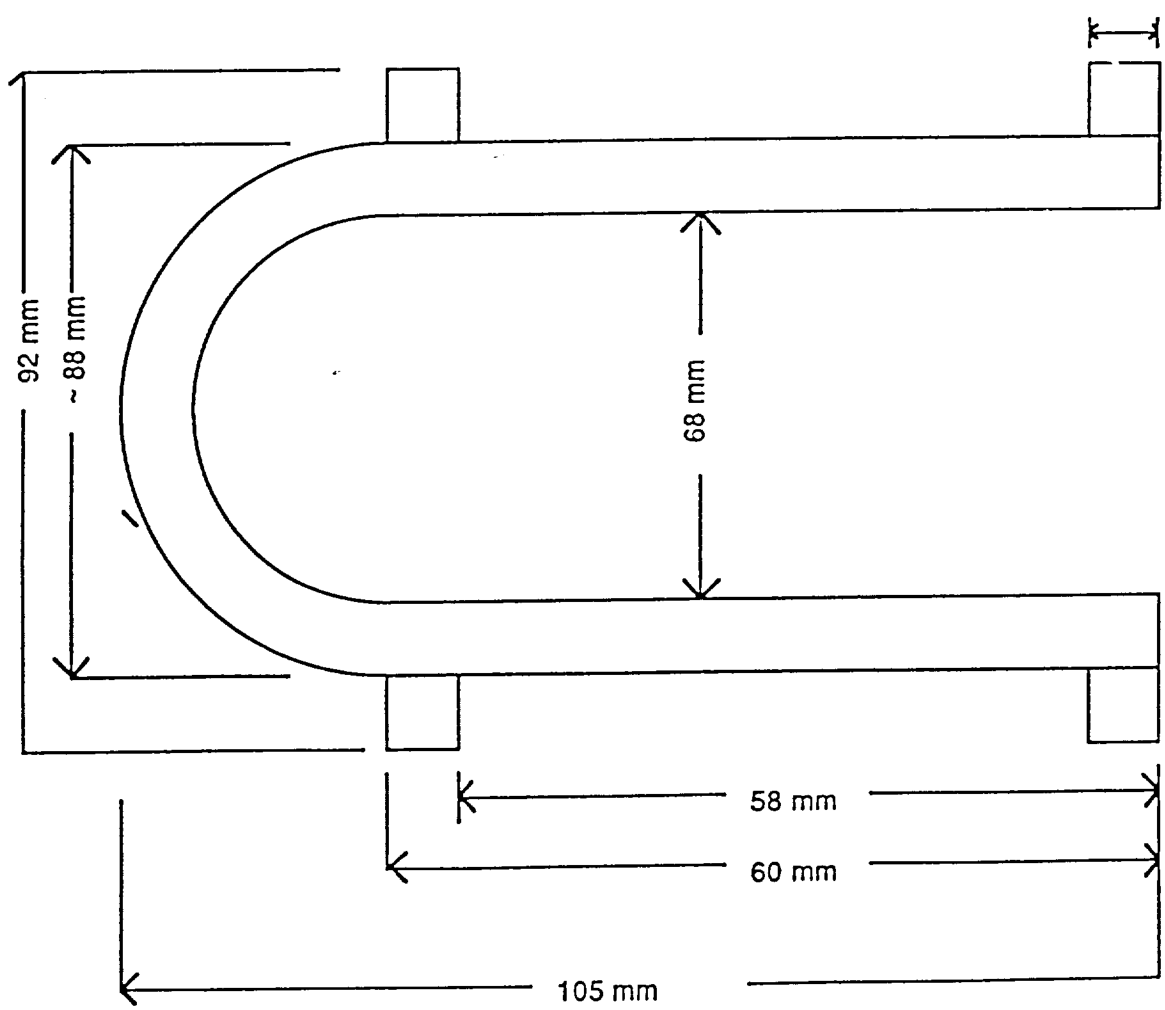

FIGURE 26 CONFIGURATION OF THE PROJECTILE MANDREL

This mandrel is made from an aluminum rod. The mandrel is then cleaned and polished with wax for 15 minutes. After the wax has been dried for another 15 minutes, the process is repeated up to 5 more coatings of wax. Finally, the mandrel is sprayed with releasing agent to deter against sticking with the composite material.

The following layup of the projectile was performed using Kevlar cloth and graphite/epoxy materials. First, the Kevlar cloth is covered over the mandrel and it is hand stretched past the tangent point of the dome/body intersection. Excess materials are then cut to exact specification. Secondly, the mandrel with first layup is taken to the tumble winder where graphite/epoxy toe is used for the filament winding of the body section. This process is repeated until the material has reached the designed goal.

After the layup, the part is ready for the bagging. The part is first bagged with release film followed by breather cloth to absorb the moisture and then bagging film. The air flow tube is inserted to check for the leaks and to pump the air out. Finally, the finished bagged part is put into autoclave to be cured for 3 hours at temperature of 300 degree Fahrenheit.

APPENDIX B

EQUATIONS OF LAMINATED PLATE THEORY

Lorentz Force $= \frac{1}{2}$ Inductance (L) x Current $(I)^2$ --(1.1)

In-plane stresses are:

$$\sigma_1^{\circ} = \frac{PD}{4h} + \frac{F}{\pi Dh} \quad \text{------------} \quad (1.2)$$

$$\sigma_2^{\circ} = \frac{PD}{2h} \quad \text{------------} \quad (1.3)$$

$$\sigma_6^{\circ} = \frac{2T}{2\pi D^2 h} \quad \text{------------} \quad (1.4)$$

In-plane strain is

$$\{\epsilon^0\} = [a^*]\{\sigma^0\} \quad \text{------------} \quad (2.1)$$

where

$$[A] = \int_{-h/2}^{h/2} [Q]\, dz \quad \text{------------} \quad (2.2)$$

$$[A^*] = \frac{[A^*]}{h} \quad \text{------------} \quad (2.3)$$

$$[a^*] = [A^*]^{-1} \quad \text{------------} \quad (2.4)$$

The displacement or changes in lengths are

$$\partial L = L\epsilon_1^{\circ} \quad \text{------------} \quad (3.1)$$

The on-axis plane stress stiffness and compliance of a unidirectional ply can be computed from the engineering constants as follows:

$$[Q] = \begin{bmatrix} \frac{E_x}{1-\nu_x \nu_y} & \nu_y Q_{yy} & 0 \\ \nu_y Q_{xx} & \frac{E_x}{1-\nu_x \nu_y} & 0 \\ 0 & 0 & E_s \end{bmatrix} \quad \text{-----} \quad (4.1)$$

where, $Q_{12} = Q_{21}$, $Q_{16} = Q_{61} = Q_{26} = Q_{62} = 0$

$$[S] = \begin{bmatrix} \frac{1}{E_x} & \frac{-\nu_y}{E_y} & 0 \\ \frac{-\nu_y}{E_x} & \frac{1}{E_y} & 0 \\ 0 & 0 & \frac{1}{E_s} \end{bmatrix} \quad \text{-------} \quad (4.2)$$

where, $S_{12} = S_{21}$, $S_{16} = S_{61} = S_{26} = S_{62} = 0$

Using the figure below to define the in-plne stress, stress resultant, and laminate stiffness by integration:

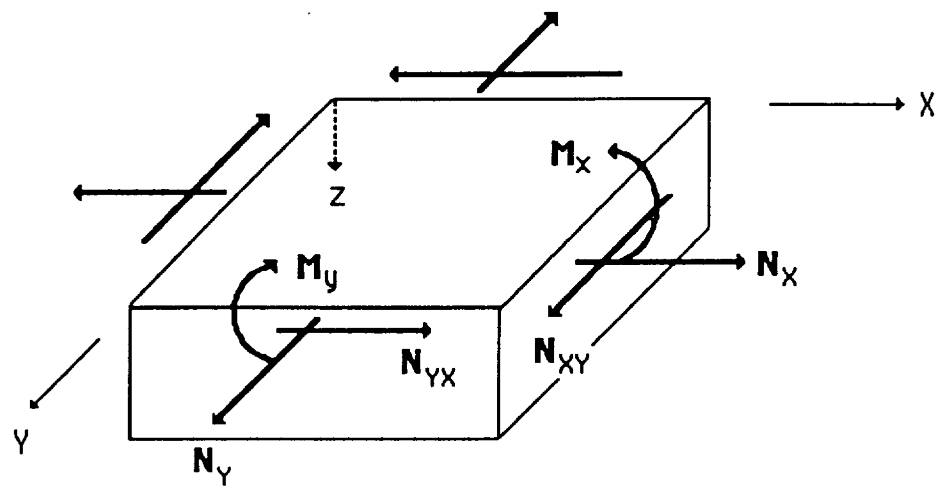

$$N_X = \int_{-h/2}^{h/2} \sigma_x \, dz$$

------------ (5.1)

$$M_X = \int_{-h/2}^{h/2} \sigma_x \, z \, dz$$

rewriting to obtain equation 5.2

$$\begin{Bmatrix} N_x \\ N_y \\ N_{xy} \end{Bmatrix} = \int_{-h/2}^{h/2} \begin{Bmatrix} \sigma_x \\ \sigma_y \\ \tau_{xy} \end{Bmatrix} dz = \sum_{k=1}^{n} \int_{-a_{k-1}}^{a_k} \begin{Bmatrix} \sigma_x \\ \sigma_y \\ \tau_{xy} \end{Bmatrix} dz$$

$$\begin{Bmatrix} N_x \\ N_y \\ N_{xy} \end{Bmatrix} = \sum_{k=1}^{n} \begin{bmatrix} \bar{Q}_{11} & \bar{Q}_{12} & \bar{Q}_{16} \\ \bar{Q}_{21} & \bar{Q}_{22} & \bar{Q}_{26} \\ \bar{Q}_{31} & \bar{Q}_{32} & \bar{Q}_{33} \end{bmatrix}_K \left(\int_{a_{k-1}}^{a_k} \begin{Bmatrix} \epsilon_x^\circ \\ \epsilon_y^\circ \\ \gamma_{xy}^\circ \end{Bmatrix} dZ + \int_{a_{k-1}}^{a_k} \begin{Bmatrix} k_x \\ k_y \\ k_{xy} \end{Bmatrix} Z\,dZ \right) \quad \text{----------} \quad (5.3)$$

Finally obtain Equation 5.4

$$\begin{Bmatrix} N_x \\ N_y \\ N_{xy} \end{Bmatrix} = \begin{bmatrix} \bar{A}_{11} & \bar{A}_{12} & \bar{A}_{16} \\ \bar{A}_{21} & \bar{A}_{22} & \bar{A}_{26} \\ \bar{A}_{31} & \bar{A}_{32} & \bar{A}_{33} \end{bmatrix} \begin{Bmatrix} \epsilon_x^\circ \\ \epsilon_y^\circ \\ \gamma_{xy}^\circ \end{Bmatrix} + \begin{bmatrix} \bar{B}_{11} & \bar{B}_{12} & \bar{B}_{16} \\ \bar{B}_{21} & \bar{B}_{22} & \bar{B}_{26} \\ \bar{B}_{31} & \bar{B}_{32} & \bar{B}_{33} \end{bmatrix} \begin{Bmatrix} k_x \\ k_y \\ k_{xy} \end{Bmatrix}$$

WHERE

$$A_{ij} = \sum_{k=1}^{n} (\bar{Q}_{ij})_k \, (a_k - a_{k-1})$$

$$B_{ij} = \sum_{k=1}^{n} (\bar{Q}_{ij})_k \, (a_k^2 - a_{k-1}^2)$$

The strain-stress relations for an axisymmetric muti-layered cylinder (Figure-3) in cylinderical coordinates are given by:

$$\epsilon_r^{(k)} = S_{rr}^{(k)}\sigma_r^{(k)} + S_{r\theta}^{(k)}\sigma_\theta^{(k)} + S_{rz}^{(k)}\sigma_z^{(k)}$$

$$\epsilon_\theta^{(k)} = S_{r\theta}^{(k)}\sigma_r^{(k)} + S_{\theta\theta}^{(k)}\sigma_\theta^{(k)} + S_{\theta z}^{(k)}\sigma_z^{(k)}$$

$$\epsilon_z^{(k)} = S_{rz}^{(k)}\sigma_r^{(k)} + S_{\theta z}^{(k)}\sigma_\theta^{(k)} + S_{zz}^{(k)}\sigma_z^{(k)}$$

where $S_{ij}^{(k)}$ $(ij = r, \theta, z)$ are components of the compliance matrix. The superscript k refers to the k-th layer.

The strain in z-direction is assumed to be constant $(\epsilon_z^{(k)} = \epsilon_z^o)$ Then strain-stress relations modify to

$$\epsilon_r^{(k)} = \beta_{rr}^{(k)}\sigma_r^{(k)} + \beta_{r\theta}^{(k)}\sigma_\theta^{(k)} + \nu_{rz}^{(k)}\epsilon_z^o$$

$$\epsilon_\theta^{(k)} = \beta_{r\theta}^{(k)}\sigma_r^{(k)} + \beta_{\theta\theta}^{(k)}\sigma_\theta^{(k)} + \nu_{z\theta}^{(k)}\epsilon_z^o$$

where $\beta_{ij}^{(k)} = S_{ij}^{(k)} - S_{iz}^{(k)} S_{jz}^{(k)} / S_{zz}^{(k)}$, $(ij = r, \theta)$

$\nu_{iz}^{(k)} = S_{iz}^{(k)} / S_{zz}^{(k)}$, $(ij = r, \theta)$

The radial, $\sigma_r^{(k)}$, and hoop, $\sigma_\theta^{(k)}$, stresses are

$$\sigma_r^{(k)} = A_k[(r/a_k)^{g(k)-1} - (a_k/r)^{g(k)+1}] + B_k[-(r/a_k)^{g(k)-1} + c_k^{2g(k)}(r/a_k)^{g(k)+1}] \quad \text{---------} \ (6.1)$$

$$\sigma_\theta^{(k)} = A_k\, g(k)[(r/a_k)^{g(k)-1} - (a_k/r)^{g(k)+1}] - B_k g(k)[-(r/a_k)^{g(k)-1} + c_k^{2g(k)}(a_k/r)^{g(k)+1}] \quad \text{---------} \ (6.2)$$

and

$$\sigma_z^{(k)} = (\epsilon_z^{o} - S_{rz}^{(k)}\sigma_r^{(k)} - S_{\theta z}^{(k)}\sigma_\theta^{(k)}) / + S_{zz}^{(k)} \quad \text{-----} \ (6.3)$$

where $A_k = (q^{(k-1)} c_k^{g(k)+1})/(1 - c_k^{2g(k)})$

$B_k = q^{(k)}/(1 - c_k^{2g(k)})$

$c_k = a_{k-1}/a_k$

$g(k) = [\beta_{rr}^{(k)}/\beta_{\theta\theta}^{(k)}]^{1/2}$

To determine ϵ_z^{o}, the axial stress,

$$\sum_{k=1}^{n} 2\pi \int_{a_{k-1}}^{a_k} \sigma_z^{(k)} r\,dr = \pi\,(q^{(i)} - q^{(e)})a^2 + F \quad \text{-----} \ (6.4)$$

Substituting $\sigma_z^{(k)}$ from Equation 6.3 and the expressions for $\sigma_r^{(k)}$ and $\sigma_\theta^{(k)}$ from Eq 6-1 and 6-2 into equation 6-4 and performing the integration, the expression for ϵ_z° is given by:

$$\epsilon_z^\circ = \left[(q^{(i)} - q^{(e)})a^2 + F/\pi - \sum_{k=1}^{n} (q^{(k-1)} \partial_k + q^{(k)}\mu_k)\right]/\Delta$$

where

$$\partial_k = -2[a_k c_k^{g(k)+1} (S_{rz}^{(k)} + g(k) S_{\theta z}^{(k)}) (a_k - c_k^{(k)} a_{k-1})/(1+g(k))$$
$$- a_{k-1} (S_{rz}^{(k)} - g(k) S_{\theta z}^{(k)}) (a_k c_k^{(k)} a_{k-1})/(1+g(k))]/\{S_{zz}^{(k)} (1-c_k^{2g(k)})\}$$

$$\mu_k = -2[a_k (S_{rz}^{(k)} + g(k) S_{\theta z}^{(k)}) (a_k - c_k^{g(k)} a_{k-1})/(1+g(k) + a_{k-1} c_k^{g(k)} (S_{rz}^{(k)}$$
$$- g(k) S_{\theta z}^{(k)}) (a_k c_k^{(k)} a_{k-1})/(1-g(k))]/\{S_{zz}^{(k)} (1-c_k^{2g(k)})\}$$

and

$$\Delta = \sum_{k=1}^{n} (a_k^2 - a_{k-1}^2)/S_{zz}^{(k)}$$

APPENDIX C

TABLE 9 MICRO-MACROMECHANIC ANALYSIS DATA

	A	B	C	D	E	F	G	H	I
1	MIC-MAC/CYLIN VESSEL: {[theta/#], . . .}total					Ply mat:	IM6/ep[Eng]		
2	READ ME	Theta 1	Theta 2	Theta 3	Theta 4				
3	[ply angle]	0.0	90.0	54.5	-54.5	[repeat]	h, #	h, E-3	[Rotate]
4	[ply#]	0	0	1	1	67.0	134.0	660.0	0.00
5									
6	R/intact	#####	#####	0.99	0.99	R/FPF	0.99	safety	1.50
7	R/degraded	#####	#####	2.59	2.59	R/LPF	2.59	R/lim*	1.73
8						R/ult	2.59	R/lim	0.99
9	size, m or in		∂L,∂D,E-3		<sg>	<sg>lim	<sg>lim*	<sg>ult	{E°}lim
10	[Length]	5.00	19.51	1	65.	65.	113.	169.	2.8
11	[Diameter]	3.60	25.79	2	128.	127.	221.	332.	7.5
12	Angle of twist,deg		0.00	6	0.	0.	0.	0.	6.9
13									
14		[Load]	[Load] lim		<ep>E-3	<ep>lim	<ep>lim*	<ep>ult	E^u/E^
15	Axial load F	10.00	9.94	1	3.90	3.88	6.73	10.10	0.33
16	Pressure P	47.00	46.71	2	7.16	7.12	12.36	18.54	0.41
17	Torque	0.00	0.00	6	0.00	0.00	0.00	0.00	0.98
18									
19		T opr	c.moist	vol/f	Em	Efx	Xm	Xfx	Em/Em°
20	Baseline	71.6	0.005	0.66	0.49	45	8.1	770	0.30
21	[Modified]	71.6	0.005	0.66	0.49	45	8.1	770	0.30
22	Mod/Base	1.000	1.000	1.000	1.000	1.000	1.000	1.000	1.000
23	Mod-Base	0.0	0.000	Hot/Wet	0.49	45	8.1	770	
24									
25									
26									
27	Ply data linked to Ply Data File:								
28	IM6/ep[Eng]	29.463	1.6255	0.32	1.2192	0.4935	251.6	320	
29	507.98258	223.51	8.1277	21.771	14.224	1.2	71.6	0.005	
30	-0.5	4925	0.66	1.6	0.516	0.5	0.2	0.9	
31	-0.166667	15.611	0	0.6	0.316	0.004	0.004	3600	
32	11.37	55.86	0.906	1.61	0	0	0	0	
33									
34									
35									
36									
37									
38									
39									

	J	K	L	M	N	O	P	Q
1	INTACT PLY DATA MODULE				Temperature deg and moisture			
2	IM6/ep[Eng]				[T] opr	72	72	1.00
3	Rigid body rotation of the entire laminate, i				[c],wet	0.005	0.005	1.00
4	Stiffness	Baseline	Modified	Mod/B	T cure	252	252	1.00
5	Ex,GPa	29.46	29.46	1.00	T glass	320	320	1.00
6	Ey,GPa	1.63	1.63	1.00	T *	1.00	1.00	1.00
7	nu/x	0.32	0.32	1.00	del T	-180	-180	1.00
8	Es,GPa	1.22	1.22	1.00				
9	ho,E-6m	4925	4925	1.00	Thermal expansion, E-6/deg			
10	Micromechanics data				alph/x	-0.17	-0.17	1.00
11	vol/f	0.66	0.66	1.00	alph/y	15.61	15.61	1.00
12	Efx	45	45	1.00	Moisture expansion,/c			
13	Em	0.49	0.49	1.00	beta/x	0.00	0.00	1.00
14	eta/y	0.52	0.52	1.00	beta/y	0.60	0.60	1.00
15	v*/y	0.27	0.27	1.00				
16	Efy,GPa	4.17	4.17	1.00	Ply & consti strengths, MPa			
17	eta/s	0.32	0.32	1.00	X	508	508	1.00
18	v*/s	0.16	0.16	1.00	X'	224	224	1.00
19	Gfx,GPa	15.85	15.85	1.00	Y	8	8	1.00
20					Y'	22	22	1.00
21	Plane stress stiffness, GPa				S	14	14	1.00
22	Qxx	29.63	29.63	1.00	[Fxy*]	-0.50	-0.50	1.00
23	Qyy	1.63	1.63	1.00	[Xf]	770	770	1.00
24	Qxy	0.52	0.52	1.00	[Xm]	8	8	1.00
25	Qss	1.22	1.22	1.00				
26	Linear combinations, GPa				Strength parameters, Pa^-18			
27	U1	12.46	12.46	1.00	Fxx	8.81	8.81	1.00
28	U2	14.00	14.00	1.00	Fyy	5651.44	5651.44	1.00
29	U3	3.17	3.17	1.00	Fxy	-111.55	-111.55	1.00
30	U4	3.69	3.69	1.00	Fss	4942.95	4942.95	1.00
31	U5=G/iso	4.39	4.39	1.00	Fx,E-9	-2.51	-2.51	1.00
32	Quasi-isotropic constants				Fy,E-9	77.10	77.10	1.00
33	E,GPa	11.37	11.37	1.00	Gxx	5821	5821	1.00
34	nu	0.30	0.30	1.00	Gyy	14915	14915	1.00
35					Gxy	-464	-464	1.00
36	Density	1.60	1.60	1.00	Gss	7347	7347	1.00
37	rho/m	1.20	1.20	1.00	Gx	-34	-34	1.00
38	rho/f	1.81	1.81	1.00	Gy	125	125	1.00
39								

	R	S	T	U	V	W	X
1	INTACT LAMINATE MODULUS MODULE - elastic and hygrothermal constants						
2							
3	[Angle]	theta/1	theta/2	theta/3	theta/4		
4	[theta]	0.0	90.0	54.5	-54.5	[REPT]	
5	[#/grp]	0.0	0.0	1.0	1.0	67	
6	2X,rad	0.00	3.14	1.90	-1.90	h/r,#	
7	4X,rad	0.00	6.28	3.80	-3.80	2.0	
8							
9	Top z*	1.00	1.00	1.00	0.50		
10	Bott z*	1.00	1.00	0.50	0.00		
11	del(z*)	0.00	0.00	0.50	0.50	h	
12						0.660	
13							
14	Stiff	[Q]/1	[Q]/2	[Q]/3	[Q]/4	[A]	[A*]
15	11	29.63	1.63	5.41	5.41	4E+00	5.41
16	22	1.63	29.63	14.53	14.53	1E+01	14.53
17	21=12	0.52	0.52	6.19	6.19	4E+00	6.19
18	66	1.22	1.22	6.88	6.88	5E+00	6.88
19	61=16	0.00	0.00	4.67	-4.67	0E+00	0.00
20	62=26	0.00	0.00	8.57	-8.57	0E+00	0.00
21					|A|	8E+01	
22	Compl	[a]		[a*]		Ei o	
23	11	5E-01		4E-01		2.78	
24	22	2E-01		1E-01		7.45	
25	21=12	-2E-01		-2E-01		0.43	
26	66	2E-01		1E-01		6.88	
27	61=16	0E+00		0E+00		0.00	
28	62=26	0E+00		0E+00		0.00	
29							
30	Nonmechanical stress and strain					V*/iA	
31	V*/1A	0.00	0.00	-0.16	-0.16	-0.33	
32	V*/3A	0.00	0.00	0.47	-0.47	0.00	
33		p^n /T	p^n /c	sig^n /T	sig^n /c	alpha o	beta o
34	1	1E-05	6E-01	2E-05	8E-01	5E+00	2E-01
35	2	-1E-05	-3E-01	1E-05	5E-01	-1E+00	-4E-02
36	6	sig^n o	eps^n o	0E+00	0E+00	0E+00	0E+00
37	1	5E-04	8E-05	e/x	3E-05		
38	2	8E-04	2E-05	e/y	2E-04		
39	6	0E+00	0E+00	e/s	0E+00		

	AF	AG	AH	AI	AJ	AK
1	STRENGTH ANALYSIS MODULE II -					
2	theta	0.0	90.0	54.5	-54.5	
3	#/group	0.0	0.0	1.0	1.0	
4	2Xtheta	#DIV/0!	#DIV/0!	1.9	-1.9	
5						
6	On-axis mech strains					(p,q,r)^n
7	eps x+	#DIV/0!	#DIV/0!	6.1E-03	6.1E-03	4.9E-05
8	eps y+	#DIV/0!	#DIV/0!	5.0E-03	5.0E-03	3.1E-05
9	eps s+	#DIV/0!	#DIV/0!	3.1E-03	-3.1E-03	0.0E+00
10						
11						
12						
13						
14	a+^m	#DIV/0!	#DIV/0!	6.3E-01	6.3E-01	
15	b+^m	#DIV/0!	#DIV/0!	4.2E-01	4.2E-01	
16	b/2a/+	#DIV/0!	#DIV/0!	3.3E-01	3.3E-01	
17						
18						
19						FPF/mech
20	R+/mech	#DIV/0!	#DIV/0!	0.972	0.972	0.972
21		#########	#########	0.972	0.972	
22	On-axis residu	0.000	0.000	0.972	0.972	
23	eps x^r	#DIV/0!	#DIV/0!	9.3E-06	9.3E-06	
24	eps y^r	#DIV/0!	#DIV/0!	-1.3E-04	-1.3E-04	
25	eps s^r	#DIV/0!	#DIV/0!	-5.9E-05	5.9E-05	
26						
27	a^r	#DIV/0!	#DIV/0!	2.8E-04	2.8E-04	
28	b^r	#DIV/0!	#DIV/0!	-1.7E-02	-1.7E-02	
29	a^r+b^r	#DIV/0!	#DIV/0!	-1.6E-02	-1.6E-02	
30	c^r	#DIV/0!	#DIV/0!	-1.0E+00	-1.0E+00	
31	b^mix/+	#DIV/0!	#DIV/0!	-2.1E-02	-2.1E-02	
32	b^Sum	#DIV/0!	#DIV/0!	4.0E-01	4.0E-01	
33	(b/2a)^Sum	#DIV/0!	#DIV/0!	3.2E-01	3.2E-01	
34						
35						
36						FPF/m+r
37	R+^m+r	#DIV/0!	#DIV/0!	0.994	0.994	9.94E-01
38		#########	#########	0.994	0.994	
39		0.000	0.000	0.994	0.994	

	Y	Z	AA	AB	AC	AD	AE
1	STRENGTH ANALYSIS MODULE I -						
2	theta	0.0	90.0	54.5	-54.5	[r]	[zc]
3	#/group	0.0	0.0	1.0	1.0	67	0.0
4	2Xtheta	#DIV/0!	#DIV/0!	1.9	-1.9	h	7E-01
5							
6	Top laminate loads & strains						
7		Ni,MN/m or kip/in		eps o,E-3		(p,q,r)eps	In-pl
8	1	4.3E+01		3.9E+00		p o	5.5E+00
9	2	8.5E+01		7.2E+00		q o	-1.6E+00
10	6	0.0E+00		0.0E+00		r o	0.0E+00
11							
12	On-axis epsilons						
13	epsx o	#DIV/0!	#DIV/0!	6.1E+00	6.1E+00		
14	epsy o	#DIV/0!	#DIV/0!	5.0E+00	5.0E+00		
15	epss o	#DIV/0!	#DIV/0!	3.1E+00	-3.1E+00		
16							
17							
18							
19							
20		<sig>	p,q,r<sig>	<eps>			
21	1	6.5E+01	9.7E+01	3.9E+00			
22	2	1.3E+02	-3.1E+01	7.2E+00			
23	6	0.0E+00	0.0E+00	0.0E+00			
24	|sig|,|eps|	1.1E+02	3.1E+01	8.2E+00			
25		max |sig|	1.1E+02	max |eps|	8.2E+00	1-4nu+nu^2	
26		|sig| quad	8388.2838	1+nu^2	1.0876793	-0.096749	
27		Q-iso	Al 2024	SS 304	Netting analysis: π/4		
28	E,GPa	11.4	69.0	210.0	[0]	0.00	1
29	X,MPa	56	200	400	[90]	0.00	1
30	rho	1.60	2.70	7.80	[45]	0.00	0
31	R=X/|sig|	0.503	1.801	3.603	[-45]	0.00	0
32	rel rho	1.00	1.69	4.88	# plies	0.00	2
33	eps/iso	9.87E+00	1.67E+00	5.50E-01			
34	rel stiff	1.210	0.205	0.067	Netting analysis: off-axis cross-ply		
35	spec stiff	1.210	0.346	0.329	N I/[0]	8.5E+01	3.382E-05
36	spec R	0.50	1.067	0.739	N II/[90]	4.3E+01	1.726E-05
37					theta/o	0	1.00
38							1.00
39							2

APPENDIX D

TABLE 10 LAMRANK DATA

Absolute laminate stiffness matrix | A B |
| B D |

Intact Materials

0.3628E+07	0.4146E+07	0.4666E+05	0.5127E+00	0.3467E+00	-0.1240E+00
0.4146E+07	0.9733E+07	0.8566E+05	0.3467E+00	0.2363E+00	-0.2285E+00
0.4666E+05	0.8566E+05	0.4612E+07	-0.1240E+00	-0.2285E+00	0.7813E-01
0.5127E+00	0.3467E+00	-0.1240E+00	0.1357E+06	0.1551E+06	0.2618E+04
0.3467E+00	0.2363E+00	-0.2285E+00	0.1551E+06	0.3641E+06	0.4806E+04
-0.1240E+00	-0.2285E+00	0.7813E-01	0.2618E+04	0.4806E+04	0.1725E+06

Degraded Materials

0.2622E+07	0.4284E+07	0.4664E+05	0.2881E+00	0.4014E+00	-0.1216E+00
0.4284E+07	0.8943E+07	0.9034E+05	0.4014E+00	0.7402E+00	-0.2393E+00
0.4664E+05	0.9034E+05	0.4497E+07	-0.1216E+00	-0.2393E+00	0.4443E+00
0.2881E+00	0.4014E+00	-0.1216E+00	0.9809E+05	0.1602E+06	0.2617E+04
0.4014E+00	0.7402E+00	-0.2393E+00	0.1602E+06	0.3345E+06	0.5069E+04
-0.1216E+00	-0.2393E+00	0.4443E+00	0.2617E+04	0.5069E+04	0.1682E+06

Absolute laminate compliance matrix | a b |
| b d |

Intact Materials

0.5371E-06	-0.2288E-06	-0.1185E-08	-0.2008E-11	0.4904E-12	0.1005E-12
-0.2288E-06	0.2002E-06	-0.1404E-08	0.4905E-12	-0.1232E-12	0.9735E-13
-0.1185E-08	-0.1404E-08	0.2169E-06	0.9514E-13	0.9903E-13	-0.1051E-12
-0.2008E-11	0.4905E-12	0.9514E-13	0.1436E-04	-0.6116E-05	-0.4752E-07
0.4904E-12	-0.1232E-12	0.9903E-13	-0.6116E-05	0.5352E-05	-0.5630E-07
0.1005E-12	0.9735E-13	-0.1051E-12	-0.4752E-07	-0.5630E-07	0.5799E-05

Degraded Materials

0.1754E-05	-0.8401E-06	-0.1312E-08	-0.6037E-11	0.2644E-11	0.9042E-13
-0.8401E-06	0.5142E-06	-0.1619E-08	0.2644E-11	-0.1400E-11	0.1295E-12
-0.1312E-08	-0.1619E-08	0.2224E-06	0.8743E-13	0.1314E-12	-0.5959E-12
-0.6037E-11	0.2644E-11	0.8743E-13	0.4688E-04	-0.2246E-04	-0.5261E-07
0.2644E-11	-0.1400E-11	0.1314E-12	-0.2246E-04	0.1375E-04	-0.6491E-07
0.9042E-13	0.1295E-12	-0.5959E-12	-0.5261E-07	-0.6491E-07	0.5947E-05

Normalized laminate stiffness matrix | A* B* | (msi)
| 3B* D* |

Intact Materials

5.4144	6.1877	.0696	0.0000	0.0000	0.0000
6.1877	14.5266	.1278	0.0000	0.0000	0.0000
.0696	.1278	6.8831	0.0000	0.0000	0.0000
0.0000	0.0000	0.0000	5.4144	6.1876	.1045
0.0000	0.0000	0.0000	6.1876	14.5266	.1918
0.0000	0.0000	0.0000	.1045	.1918	6.8831

Degraded Materials

3.9136	6.3934	.0696	0.0000	0.0000	0.0000
6.3934	13.3470	.1348	0.0000	0.0000	0.0000
.0696	.1348	6.7125	0.0000	0.0000	0.0000
0.0000	0.0000	0.0000	3.9136	6.3934	.1044
0.0000	0.0000	0.0000	6.3934	13.3470	.2022
0.0000	0.0000	0.0000	.1044	.2022	6.7125

Normalized laminate compliance matrix | a* b*/3| 1/(10**9 psi)
| b*t d* |

Intact Materials

359.8779	-153.2842	-.7940	-.0002	0.0000	0.0000
-153.2841	134.1394	-.9407	0.0000	0.0000	0.0000
-.7940	-.9407	145.3090	0.0000	0.0000	0.0000
-.0005	.0001	0.0000	359.8839	-153.2781	-1.1911
.0001	0.0000	0.0000	-153.2781	134.1473	-1.4112
0.0000	0.0000	0.0000	-1.1911	-1.4112	145.3413

Degraded Materials

1175.0280	-562.8461	-.8788	-.0005	.0002	0.0000
-562.8461	344.5452	-1.0844	.0002	-.0001	0.0000
-.8788	-1.0844	149.0075	0.0000	0.0000	0.0000
-.0014	.0006	0.0000	1175.0450	-562.8431	-1.3185
.0006	-.0003	0.0000	-562.8432	344.5575	-1.6269
0.0000	0.0000	-.0001	-1.3185	-1.6269	149.0460

Engineering Constants (Intact Materials) (msi)

E1o =	2.7787	E2o =	7.4549	E6o =	6.8819
E1f =	2.7787	E2f =	7.4545	E6f =	6.8804

Coupling Coefficients

Nu21o = .4259	Nu61o = -.0022	Nu62o = -.0070
Nu12o = 1.1427	Nu16o = -.0055	Nu26o = -.0065
Nu21f = .4259	Nu61f = -.0033	Nu62f = -.0105
Nu12f = 1.1426	Nu16f = -.0082	Nu26f = -.0097

Engineering Constants (Degraded Materials) (msi)

E1o =	.8510	E2o =	2.9024	E6o =	6.7111
E1f =	.8510	E2f =	2.9023	E6f =	6.7093

Coupling Coefficients

Nu21o = .4790	Nu61o = -.0007	Nu62o = -.0031
Nu12o = 1.6336	Nu16o = -.0059	Nu26o = -.0073
Nu21f = .4790	Nu61f = -.0011	Nu62f = -.0047
Nu12f = 1.6335	Nu16f = -.0088	Nu26f = -.0109

Load Case No 1 (Intact Materials)

Eps1	Eps2	Eps6	k1	k2	k6
0.1315E-02	0.4994E-03	-0.2601E-04	-0.5633E-08	0.7867E-09	0.1924E-08

Eps1o	Eps2o	Eps6o	Eps1f	Eps2f	Eps6f *E-3
1.3149	.4994	-.0260	0.0000	0.0000	0.0000

N1	N2	N6	M1	M2	M6
0.4300E+04	0.8500E+04	0.0000E+00	0.0000E+00	0.0000E+00	0.0000E+00

Sig1o	Sig2o	Sig6o	Sig1f	Sig2f	Sig6f (ksi)
6.4179	12.6866	.0000	.0000	.0000	.0000

APPENDIX E

TABLE 11 TEXGAP2D ANALYSIS DATA

```
DIRECT LIST OF TRANSLATED DATA

ISO,BULLET, 10,0.250000E+08,0.300000E+00,0.000000E+00,0.165600E-03
END,MATERIALS
POINT,  1,  1,0.000000E+00,0.796000E+02
POINT,  2,  1,0.000000E+00,0.792750E+02
POINT,  3,  1,0.281092E+01,0.794326E+02
POINT,  4,  1,0.000000E+00,0.789500E+02
POINT,  5,  1,0.270272E+01,0.787908E+02
POINT,  6,  1,0.000000E+00,0.786250E+02
POINT,  7,  1,0.000000E+00,0.783000E+02
POINT,  8,  1,0.259453E+01,0.781490E+02
POINT,  9,  1,0.000000E+00,0.779750E+02
POINT, 10,  1,0.000000E+00,0.776500E+02
POINT, 11,  1,0.248754E+01,0.775070E+02
POINT, 12,  1,0.000000E+00,0.770000E+02
POINT, 13,  1,0.000000E+00,0.773250E+02
POINT, 14,  1,0.237929E+01,0.768652E+02
POINT, 15,  1,0.558232E+01,0.789314E+02
POINT, 16,  1,0.547570E+01,0.786227E+02
POINT, 17,  1,0.536907E+01,0.783139E+02
POINT, 18,  1,0.526245E+01,0.780051E+02
POINT, 19,  1,0.515583E+01,0.776964E+02
POINT, 20,  1,0.504920E+01,0.773876E+02
POINT,  1,  2,0.494258E+01,0.770788E+02
POINT,  2,  2,0.472933E+01,0.764613E+02
POINT,  3,  2,0.483596E+01,0.767701E+02
POINT,  4,  2,0.821986E+01,0.781232E+02
POINT,  5,  2,0.790869E+01,0.775445E+02
POINT,  6,  2,0.759869E+01,0.769653E+02
POINT,  7,  2,0.728747E+01,0.763867E+02
POINT,  8,  2,0.697625E+01,0.758080E+02
POINT,  9,  2,0.107465E+02,0.770116E+02
POINT, 10,  2,0.105452E+02,0.767487E+02
POINT, 11,  2,0.103440E+02,0.764858E+02
POINT, 12,  2,0.101428E+02,0.762229E+02
POINT, 13,  2,0.994162E+01,0.759600E+02
POINT, 14,  2,0.974042E+01,0.756971E+02
POINT, 15,  2,0.953921E+01,0.754342E+02
POINT, 16,  2,0.913680E+01,0.749084E+02
POINT, 17,  2,0.933800E+01,0.751713E+02
POINT, 18,  2,0.131115E+02,0.756226E+02
POINT, 19,  2,0.126268E+02,0.751623E+02
POINT, 20,  2,0.121421E+02,0.747019E+02
POINT,  1,  3,0.116574E+02,0.742415E+02
POINT,  2,  3,0.111727E+02,0.737812E+02
POINT,  3,  3,0.152998E+02,0.739691E+02
POINT,  4,  3,0.150213E+02,0.737775E+02
POINT,  5,  3,0.147427E+02,0.735858E+02
POINT,  6,  3,0.144642E+02,0.733942E+02
POINT,  7,  3,0.141857E+02,0.732025E+02
POINT,  8,  3,0.139072E+02,0.730109E+02
POINT,  9,  3,0.136287E+02,0.728192E+02
POINT, 10,  3,0.130716E+02,0.724359E+02
POINT, 11,  3,0.133502E+02,0.726276E+02
POINT, 12,  3,0.172936E+02,0.720602E+02
POINT, 13,  3,0.166753E+02,0.717649E+02
POINT, 14,  3,0.160561E+02,0.714705E+02
```

DIRECT LIST OF TRANSLATED DATA

```
POINT, 11,  6,0.215378E+02,0.614960E+02
POINT, 12,  6,0.202844E+02,0.614355E+02
POINT, 13,  6,0.260000E+02,0.610000E+02
POINT, 14,  6,0.253092E+02,0.609591E+02
POINT, 15,  6,0.246184E+02,0.609182E+02
POINT, 16,  6,0.239276E+02,0.608773E+02
POINT, 17,  6,0.232368E+02,0.608364E+02
POINT, 18,  6,0.225459E+02,0.607955E+02
POINT, 19,  6,0.218551E+02,0.607546E+02
POINT, 20,  6,0.204735E+02,0.606728E+02
POINT,  1,  7,0.211643E+02,0.607137E+02
POINT,  2,  7,0.260000E+02,0.601667E+02
POINT,  3,  7,0.246585E+02,0.601009E+02
POINT,  4,  7,0.233170E+02,0.600351E+02
POINT,  5,  7,0.219755E+02,0.599694E+02
POINT,  6,  7,0.206340E+02,0.599036E+02
POINT,  7,  7,0.260000E+02,0.593333E+02
POINT,  8,  7,0.253457E+02,0.593078E+02
POINT,  9,  7,0.246914E+02,0.592824E+02
POINT, 10,  7,0.240371E+02,0.592569E+02
POINT, 11,  7,0.233828E+02,0.592314E+02
POINT, 12,  7,0.227284E+02,0.592059E+02
POINT, 13,  7,0.220741E+02,0.591804E+02
POINT, 14,  7,0.207655E+02,0.591294E+02
POINT, 15,  7,0.214198E+02,0.591549E+02
POINT, 16,  7,0.260000E+02,0.585000E+02
POINT, 17,  7,0.247170E+02,0.584628E+02
POINT, 18,  7,0.234340E+02,0.584256E+02
POINT, 19,  7,0.221510E+02,0.583884E+02
POINT, 20,  7,0.208680E+02,0.583512E+02
POINT,  1,  8,0.260000E+02,0.576667E+02
POINT,  2,  8,0.253677E+02,0.576545E+02
POINT,  3,  8,0.247353E+02,0.576424E+02
POINT,  4,  8,0.241030E+02,0.576303E+02
POINT,  5,  8,0.234706E+02,0.576182E+02
POINT,  6,  8,0.228383E+02,0.576060E+02
POINT,  7,  8,0.222059E+02,0.575939E+02
POINT,  8,  8,0.209412E+02,0.575697E+02
POINT,  9,  8,0.215736E+02,0.575818E+02
POINT, 10,  8,0.260000E+02,0.568333E+02
POINT, 11,  8,0.247463E+02,0.568214E+02
POINT, 12,  8,0.234926E+02,0.568095E+02
POINT, 13,  8,0.222390E+02,0.567976E+02
POINT, 14,  8,0.209853E+02,0.567856E+02
POINT, 15,  8,0.253750E+02,0.560000E+02
POINT, 16,  8,0.260000E+02,0.560000E+02
POINT, 17,  8,0.247500E+02,0.560000E+02
POINT, 18,  8,0.241250E+02,0.560000E+02
POINT, 19,  8,0.235000E+02,0.560000E+02
POINT, 20,  8,0.228750E+02,0.560000E+02
POINT,  1,  9,0.222500E+02,0.560000E+02
POINT,  2,  9,0.210000E+02,0.560000E+02
POINT,  3,  9,0.216250E+02,0.560000E+02
POINT,  4,  9,0.247500E+02,0.553333E+02
POINT,  5,  9,0.260000E+02,0.553333E+02
POINT,  6,  9,0.263333E+02,0.560000E+02
```

DIRECT LIST OF TRANSLATED DATA

```
POINT, 15,  3,0.154378E+02,0.711751E+02
POINT, 16,  3,0.148196E+02,0.708797E+02
POINT, 17,  3,0.190497E+02,0.699328E+02
POINT, 18,  3,0.187164E+02,0.698335E+02
POINT, 19,  3,0.183830E+02,0.697343E+02
POINT, 20,  3,0.180497E+02,0.696350E+02
POINT,  1,  4,0.177164E+02,0.695358E+02
POINT,  2,  4,0.173831E+02,0.694365E+02
POINT,  3,  4,0.170497E+02,0.693372E+02
POINT,  4,  4,0.163831E+02,0.691387E+02
POINT,  5,  4,0.167164E+02,0.692380E+02
POINT,  6,  4,0.205733E+02,0.675641E+02
POINT,  7,  4,0.198718E+02,0.674720E+02
POINT,  8,  4,0.191703E+02,0.673799E+02
POINT,  9,  4,0.184681E+02,0.672888E+02
POINT, 10,  4,0.177666E+02,0.671966E+02
POINT, 11,  4,0.218036E+02,0.650312E+02
POINT, 12,  4,0.214432E+02,0.650412E+02
POINT, 13,  4,0.210828E+02,0.650513E+02
POINT, 14,  4,0.207224E+02,0.650613E+02
POINT, 15,  4,0.203620E+02,0.650713E+02
POINT, 16,  4,0.200016E+02,0.650814E+02
POINT, 17,  4,0.196412E+02,0.650914E+02
POINT, 18,  4,0.189204E+02,0.651115E+02
POINT, 19,  4,0.192808E+02,0.651014E+02
POINT, 20,  4,0.225030E+02,0.643593E+02
POINT,  1,  5,0.216893E+02,0.643688E+02
POINT,  2,  5,0.208745E+02,0.643796E+02
POINT,  3,  5,0.200610E+02,0.643891E+02
POINT,  4,  5,0.192480E+02,0.643972E+02
POINT,  5,  5,0.232024E+02,0.636875E+02
POINT,  6,  5,0.227457E+02,0.636855E+02
POINT,  7,  5,0.222889E+02,0.636835E+02
POINT,  8,  5,0.218322E+02,0.636816E+02
POINT,  9,  5,0.213755E+02,0.636796E+02
POINT, 10,  5,0.209187E+02,0.636776E+02
POINT, 11,  5,0.204620E+02,0.636757E+02
POINT, 12,  5,0.195485E+02,0.636717E+02
POINT, 13,  5,0.200053E+02,0.636737E+02
POINT, 14,  5,0.239018E+02,0.630156E+02
POINT, 15,  5,0.228806E+02,0.629970E+02
POINT, 16,  5,0.218608E+02,0.629771E+02
POINT, 17,  5,0.208409E+02,0.629571E+02
POINT, 18,  5,0.198216E+02,0.629357E+02
POINT, 19,  5,0.246012E+02,0.623437E+02
POINT, 20,  5,0.240344E+02,0.623245E+02
POINT,  1,  6,0.234676E+02,0.623053E+02
POINT,  2,  6,0.229009E+02,0.622861E+02
POINT,  3,  6,0.223341E+02,0.622669E+02
POINT,  4,  6,0.217673E+02,0.622477E+02
POINT,  5,  6,0.212005E+02,0.622285E+02
POINT,  6,  6,0.200670E+02,0.621901E+02
POINT,  7,  6,0.206337E+02,0.622093E+02
POINT,  8,  6,0.253006E+02,0.616719E+02
POINT,  9,  6,0.240454E+02,0.616141E+02
POINT, 10,  6,0.227916E+02,0.615551E+02
```

DIRECT LIST OF TRANSLATED DATA

```
POINT,  7,  9,0.266667E+02,0.560000E+02
POINT,  8,  9,0.266667E+02,0.553333E+02
POINT,  9,  9,0.235000E+02,0.553333E+02
POINT, 10,  9,0.222500E+02,0.553333E+02
POINT, 11,  9,0.210000E+02,0.553333E+02
POINT, 12,  9,0.270000E+02,0.560000E+02
POINT, 13,  9,0.273333E+02,0.560000E+02
POINT, 14,  9,0.273333E+02,0.553333E+02
POINT, 15,  9,0.280000E+02,0.560000E+02
POINT, 16,  9,0.276667E+02,0.560000E+02
POINT, 17,  9,0.280000E+02,0.553333E+02
POINT, 18,  9,0.280000E+02,0.546667E+02
POINT, 19,  9,0.276667E+02,0.546667E+02
POINT, 20,  9,0.280000E+02,0.540000E+02
POINT,  1, 10,0.280000E+02,0.533333E+02
POINT,  2, 10,0.276667E+02,0.533333E+02
POINT,  3, 10,0.280000E+02,0.520000E+02
POINT,  4, 10,0.276667E+02,0.520000E+02
POINT,  5, 10,0.280000E+02,0.526667E+02
POINT,  6, 10,0.253750E+02,0.546667E+02
POINT,  7, 10,0.247500E+02,0.546667E+02
POINT,  8, 10,0.260000E+02,0.546667E+02
POINT,  9, 10,0.263333E+02;0.546667E+02
POINT, 10, 10,0.266667E+02,0.546667E+02
POINT, 11, 10,0.241250E+02,0.546667E+02
POINT, 12, 10,0.235000E+02,0.546667E+02
POINT, 13, 10,0.228750E+02,0.546667E+02
POINT, 14, 10,0.222500E+02,0.546667E+02
POINT, 15, 10,0.210000E+02,0.546667E+02
POINT, 16, 10,0.216250E+02,0.546667E+02
POINT, 17, 10,0.270000E+02,0.546667E+02
POINT, 18, 10,0.273333E+02,0.546667E+02
POINT, 19, 10,0.273333E+02,0.540000E+02
POINT, 20, 10,0.273333E+02,0.533333E+02
POINT,  1, 11,0.273333E+02,0.520000E+02
POINT,  2, 11,0.273333E+02,0.526667E+02
POINT,  3, 11,0.247500E+02,0.540000E+02
POINT,  4, 11,0.260000E+02,0.540000E+02
POINT,  5, 11,0.235000E+02,0.540000E+02
POINT,  6, 11,0.266667E+02,0.540000E+02
POINT,  7, 11,0.270000E+02,0.533333E+02
POINT,  8, 11,0.222500E+02,0.540000E+02
POINT,  9, 11,0.210000E+02,0.540000E+02
POINT, 10, 11,0.270000E+02,0.520000E+02
POINT, 11, 11,0.253750E+02,0.533333E+02
POINT, 12, 11,0.247500E+02,0.533333E+02
POINT, 13, 11,0.260000E+02,0.533333E+02
POINT, 14, 11,0.241250E+02,0.533333E+02
POINT, 15, 11,0.235000E+02,0.533333E+02
POINT, 16, 11,0.263333E+02,0.533333E+02
POINT, 17, 11,0.266667E+02,0.533333E+02
POINT, 18, 11,0.228750E+02,0.533333E+02
POINT, 19, 11,0.222500E+02,0.533333E+02
POINT, 20, 11,0.210000E+02,0.533333E+02
POINT,  1, 12,0.216250E+02,0.533333E+02
POINT,  2, 12,0.266667E+02,0.520000E+02
```

DIRECT LIST OF TRANSLATED DATA

```
POINT,  3, 12,0.266667E+02,0.526667E+02
POINT,  4, 12,0.247500E+02,0.526667E+02
POINT,  5, 12,0.260000E+02,0.526667E+02
POINT,  6, 12,0.235000E+02,0.526667E+02
POINT,  7, 12,0.263333E+02,0.520000E+02
POINT,  8, 12,0.222500E+02,0.526667E+02
POINT,  9, 12,0.210000E+02,0.526667E+02
POINT, 10, 12,0.253750E+02,0.520000E+02
POINT, 11, 12,0.260000E+02,0.520000E+02
POINT, 12, 12,0.247500E+02,0.520000E+02
POINT, 13, 12,0.241250E+02,0.520000E+02
POINT, 14, 12,0.235000E+02,0.520000E+02
POINT, 15, 12,0.228750E+02,0.520000E+02
POINT, 16, 12,0.222500E+02,0.520000E+02
POINT, 17, 12,0.210000E+02,0.520000E+02
POINT, 18, 12,0.216250E+02,0.520000E+02
POINT, 19, 12,0.260000E+02,0.493333E+02
POINT, 20, 12,0.247500E+02,0.493333E+02
POINT,  1, 13,0.235000E+02,0.493333E+02
POINT,  2, 13,0.222500E+02,0.493333E+02
POINT,  3, 13,0.210000E+02,0.493333E+02
POINT,  4, 13,0.260000E+02,0.466667E+02
POINT,  5, 13,0.253750E+02,0.466667E+02
POINT,  6, 13,0.247500E+02,0.466667E+02
POINT,  7, 13,0.241250E+02,0.466667E+02
POINT,  8, 13,0.235000E+02,0.466667E+02
POINT,  9, 13,0.228750E+02,0.466667E+02
POINT, 10, 13,0.222500E+02,0.466667E+02
POINT, 11, 13,0.210000E+02,0.466667E+02
POINT, 12, 13,0.216250E+02,0.466667E+02
POINT, 13, 13,0.260000E+02,0.440000E+02
POINT, 14, 13,0.247500E+02,0.440000E+02
POINT, 15, 13,0.235000E+02,0.440000E+02
POINT, 16, 13,0.222500E+02,0.440000E+02
POINT, 17, 13,0.210000E+02,0.440000E+02
POINT, 18, 13,0.260000E+02,0.413333E+02
POINT, 19, 13,0.253750E+02,0.413333E+02
POINT, 20, 13,0.247500E+02,0.413333E+02
POINT,  1, 14,0.241250E+02,0.413333E+02
POINT,  2, 14,0.235000E+02,0.413333E+02
POINT,  3, 14,0.228750E+02,0.413333E+02
POINT,  4, 14,0.222500E+02,0.413333E+02
POINT,  5, 14,0.210000E+02,0.413333E+02
POINT,  6, 14,0.216250E+02,0.413333E+02
POINT,  7, 14,0.260000E+02,0.386667E+02
POINT,  8, 14,0.247500E+02,0.386667E+02
POINT,  9, 14,0.235000E+02,0.386667E+02
POINT, 10, 14,0.222500E+02,0.386667E+02
POINT, 11, 14,0.210000E+02,0.386667E+02
POINT, 12, 14,0.260000E+02,0.360000E+02
POINT, 13, 14,0.253750E+02,0.360000E+02
POINT, 14, 14,0.247500E+02,0.360000E+02
POINT, 15, 14,0.241250E+02,0.360000E+02
POINT, 16, 14,0.235000E+02,0.360000E+02
POINT, 17, 14,0.228750E+02,0.360000E+02
POINT, 18, 14,0.222500E+02,0.360000E+02
```

DIRECT LIST OF TRANSLATED DATA

```
POINT, 19, 14,0.210000E+02,0.360000E+02
POINT, 20, 14,0.216250E+02,0.360000E+02
POINT,  1, 15,0.260000E+02,0.333333E+02
POINT,  2, 15,0.247500E+02,0.333333E+02
POINT,  3, 15,0.235000E+02,0.333333E+02
POINT,  4, 15,0.222500E+02,0.333333E+02
POINT,  5, 15,0.210000E+02,0.333333E+02
POINT,  6, 15,0.260000E+02,0.306667E+02
POINT,  7, 15,0.253750E+02,0.306667E+02
POINT,  8, 15,0.247500E+02,0.306667E+02
POINT,  9, 15,0.241250E+02,0.306667E+02
POINT, 10, 15,0.235000E+02,0.306667E+02
POINT, 11, 15,0.228750E+02,0.306667E+02
POINT, 12, 15,0.222500E+02,0.306667E+02
POINT, 13, 15,0.210000E+02,0.306667E+02
POINT, 14, 15,0.216250E+02,0.306667E+02
POINT, 15, 15,0.260000E+02,0.280000E+02
POINT, 16, 15,0.247500E+02,0.280000E+02
POINT, 17, 15,0.235000E+02,0.280000E+02
POINT, 18, 15,0.222500E+02,0.280000E+02
POINT, 19, 15,0.210000E+02,0.280000E+02
POINT, 20, 15,0.260000E+02,0.253333E+02
POINT,  1, 16,0.253750E+02,0.253333E+02
POINT,  2, 16,0.247500E+02,0.253333E+02
POINT,  3, 16,0.241250E+02,0.253333E+02
POINT,  4, 16,0.235000E+02,0.253333E+02
POINT,  5, 16,0.228750E+02,0.253333E+02
POINT,  6, 16,0.222500E+02,0.253333E+02
POINT,  7, 16,0.210000E+02,0.253333E+02
POINT,  8, 16,0.216250E+02,0.253333E+02
POINT,  9, 16,0.260000E+02,0.226667E+02
POINT, 10, 16,0.247500E+02,0.226667E+02
POINT, 11, 16,0.235000E+02,0.226667E+02
POINT, 12, 16,0.222500E+02,0.226667E+02
POINT, 13, 16,0.210000E+02,0.226667E+02
POINT, 14, 16,0.260000E+02,0.200000E+02
POINT, 15, 16,0.253750E+02,0.200000E+02
POINT, 16, 16,0.247500E+02,0.200000E+02
POINT, 17, 16,0.241250E+02,0.200000E+02
POINT, 18, 16,0.235000E+02,0.200000E+02
POINT, 19, 16,0.228750E+02,0.200000E+02
POINT, 20, 16,0.222500E+02,0.200000E+02
POINT,  1, 17,0.210000E+02,0.200000E+02
POINT,  2, 17,0.216250E+02,0.200000E+02
POINT,  3, 17,0.260000E+02,0.173333E+02
POINT,  4, 17,0.247500E+02,0.173333E+02
POINT,  5, 17,0.235000E+02,0.173333E+02
POINT,  6, 17,0.222500E+02,0.173333E+02
POINT,  7, 17,0.210000E+02,0.173333E+02
POINT,  8, 17,0.280000E+02,0.400000E+01
POINT,  9, 17,0.280000E+02,0.333334E+01
POINT, 10, 17,0.276667E+02,0.400000E+01
POINT, 11, 17,0.280000E+02,0.266666E+01
POINT, 12, 17,0.276667E+02,0.266666E+01
POINT, 13, 17,0.280000E+02,0.200000E+01
POINT, 14, 17,0.280000E+02,0.133334E+01
```

DIRECT LIST OF TRANSLATED DATA

```
POINT, 15, 17,0.276667E+02,0.133334E+01
POINT, 16, 17,0.280000E+02,0.000000E+00
POINT, 17, 17,0.276667E+02,0.000000E+00
POINT, 18, 17,0.280000E+02,0.666664E+00
POINT, 19, 17,0.260000E+02,0.146667E+02
POINT, 20, 17,0.253750E+02,0.146667E+02
POINT,  1, 18,0.247500E+02,0.146667E+02
POINT,  2, 18,0.241250E+02,0.146667E+02
POINT,  3, 18,0.235000E+02,0.146667E+02
POINT,  4, 18,0.228750E+02,0.146667E+02
POINT,  5, 18,0.222500E+02,0.146667E+02
POINT,  6, 18,0.210000E+02,0.146667E+02
POINT,  7, 18,0.216250E+02,0.146667E+02
POINT,  8, 18,0.273333E+02,0.400000E+01
POINT,  9, 18,0.273333E+02,0.333334E+01
POINT, 10, 18,0.273333E+02,0.266666E+01
POINT, 11, 18,0.273333E+02,0.200000E+01
POINT, 12, 18,0.273333E+02,0.133334E+01
POINT, 13, 18,0.273333E+02,0.000000E+00
POINT, 14, 18,0.273333E+02,0.666664E+00
POINT, 15, 18,0.260000E+02,0.120000E+02
POINT, 16, 18,0.247500E+02,0.120000E+02
POINT, 17, 18,0.235000E+02,0.120000E+02
POINT, 18, 18,0.222500E+02,0.120000E+02
POINT, 19, 18,0.210000E+02,0.120000E+02
POINT, 20, 18,0.270000E+02,0.400000E+01
POINT,  1, 19,0.270000E+02,0.266666E+01
POINT,  2, 19,0.270000E+02,0.133334E+01
POINT,  3, 19,0.270000E+02,0.000000E+00
POINT,  4, 19,0.260000E+02,0.933333E+01
POINT,  5, 19,0.253750E+02,0.933333E+01
POINT,  6, 19,0.247500E+02,0.933333E+01
POINT,  7, 19,0.241250E+02,0.933333E+01
POINT,  8, 19,0.235000E+02,0.933332E+01
POINT,  9, 19,0.228750E+02,0.933332E+01
POINT, 10, 19,0.222500E+02,0.933333E+01
POINT, 11, 19,0.210000E+02,0.933333E+01
POINT, 12, 19,0.216250E+02,0.933333E+01
POINT, 13, 19,0.266667E+02,0.400000E+01
POINT, 14, 19,0.266667E+02,0.333334E+01
POINT, 15, 19,0.266667E+02,0.266666E+01
POINT, 16, 19,0.266667E+02,0.200000E+01
POINT, 17, 19,0.266667E+02,0.133334E+01
POINT, 18, 19,0.266667E+02,0.000000E+00
POINT, 19, 19,0.266667E+02,0.666664E+00
POINT, 20, 19,0.260000E+02,0.666666E+01
POINT,  1, 20,0.247500E+02,0.666666E+01
POINT,  2, 20,0.235000E+02,0.666666E+01
POINT,  3, 20,0.222500E+02,0.666666E+01
POINT,  4, 20,0.210000E+02,0.666666E+01
POINT,  5, 20,0.263333E+02,0.400000E+01
POINT,  6, 20,0.263333E+02,0.266666E+01
POINT,  7, 20,0.263333E+02,0.133334E+01
POINT,  8, 20,0.263333E+02,0.000000E+00
POINT,  9, 20,0.253750E+02,0.400000E+01
POINT, 10, 20,0.260000E+02,0.400000E+01
```

DIRECT LIST OF TRANSLATED DATA

```
POINT, 11, 20,0.247500E+02,0.400000E+01
POINT, 12, 20,0.241250E+02,0.400000E+01
POINT, 13, 20,0.235000E+02,0.400000E+01
POINT, 14, 20,0.228750E+02,0.400000E+01
POINT, 15, 20,0.222500E+02,0.400000E+01
POINT, 16, 20,0.210000E+02,0.400000E+01
POINT, 17, 20,0.216250E+02,0.400000E+01
POINT, 18, 20,0.260000E+02,0.333334E+01
POINT, 19, 20,0.260000E+02,0.266666E+01
POINT, 20, 20,0.260000E+02,0.200000E+01
POINT,  1, 21,0.260000E+02,0.133334E+01
POINT,  2, 21,0.260000E+02,0.000000E+00
POINT,  3, 21,0.260000E+02,0.666664E+00
POINT,  4, 21,0.247500E+02,0.333334E+01
POINT,  5, 21,0.253750E+02,0.266666E+01
POINT,  6, 21,0.235000E+02,0.333334E+01
POINT,  7, 21,0.222500E+02,0.333334E+01
POINT,  8, 21,0.210000E+02,0.333334E+01
POINT,  9, 21,0.253750E+02,0.133334E+01
POINT, 10, 21,0.253750E+02,0.000000E+00
POINT, 11, 21,0.247500E+02,0.266666E+01
POINT, 12, 21,0.241250E+02,0.266666E+01
POINT, 13, 21,0.235000E+02,0.266666E+01
POINT, 14, 21,0.228750E+02,0.266666E+01
POINT, 15, 21,0.222500E+02,0.266666E+01
POINT, 16, 21,0.210000E+02,0.266666E+01
POINT, 17, 21,0.216250E+02,0.266666E+01
POINT, 18, 21,0.247500E+02,0.200000E+01
POINT, 19, 21,0.247500E+02,0.133334E+01
POINT, 20, 21,0.247500E+02,0.000000E+00
POINT,  1, 22,0.247500E+02,0.666664E+00
POINT,  2, 22,0.235000E+02,0.200000E+01
POINT,  3, 22,0.241250E+02,0.133334E+01
POINT,  4, 22,0.222500E+02,0.200000E+01
POINT,  5, 22,0.210000E+02,0.200000E+01
POINT,  6, 22,0.210000E+02,0.133334E+01
POINT,  7, 22,0.216250E+02,0.133334E+01
POINT,  8, 22,0.241250E+02,0.000000E+00
POINT,  9, 22,0.210000E+02,0.000000E+00
POINT, 10, 22,0.210000E+02,0.666664E+00
POINT, 11, 22,0.216250E+02,0.000000E+00
POINT, 12, 22,0.235000E+02,0.133334E+01
POINT, 13, 22,0.228750E+02,0.133334E+01
POINT, 14, 22,0.222500E+02,0.133334E+01
POINT, 15, 22,0.235000E+02,0.000000E+00
POINT, 16, 22,0.235000E+02,0.666664E+00
POINT, 17, 22,0.222500E+02,0.000000E+00
POINT, 18, 22,0.222500E+02,0.666664E+00
POINT, 19, 22,0.228750E+02,0.000000E+00
END,GRID
QQ,CS24,BULLET,  1,  1,  4,  1, 17,  1, 15,  1,  2,  1,  5,  1, 16,  1,  3,  1
QQ,CS24,BULLET,  4,  1,  7,  1, 19,  1, 17,  1,  6,  1,  8,  1, 18,  1,  5,  1
QQ,CS24,BULLET,  7,  1, 10,  1,  1,  2, 19,  1,  9,  1, 11,  1, 20,  1,  3,  1
QQ,CS24,BULLET, 10,  1, 12,  1,  2,  2,  1,  2, 13,  1, 14,  1,  3,  2, 11,  1
QQ,CS24,BULLET, 15,  1, 17,  1, 11,  2,  9,  2, 16,  1,  5,  2, 10,  2,  4,  2
QQ,CS24,BULLET, 17,  1, 19,  1, 13,  2, 11,  2, 18,  1,  6,  2, 12,  2,  5,  2
```

DIRECT LIST OF TRANSLATED DATA

```
QQ,CS24,BULLET, 19,  1,  1,  2, 15,  2, 13,  2, 20,  1,  7,  2, 14,  2,  6,  2
QQ,CS24,BULLET,  1,  2,  2,  2, 16,  2, 15,  2,  3,  2,  8,  2, 17,  2,  7,  2
QQ,CS24,BULLET,  9,  2, 11,  2,  5,  3,  3,  3, 10,  2, 19,  2,  4,  3, 18,  2
QQ,CS24,BULLET, 11,  2, 13,  2,  7,  3,  5,  3, 12,  2, 20,  2,  6,  3, 19,  2
QQ,CS24,BULLET, 13,  2, 15,  2,  9,  3,  7,  3, 14,  2,  1,  3,  8,  3, 20,  2
QQ,CS24,BULLET, 15,  2, 16,  2, 10,  3,  9,  3, 17,  2,  2,  3, 11,  3,  1,  3
QQ,CS24,BULLET,  3,  3,  5,  3, 19,  3, 17,  3,  4,  3, 13,  3, 18,  3, 12,  3
QQ,CS24,BULLET,  5,  3,  7,  3,  1,  4, 19,  3,  6,  3, 14,  3, 20,  3, 13,  3
QQ,CS24,BULLET,  7,  3,  9,  3,  3,  4,  1,  4,  8,  3, 15,  3,  2,  4, 14,  3
QQ,CS24,BULLET,  9,  3, 10,  3,  4,  4,  3,  4, 11,  3, 16,  3,  5,  4, 15,  3
QQ,CS24,BULLET, 17,  3, 19,  3, 13,  4, 11,  4, 18,  3,  7,  4, 12,  4,  6,  4
QQ,CS24,BULLET, 19,  3,  1,  4, 15,  4, 13,  4, 20,  3,  8,  4, 14,  4,  7,  4
QQ,CS24,BULLET,  1,  4,  3,  4, 17,  4, 15,  4,  2,  4,  9,  4, 16,  4,  3,  4
QQ,CS24,BULLET,  3,  4,  4,  4, 18,  4, 17,  4,  5,  4, 10,  4, 19,  4,  9,  4
QQ,CS24,BULLET, 11,  4, 13,  4,  7,  5,  5,  5, 12,  4,  1,  5,  6,  5, 20,  4
QQ,CS1234,BULLET, 13,  4, 15,  4,  9,  5,  7,  5, 14,  4,  2,  5,  8,  5,  1,  5
!
QQ,CS234,BULLET, 15,  4, 17,  4, 11,  5,  9,  5, 16,  4,  3,  5, 10,  5,  2,  5
QQ,CS1234,BULLET, 17,  4, 18,  4, 12,  5, 11,  5, 19,  4,  4,  5, 13,  5,  3,  5
!
QQ,CS234,BULLET,  5,  5,  7,  5,  1,  6, 19,  5,  6,  5, 15,  5, 20,  5, 14,  5
QQ,CS1234,BULLET,  7,  5,  9,  5,  3,  6,  1,  6,  8,  5, 16,  5,  2,  6, 15,  5
!
QQ,CS1234,BULLET,  9,  5, 11,  5,  5,  6,  3,  6, 10,  5, 17,  5,  4,  6, 16,  5
!
QQ,CS1234,BULLET, 11,  5, 12,  5,  6,  6,  5,  6, 13,  5, 18,  5,  7,  6, 17,  5
!
QQ,CS1234,BULLET, 19,  5,  1,  6, 15,  6, 13,  6, 20,  5,  9,  6, 14,  6,  8,  6
!
QQ,CS1234,BULLET,  1,  6,  3,  6, 17,  6, 15,  6,  2,  6, 10,  6, 16,  6,  9,  6
!
QQ,CS124,BULLET,  3,  6,  5,  6, 19,  6, 17,  6,  4,  6, 11,  6, 18,  6, 10,  6
QQ,CS124,BULLET,  5,  6,  6,  6, 20,  6, 19,  6,  7,  6, 12,  6,  1,  7, 11,  6
QQ,CS123,BULLET, 13,  6, 15,  6,  9,  7,  7,  7, 14,  6,  3,  7,  8,  7,  2,  7
QQ,CS1234,BULLET, 15,  6, 17,  6, 11,  7,  9,  7, 16,  6,  4,  7, 10,  7,  3,  7
!
QQ,CS24,BULLET, 17,  6, 19,  6, 13,  7, 11,  7, 18,  6,  5,  7, 12,  7,  4,  7
QQ,CS234,BULLET, 19,  6, 20,  6, 14,  7, 13,  7,  1,  7,  6,  7, 15,  7,  5,  7
QQ,CS12,BULLET,  7,  7,  9,  7,  3,  8,  1,  8,  8,  7, 17,  7,  2,  8, 16,  7
QQ,CS124,BULLET,  9,  7, 11,  7,  5,  8,  3,  8, 10,  7, 18,  7,  4,  8, 17,  7
QQ,CS24,BULLET, 11,  7, 13,  7,  7,  8,  5,  8, 12,  7, 19,  7,  6,  8, 18,  7
QQ,CS1234,BULLET, 13,  7, 14,  7,  8,  8,  7,  8, 15,  7, 20,  7,  9,  8, 19,  7
!
QQ,CS2,BULLET,  1,  8,  3,  8, 17,  8, 16,  8,  2,  8, 11,  8, 15,  8, 10,  8
QQ,CS24,BULLET,  3,  8,  5,  8, 19,  8, 17,  8,  4,  8, 12,  8, 18,  8, 11,  8
QQ,CS24,BULLET,  5,  8,  7,  8,  1,  9, 19,  8,  6,  8, 13,  8, 20,  8, 12,  8
QQ,CS1234,BULLET,  7,  8,  8,  8,  2,  9,  1,  9,  9,  8, 14,  8,  3,  9, 13,  8
!
QQ,,BULLET, 11, 12, 12, 12,  6, 13,  4, 13, 10, 12, 20, 12,  5, 13, 19, 12
QQ,,BULLET, 12, 12, 14, 12,  8, 13,  6, 13, 13, 12,  1, 13,  7, 13, 20, 12
QQ,,BULLET, 14, 12, 16, 12, 10, 13,  8, 13, 15, 12,  2, 13,  9, 13,  1, 13
QQ,,BULLET, 16, 12, 17, 12, 11, 13, 10, 13, 18, 12,  3, 13, 12, 13,  2, 13
QQ,,BULLET,  4, 13,  6, 13, 20, 13, 18, 13,  5, 13, 14, 13, 19, 13, 13, 13
QQ,,BULLET,  6, 13,  8, 13,  2, 14, 20, 13,  7, 13, 15, 13,  1, 14, 14, 13
QQ,,BULLET,  8, 13, 10, 13,  4, 14,  2, 14,  9, 13, 16, 13,  3, 14, 15, 13
QQ,,BULLET, 10, 13, 11, 13,  5, 14,  4, 14, 12, 13, 17, 13,  6, 14, 16, 13
QQ,,BULLET, 18, 13, 20, 13, 14, 14, 12, 14, 19, 13,  8, 14, 13, 14,  7, 14
QQ,,BULLET, 20, 13,  2, 14, 16, 14, 14, 14,  1, 14,  9, 14, 15, 14,  8, 14
QQ,,BULLET,  2, 14,  4, 14, 18, 14, 16, 14,  3, 14, 10, 14, 17, 14,  9, 14
QQ,,BULLET,  4, 14,  5, 14, 19, 14, 18, 14,  6, 14, 11, 14, 20, 14, 10, 14
QQ,,BULLET, 12, 14, 14, 14,  8, 15,  6, 15, 13, 14,  2, 15,  7, 15,  1, 15
QQ,,BULLET, 14, 14, 16, 14, 10, 15,  8, 15, 15, 14,  3, 15,  9, 15,  2, 15
QQ,,BULLET, 16, 14, 18, 14, 12, 15, 10, 15, 17, 14,  4, 15, 11, 15,  3, 15
QQ,,BULLET, 18, 14, 19, 14, 13, 15, 12, 15, 20, 14,  5, 15, 14, 15,  4, 15
```

```
QQ,,BULLET,  6, 15,  8, 15,  2, 16, 20, 15,  7, 15, 16, 15,  1, 16, 15, 15
QQ,,BULLET,  8, 15, 10, 15,  4, 16,  2, 16,  9, 15, 17, 15,  3, 16, 16, 15
QQ,,BULLET, 10, 15, 12, 15,  6, 16,  4, 16, 11, 15, 18, 15,  5, 16, 17, 15
QQ,,BULLET, 12, 15, 13, 15,  7, 16,  6, 16, 14, 15, 19, 15,  8, 16, 18, 15
QQ,,BULLET, 20, 15,  2, 16, 16, 16, 14, 16,  1, 16, 10, 16, 15, 16,  9, 16
QQ,,BULLET,  2, 16,  4, 16, 18, 16, 16, 16,  3, 16, 11, 16, 17, 16, 10, 16
QQ,,BULLET,  4, 16,  6, 16, 20, 16, 18, 16,  5, 16, 12, 16, 19, 16, 11, 16
```

DIRECT LIST OF TRANSLATED DATA

```
QQ,,BULLET,  6, 16,  7, 16,  1, 17, 20, 16,  8, 16, 13, 16,  2, 17, 12, 16
QQ,,BULLET, 14, 16, 16, 16,  1, 18, 19, 17, 15, 16,  4, 17, 20, 17,  3, 17
QQ,,BULLET, 16, 16, 18, 16,  3, 18,  1, 18, 17, 16,  5, 17,  2, 18,  4, 17
QQ,,BULLET, 18, 16, 20, 16,  5, 18,  3, 18, 19, 16,  6, 17,  4, 18,  5, 17
QQ,,BULLET, 20, 16,  1, 17,  6, 18,  5, 18,  2, 17,  7, 17,  7, 18,  6, 17
QQ,,BULLET, 19, 17,  1, 18,  6, 19,  4, 19, 20, 17, 16, 18,  5, 19, 15, 18
QQ,,BULLET,  1, 18,  3, 18,  8, 19,  6, 19,  2, 18, 17, 18,  7, 19, 16, 18
QQ,,BULLET,  3, 18,  5, 18, 10, 19,  8, 19,  4, 18, 18, 18,  9, 19, 17, 18
QQ,,BULLET,  5, 18,  6, 18, 11, 19, 10, 19,  7, 18, 19, 18, 12, 19, 18, 18
QQ,,BULLET,  4, 19,  6, 19, 11, 20, 10, 20,  5, 19,  1, 20,  9, 20, 20, 19
QQ,,BULLET,  6, 19,  8, 19, 13, 20, 11, 20,  7, 19,  2, 20, 12, 20,  1, 20
QQ,,BULLET,  8, 19, 10, 19, 15, 20, 13, 20,  9, 19,  3, 20, 14, 20,  2, 20
QQ,,BULLET, 10, 19, 11, 19, 16, 20, 15, 20, 12, 19,  4, 20, 17, 20,  3, 20
QQ,,BULLET, 10, 20, 11, 20, 11, 21, 19, 20,  9, 20,  4, 21,  5, 21, 18, 20
QQ,,BULLET, 11, 20, 13, 20, 13, 21, 11, 21, 12, 20,  6, 21, 12, 21,  4, 21
QQ,,BULLET, 13, 20, 15, 20, 15, 21, 13, 21, 14, 20,  7, 21, 14, 21,  6, 21
QQ,,BULLET, 15, 20, 16, 20, 16, 21, 15, 21, 17, 20,  8, 21, 17, 21,  7, 21
QQ,,BULLET, 19, 20, 11, 21, 19, 21,  1, 21,  5, 21, 18, 21,  9, 21, 20, 20
QQ,,BULLET, 11, 21, 13, 21, 12, 22, 19, 21, 12, 21,  2, 22,  3, 22, 18, 21
QQ,,BULLET, 13, 21, 15, 21, 14, 22, 12, 22, 14, 21,  4, 22, 13, 22,  2, 22
QQ,,BULLET, 15, 21, 16, 21,  6, 22, 14, 22, 17, 21,  5, 22,  7, 22,  4, 22
QQ,,BULLET,  1, 21, 19, 21, 20, 21,  2, 21,  9, 21,  1, 22, 10, 21,  3, 21
QQ,,BULLET, 19, 21, 12, 22, 15, 22, 20, 21,  3, 22, 16, 22,  8, 22,  1, 22
QQ,,BULLET, 12, 22, 14, 22, 17, 22, 15, 22, 13, 22, 18, 22, 19, 22, 16, 22
QQ,,BULLET, 14, 22,  6, 22,  9, 22, 17, 22,  7, 22, 10, 22, 11, 22, 18, 22
QQ,,BULLET, 16,  8, 17,  8,  7, 10,  8, 10, 15,  8,  4,  9,  6, 10,  5,  9
QQ,,BULLET, 17,  8, 19,  8, 12, 10,  7, 10, 18,  8,  9,  9, 11, 10,  4,  9
QQ,,BULLET, 19,  8,  1,  9, 14, 10, 12, 10, 20,  8, 10,  9, 13, 10,  9,  9
QQ,CS13,BULLET,  1,  9,  2,  9, 15, 10, 14, 10,  3,  9, 11,  9, 16, 10, 10,  9
QQ,,BULLET,  8, 10,  7, 10, 12, 11, 13, 11,  6, 10,  3, 11, 11, 11,  4, 11
QQ,,BULLET,  7, 10, 12, 10, 15, 11, 12, 11, 11, 10,  5, 11, 14, 11,  3, 11
QQ,,BULLET, 12, 10, 14, 10, 19, 11, 15, 11, 13, 10,  8, 11, 18, 11,  5, 11
QQ,CS13,BULLET, 14, 10, 15, 10, 20, 11, 19, 11, 16, 10,  9, 11,  1, 12,  8, 11
QQ,,BULLET, 13, 11, 12, 11, 12, 12, 11, 12, 11, 11,  4, 12, 10, 12,  5, 12
QQ,,BULLET, 12, 11, 15, 11, 14, 12, 12, 12, 14, 11,  6, 12, 13, 12,  4, 12
QQ,,BULLET, 15, 11, 19, 11, 16, 12, 14, 12, 18, 11,  8, 12, 15, 12,  6, 12
QQ,CS13,BULLET, 19, 11, 20, 11, 17, 12, 16, 12,  1, 12,  9, 12, 18, 12,  8, 12
QQ,,BULLET, 15,  9, 13,  9, 18, 10, 18,  9, 16,  9, 14,  9, 19,  9, 17,  9
QQ,,BULLET, 13,  9,  7,  9, 10, 10, 18, 10, 12,  9,  8,  9, 17, 10, 14,  9
QQ,,BULLET,  7,  9, 16,  8,  8, 10, 10, 10,  6,  9,  5,  9,  9, 10,  8,  9
QQ,,BULLET, 18,  9, 18, 10, 20, 10,  1, 10, 19,  9, 19, 10,  2, 10, 20,  9
QQ,,BULLET, 18, 10, 10, 10, 17, 11, 20, 10, 17, 10,  6, 11,  7, 11, 19, 10
QQ,,BULLET, 10, 10,  8, 10, 13, 11, 17, 11,  9, 10,  4, 11, 16, 11,  6, 11
QQ,,BULLET,  1, 10, 20, 10,  1, 11,  3, 10,  2, 10,  2, 11,  4, 10,  5, 10
QQ,,BULLET, 20, 10, 17, 11,  2, 12,  1, 11,  7, 11,  3, 12, 10, 11,  2, 11
QQ,,BULLET, 17, 11, 13, 11, 11, 12,  2, 12, 16, 11,  5, 12,  7, 12,  3, 12
QQ,,BULLET, 10, 20, 19, 20, 15, 19, 13, 19, 18, 20,  6, 20, 14, 19,  5, 20
QQ,,BULLET, 19, 20,  1, 21, 17, 19, 15, 19, 20, 20,  7, 20, 16, 19,  6, 20
QQ,,BULLET,  1, 21,  2, 21, 18, 19, 17, 19,  3, 21,  8, 20, 19, 19,  7, 20
QQ,,BULLET, 13, 19, 15, 19, 10, 18,  8, 18, 14, 19,  1, 19,  9, 18, 20, 18
QQ,,BULLET, 15, 19, 17, 19, 12, 18, 10, 18, 16, 19,  2, 19, 11, 18,  1, 19
QQ,,BULLET, 17, 19, 18, 19, 13, 18, 12, 18, 19, 19,  3, 19, 14, 18,  2, 19
QQ,,BULLET,  8, 18, 10, 18, 11, 17,  8, 17,  9, 18, 12, 17,  9, 17, 10, 17
QQ,,BULLET, 10, 18, 12, 18, 14, 17, 11, 17, 11, 18, 15, 17, 13, 17, 12, 17
QQ,,BULLET, 12, 18, 13, 18, 16, 17, 14, 17, 14, 18, 17, 17, 18, 17, 15, 17
BC,PRESSURE, 10,  1,  2,0.250000E+02,0.250000E+02
```

DIRECT LIST OF TRANSLATED DATA

```
BC,PRESSURE,  1,  2,  2,0.250000E+02,0.250000E+02
BC,PRESSURE, 15,  2,  2,0.250000E+02,0.250000E+02
BC,PRESSURE,  9,  3,  2,0.250000E+02,0.250000E+02
BC,PRESSURE,  3,  4,  2,0.250000E+02,0.250000E+02
BC,PRESSURE, 17,  4,  2,0.250000E+02,0.250000E+02
BC,PRESSURE, 11,  5,  2,0.250000E+02,0.250000E+02
BC,PRESSURE,  5,  6,  2,0.250000E+02,0.250000E+02
BC,PRESSURE, 19,  6,  2,0.250000E+02,0.250000E+02
BC,PRESSURE, 13,  7,  2,0.250000E+02,0.250000E+02
BC,PRESSURE,  7,  8,  2,0.250000E+02,0.250000E+02
BC,PRESSURE, 16, 12,  2,0.250000E+02,0.250000E+02
BC,PRESSURE, 10, 13,  2,0.250000E+02,0.250000E+02
BC,PRESSURE,  4, 14,  2,0.250000E+02,0.250000E+02
BC,PRESSURE, 18, 14,  2,0.250000E+02,0.250000E+02
BC,PRESSURE, 12, 15,  2,0.250000E+02,0.250000E+02
BC,PRESSURE,  6, 16,  2,0.250000E+02,0.250000E+02
BC,PRESSURE, 20, 16,  2,0.250000E+02,0.250000E+02
BC,PRESSURE,  5, 18,  2,0.250000E+02,0.250000E+02
BC,PRESSURE, 10, 19,  2,0.250000E+02,0.250000E+02
BC,PRESSURE, 15, 20,  2,0.250000E+02,0.250000E+02
BC,PRESSURE, 15, 21,  2,0.250000E+02,0.250000E+02
BC,SHEAR,  1, 21,  3,0.250000E+02,0.250000E+02
BC,SHEAR, 19, 21,  3,0.250000E+02,0.250000E+02
BC,SHEAR, 12, 22,  3,0.250000E+02,0.250000E+02
BC,PRESSURE, 14, 22,  2,0.250000E+02,0.250000E+02
BC,SHEAR, 14, 22,  3,0.250000E+02,0.250000E+02
BC,PRESSURE,  1,  9,  2,0.250000E+02,0.250000E+02
BC,PRESSURE, 14, 10,  2,0.250000E+02,0.250000E+02
BC,PRESSURE, 19, 11,  2,0.250000E+02,0.250000E+02
BC,PRESSURE,  1, 21,  2,0.250000E+02,0.250000E+02
BC,PRESSURE, 17, 19,  2,0.250000E+02,0.250000E+02
BC,PRESSURE, 12, 18,  2,0.250000E+02,0.250000E+02
BC,SLOPE,  1,  1,  1,0.000000E+00,0.000000E+00
BC,SLOPE,  4,  1,  1,0.000000E+00,0.000000E+00
BC,SLOPE,  7,  1,  1,0.000000E+00,0.000000E+00
BC,SLOPE, 10,  1,  1,0.000000E+00,0.000000E+00
BC,SLOPE, 12, 18,  2,0.000000E+00,0.000000E+00
BC,SLOPE, 17, 19,  2,0.000000E+00,0.000000E+00
BC,SLOPE,  1, 21,  2,0.000000E+00,0.000000E+00
BC,SLOPE,  1, 21,  3,0.000000E+00,0.000000E+00
BC,SLOPE, 19, 21,  3,0.000000E+00,0.000000E+00
BC,SLOPE, 14, 22,  3,0.000000E+00,0.000000E+00
BC,SLOPE, 12, 22,  3,0.000000E+00,0.000000E+00
END,ELEMENTS
           5    BODY,FORCE,,16100
  613
           6    SOLVE
  614
           7    STRESS,2
  615
           8    TRANSLATE
  616
           9    STOP
  617
```

ELEMENT DATA

ELEMENT NO.	TYPE	MAT NO.	NODE NO.	NODE I,J	R	Z
1	QQ	10	1	1,1	0.000	79.600
			2	4,1	0.000	78.950
			3	17,1	5.369	78.314
			4	15,1	5.582	78.931
			5	2,1	0.000	79.275
			6	5,1	2.703	78.791
			7	16,1	5.476	78.623
			8	3,1	2.811	79.433
2	QQ	10	1	4,1	0.000	78.950
			2	7,1	0.000	78.300
			3	19,1	5.156	77.696
			4	17,1	5.369	78.314
			5	6,1	0.000	78.625
			6	8,1	2.596	78.149
			7	18,1	5.262	78.005
			8	5,1	2.703	78.791
3	QQ	10	1	7,1	0.000	78.300
			2	10,1	0.000	77.650
			3	1,2	4.943	77.079
			4	19,1	5.156	77.696
			5	9,1	0.000	77.975
			6	11,1	2.488	77.507
			7	20,1	5.049	77.388
			8	8,1	2.596	78.149
4	QQ	10	1	10,1	0.000	77.650
			2	12,1	0.000	77.000
			3	2,2	4.729	76.461
			4	1,2	4.943	77.079
			5	13,1	0.000	77.325
			6	14,1	2.380	76.865
			7	3,2	4.836	76.770
			8	11,1	2.488	77.507
5	QQ	10	1	15,1	5.582	78.931
			2	17,1	5.369	78.314
			3	11,2	10.344	76.486
			4	9,2	10.746	77.012
			5	16,1	5.476	78.623
			6	5,2	7.910	77.544
			7	10,2	10.545	76.749
			8	4,2	8.221	78.123
6	QQ	10	1	17,1	5.369	78.314
			2	19,1	5.156	77.696
			3	13,2	9.942	75.960
			4	11,2	10.344	76.486
			5	18,1	5.262	78.005
			6	6,2	7.599	76.965
			7	12,2	10.143	76.223
			8	5,2	7.910	77.544
7	QQ	10	1	19,1	5.156	77.696
			2	1,2	4.943	77.079
			3	15,2	9.539	75.434
			4	13,2	9.942	75.960
			5	20,1	5.049	77.388
			6	7,2	7.287	76.387
			7	14,2	9.740	75.697
			8	6,2	7.599	76.965
8	QQ	10	1	1,2	4.943	77.079
			2	2,2	4.729	76.461
			3	16,2	9.137	74.908
			4	15,2	9.539	75.434
			5	3,2		

4.836 76.770 6 8,2 6.976 75.808
7 17,2 9.338 75.171 8 7,2
7.287 76.387

9 QQ 10 1 9,2 10.746 77.012 2 11,2
10.344 76.486 3 5,3 14.743 73.586
4 3,3 15.300 73.969 5 10,2
10.545 76.749 6 19,2 12.627 75.162
7 4,3 15.021 73.777 8 18,2
13.112 75.623

10 QQ 10 1 11,2 10.344 76.486 2 13,2
9.942 75.960 3 7,3 14.186 73.203
4 5,3 14.743 73.586 5 12,2
10.143 76.223 6 20,2 12.142 74.702
7 6,3 14.464 73.394 8 19,2
12.627 75.162

11 QQ 10 1 13,2 9.942 75.960 2 15,2
9.539 75.434 3 9,3 13.629 72.819
4 7,3 14.186 73.203 5 14,2
9.740 75.697 6 1,3 11.657 74.242
7 8,3 13.907 73.011 8 20,2
12.142 74.702

12 QQ 10 1 15,2 9.539 75.434 2 16,2
9.137 74.908 3 10,3 13.072 72.436
4 9,3 13.629 72.819 5 17,2
9.338 75.171 6 2,3 11.173 73.781
7 11,3 13.350 72.628 8 1,3
11.657 74.242

13 QQ 10 1 3,3 15.300 73.969 2 5,3
14.743 73.586 3 19,3 18.383 69.734
4 17,3 19.050 69.933 5 4,3
15.021 73.777 6 13,3 16.675 71.766
7 18,3 18.716 69.834 8 12,3
17.293 72.061

projectile

ELEMENT DATA

ELEMENT NO.	TYPE	MAT NO.	NODE NO.	NODE I,J	R	Z
14	QQ	10	1	5,3	14.743	73.586
			2	7,3	14.186	73.203
			3	1,4	17.716	69.536
			4	19,3	18.383	69.734
			5	6,3	14.464	73.394
			6	14,3	16.056	71.470
			7	20,3	18.050	69.635
			8	13,3	16.675	71.766
15	QQ	10	1	7,3	14.186	73.203
			2	9,3	13.629	72.819
			3	3,4	17.050	69.337
			4	1,4	17.716	69.536
			5	8,3	13.907	73.011
			6	15,3	15.438	71.175
			7	2,4	17.383	69.436
			8	14,3	16.056	71.470
16	QQ	10	1	9,3	13.629	72.819
			2	10,3	13.072	72.436
			3	4,4	16.383	69.139
			4	3,4	17.050	69.337
			5	11,3	13.350	72.628
			6	16,3	14.819	70.880
			7	5,4	16.716	69.238
			8	15,3	15.438	71.175
17	QQ	10	1	17,3	19.050	69.933
			2	19,3	18.383	69.734
			3	13,4	21.083	65.051
			4	11,4	21.804	65.031
			5	18,3	18.716	69.834
			6	7,4	19.871	67.473
			7	12,4	21.443	65.041
			8	6,4	20.573	67.564
18	QQ	10	1	19,3	18.383	69.734
			2	1,4	17.716	69.536
			3	15,4	20.362	65.071
			4	13,4	21.083	65.051
			5	20,3	18.050	69.635
			6	8,4	19.170	67.381
			7	14,4	20.722	65.061
			8	7,4	19.871	67.473
19	QQ	10	1	1,4	17.716	69.536
			2	3,4	17.050	69.337
			3	17,4	19.641	65.091
			4	15,4	20.362	65.071
			5	2,4	17.383	69.436
			6	9,4	18.468	67.289
			7	16,4	20.002	65.081
			8	8,4	19.170	67.381
20	QQ	10	1	3,4	17.050	69.337
			2	4,4	16.383	69.139
			3	18,4	18.920	65.111
			4	17,4	19.641	65.091
			5	5,4	16.716	69.238
			6	10,4	17.766	67.197
			7	19,4	19.281	65.101
			8	9,4	18.468	67.289
21	QQ	10	1	11,4	21.804	65.031
			2	13,4	21.083	65.051
			3	7,5	22.289	63.684
			4	5.5	23.202	63.687
			5	12,4		

21.443 65.041 6 1,5 21.688 64.370

7 6,5 22.746 63.686 8 20,4

22.503 64.359

22 QQ 10 1 13,4 21.083 65.051 2 15,4

20.362 65.071 3 9,5 21.375 63.680

4 7,5 22.289 63.684 5 14,4

20.722 65.061 6 2,5 20.875 64.380

7 8,5 21.832 63.682 8 1,5

21.688 64.370

23 QQ 10 1 15,4 20.362 65.071 2 17,4

19.641 65.091 3 11,5 20.462 63.676

4 9,5 21.375 63.680 5 16,4

20.002 65.081 6 3,5 20.061 64.389

7 10,5 20.919 63.678 8 2,5

20.875 64.380

24 QQ 10 1 17,4 19.641 65.091 2 18,4

18.920 65.111 3 12,5 19.549 63.672

4 11,5 20.462 63.676 5 19,4

19.281 65.101 6 4,5 19.248 64.397

7 13,5 20.005 63.674 8 3,5

20.061 64.389

25 QQ 10 1 5,5 23.202 63.687 2 7,5

22.289 63.684 3 1,6 23.468 62.305

4 19,5 24.601 62.344 5 6,5

22.746 63.686 6 15,5 22.881 62.997

7 20,5 24.034 62.325 8 14,5

23.902 63.016

26 QQ 10 1 7,5 22.289 63.684 2 9,5

21.375 63.680 3 3,6 22.334 62.267

4 1,6 23.468 62.305 5 8,5

21.832 63.682 6 16,5 21.861 62.977

7 2,6 22.901 62.286 8 15,5

22.881 62.997

T E X G A P 8 4 - 2 D VERSION

238AUG-90

PAGE 4

projectile

ELEMENT DATA

ELEMENT NO.	TYPE	MAT	NODE NO.	NODE I,J	R	Z
27	QQ	10	1	9,5	21.375	63.680
			2	11,5	20.462	63.676
			3	5,6	21.201	62.229
			4	3,6	22.334	62.267
			5	10,5	20.919	63.678
			6	17,5	20.841	62.957
			7	4,6	21.767	62.248
			8	16,5	21.861	62.977
28	QQ	10	1	11,5	20.462	63.676
			2	12,5	19.549	63.672
			3	6,6	20.067	62.190
			4	5,6	21.201	62.229
			5	13,5	20.005	63.674
			6	18,5	19.822	62.936
			7	7,6	20.634	62.209
			8	17,5	20.841	62.957
29	QQ	10	1	19,5	24.601	62.344
			2	1,6	23.468	62.305
			3	15,6	24.618	60.918
			4	13,6	26.000	61.000
			5	20,5	24.034	62.325
			6	9,6	24.046	61.614
			7	14,6	25.309	60.959
			8	8,6	25.301	61.672
30	QQ	10	1	1,6	23.468	62.305
			2	3,6	22.334	62.267
			3	17,6	23.237	60.836
			4	15,6	24.618	60.918
			5	2,6	22.901	62.286
			6	10,6	22.791	61.555
			7	16,6	23.928	60.877
			8	9,6	24.046	61.614
31	QQ	10	1	3,6	22.334	62.267
			2	5,6	21.201	62.229
			3	19,6	21.855	60.755
			4	17,6	23.237	60.836
			5	4,6	21.767	62.248
			6	11,6	21.538	61.496
			7	18,6	22.546	60.796
			8	10,6	22.791	61.555
32	QQ	10	1	5,6	21.201	62.229
			2	6,5	20.067	62.190
			3	20,6	20.474	60.673
			4	19,6	21.855	60.755
			5	7,6	20.634	62.209
			6	12,6	20.284	61.435
			7	1,7	21.164	60.714
			8	11,6	21.538	61.496
33	QQ	10	1	13,6	26.000	61.000
			2	15,6	24.618	60.918
			3	9,7	24.691	59.282
			4	7,7	26.000	59.333
			5	14,6	25.309	60.959
			6	3,7	24.659	60.100
			7	8,7	25.346	59.308
			8	2,7	26.000	60.167
34	QQ	10	1	15,6	24.618	60.918
			2	17,6	23.237	60.836
			3	11,7	23.383	59.231
			4	9.7	24.691	59.282
			5	16,6		

23.928 60.877 6 4,7 23.317 60.035
7 10,7 24.037 59.257 8 3,7

24.659 60.100

35 QQ 10 1 17,6 23.237 60.836 2 19,6
21.855 60.755 3 13,7 22.074 59.180
4 11,7 23.383 59.231 5 18,6
22.546 60.796 6 5,7 21.976 59.969
7 12,7 22.728 59.206 8 4,7

23.317 60.035

36 QQ 10 1 19,6 21.855 60.755 2 20,6
20.474 60.673 3 14,7 20.766 59.129
4 13,7 22.074 59.180 5 1,7
21.164 60.714 6 6,7 20.634 59.904
7 15,7 21.420 59.155 8 5,7

21.976 59.969

37 QQ 10 1 7,7 26.000 59.333 2 9,7
24.691 59.282 3 3,8 24.735 57.642
4 1,8 26.000 57.667 5 8,7
25.346 59.308 6 17,7 24.717 58.462
7 2,8 25.368 57.655 8 16,7

26.000 58.500

38 QQ 10 1 9,7 24.691 59.282 2 11,7
23.383 59.231 3 5,8 23.471 57.618
4 3,8 24.735 57.642 5 10,7
24.037 59.257 6 18,7 23.434 58.425
7 4,8 24.103 57.630 8 17,7

24.717 58.462

39 QQ 10 1 11,7 23.383 59.231 2 13,7
22.074 59.180 3 7,8 22.206 57.594
4 5,8 23.471 57.618 5 12,7
22.728 59.206 6 19,7 22.151 58.388
7 6,8 22.838 57.606 8 18,7

23.434 58.425

T E X G A P 8 4 - 2 D VERSION

238AUG-90

PAGE 5

projectile

ELEMENT DATA

ELEMENT NO. R	TYPE Z	MAT	NO.	NODE NO. I,J	NODE I,J R	R Z	Z	NODE NO.	I,J
40	QQ	10		1	13,7	22.074	59.180	2	14,7
20.766	59.129		3	8,8		20.941	57.570		
				4	7,8	22.206	57.594	5	15,7
21.420	59.155		6	20,7		20.868	58.351		
				7	9,8	21.574	57.582	8	19,7
22.151	58.388								
41	QQ	10		1	1,8	26.000	57.667	2	3,8
24.735	57.642		3	17,8		24.750	56.000		
				4	16,8	26.000	56.000	5	2,8
25.368	57.655		6	11,8		24.746	56.821		
				7	15,8	25.375	56.000	8	10,8
26.000	56.833								
42	QQ	10		1	3,8	24.735	57.642	2	5,8
23.471	57.618		3	19,8		23.500	56.000		
				4	17,8	24.750	56.000	5	4,8
24.103	57.630		6	12,8		23.493	56.809		
				7	18,8	24.125	56.000	8	11,8
24.746	56.821								
43	QQ	10		1	5,8	23.471	57.618	2	7,8
22.206	57.594		3	1,9		22.250	56.000		
				4	19,8	23.500	56.000	5	6,8
22.838	57.606		6	13,8		22.239	56.797		
				7	20,8	22.875	56.000	8	12,8
23.493	56.809								
44	QQ	10		1	7,8	22.206	57.594	2	8,8
20.941	57.570		3	2,9		21.000	56.000		
				4	1,9	22.250	56.000	5	9,8
21.574	57.582		6	14,8		20.985	56.785		
				7	3,9	21.625	56.000	8	13,8
22.239	56.797								
45	QQ	10		1	11,12	26.000	52.000	2	12,12
24.750	52.000		3	6,13		24.750	46.667		
				4	4,13	26.000	46.667	5	10,12
25.375	52.000		6	20,12		24.750	49.333		
				7	5,13	25.375	46.667	8	19,12
26.000	49.333								
46	QQ	10		1	12,12	24.750	52.000	2	14,12
23.500	52.000		3	8,13		23.500	46.667		
				4	6,13	24.750	46.667	5	13,12
24.125	52.000		6	1,13		23.500	49.333		
				7	7,13	24.125	46.667	8	20,12
24.750	49.333								
47	QQ	10		1	14,12	23.500	52.000	2	16,12
22.250	52.000		3	10,13		22.250	46.667		
				4	8,13	23.500	46.667	5	15,12

22.875 52.000 6 2,13 22.250 49.333
7 9,13 22.875 46.667 8 1,13
23.500 49.333

48 QQ 10 1 16,12 22.250 52.000 2 17,12
21.000 52.000 3 11,13 21.000 46.667
4 10,13 22.250 46.667 5 18,12
21.625 52.000 6 3,13 21.000 49.333
7 12,13 21.625 46.667 8 2,13
22.250 49.333

49 QQ 10 1 4,13 26.000 46.667 2 6,13
24.750 46.667 3 20,13 24.750 41.333
4 18,13 26.000 41.333 5 5,13
25.375 46.667 6 14,13 24.750 44.000
7 19,13 25.375 41.333 8 13,13
26.000 44.000

50 QQ 10 1 6,13 24.750 46.667 2 8,13
23.500 46.667 3 2,14 23.500 41.333
4 20,13 24.750 41.333 5 7,13
24.125 46.667 6 15,13 23.500 44.000
7 1,14 24.125 41.333 8 14,13
24.750 44.000

51 QQ 10 1 8,13 23.500 46.667 2 10,13
22.250 46.667 3 4,14 22.250 41.333
4 2,14 23.500 41.333 5 9,13
22.875 46.667 6 16,13 22.250 44.000
7 3,14 22.875 41.333 8 15,13
23.500 44.000

52 QQ 10 1 10,13 22.250 46.667 2 11,13
21.000 46.667 3 5,14 21.000 41.333
4 4,14 22.250 41.333 5 12,13
21.625 46.667 6 17,13 21.000 44.000
7 6,14 21.625 41.333 8 16,13
22.250 44.000

projectile

ELEMENT DATA

ELEMENT NO.	TYPE	MAT	NODE NO.	NODE I,J	R	Z
53	QQ	10	1	18,13	26.000	41.333
			2	20,13	24.750	41.333
			3	14,14	24.750	36.000
			4	12,14	26.000	36.000
			5	19,13	25.375	41.333
			6	8,14	24.750	38.667
			7	13,14	25.375	36.000
			8	7,14	26.000	38.667
54	QQ	10	1	20,13	24.750	41.333
			2	2,14	23.500	41.333
			3	16,14	23.500	36.000
			4	14,14	24.750	36.000
			5	1,14	24.125	41.333
			6	9,14	23.500	38.667
			7	15,14	24.125	36.000
			8	8,14	24.750	38.667
55	QQ	10	1	2,14	23.500	41.333
			2	4,14	22.250	41.333
			3	18,14	22.250	36.000
			4	16,14	23.500	36.000
			5	3,14	22.875	41.333
			6	10,14	22.250	38.667
			7	17,14	22.875	36.000
			8	9,14	23.500	38.667
56	QQ	10	1	4,14	22.250	41.333
			2	5,14	21.000	41.333
			3	19,14	21.000	36.000
			4	18,14	22.250	36.000
			5	6,14	21.625	41.333
			6	11,14	21.000	38.667
			7	20,14	21.625	36.000
			8	10,14	22.250	38.667
57	QQ	10	1	12,14	26.000	36.000
			2	14,14	24.750	36.000
			3	8,15	24.750	30.667
			4	6,15	26.000	30.667
			5	13,14	25.375	36.000
			6	2,15	24.750	33.333
			7	7,15	25.375	30.667
			8	1,15	26.000	33.333
58	QQ	10	1	14,14	24.750	36.000
			2	16,14	23.500	36.000
			3	10,15	23.500	30.667
			4	8,15	24.750	30.667
			5	15,14	24.125	36.000
			6	3,15	23.500	33.333
			7	9,15	24.125	30.667
			8	2,15	24.750	33.333
59	QQ	10	1	16,14	23.500	36.000
			2	18,14	22.250	36.000
			3	12,15	22.250	30.667
			4	10,15	23.500	30.667
			5	17,14	22.875	36.000
			6	4,15	22.250	33.333
			7	11,15	22.875	30.667
			8	3,15	23.500	33.333
60	QQ	10	1	18,14	22.250	36.000
			2	19,14	21.000	36.000
			3	13,15	21.000	30.667
			4	12,15	22.250	30.667
			5	20,14		

```
21.625    36.000        6    5,15       21.000    33.333
                             7     14,15       21.625    30.667        8    4,15
22.250    33.333

  61       QQ      10        1     6,15        26.000    30.667        2    8,15
24.750    30.667        3    2,16       24.750    25.333
                             4     20,15       26.000    25.333        5    7,15
25.375    30.667        6    16,15      24.750    28.000
                             7     1,16        25.375    25.333        8    15,15
26.000    28.000

  62       QQ      10        1     8,15        24.750    30.667        2    10,15
23.500    30.667        3    4,16       23.500    25.333
                             4     2,16        24.750    25.333        5    9,15
24.125    30.667        6    17,15      23.500    28.000
                             7     3,16        24.125    25.333        8    16,15
24.750    28.000

  63       QQ      10        1     10,15       23.500    30.667        2    12,15
22.250    30.667        3    6,16       22.250    25.333
                             4     4,16        23.500    25.333        5    11,15
22.875    30.667        6    18,15      22.250    28.000
                             7     5,16        22.875    25.333        8    17,15
23.500    28.000

  64       QQ      10        1     12,15       22.250    30.667        2    13,15
21.000    30.667        3    7,16       21.000    25.333
                             4     6,16        22.250    25.333        5    14,15
21.625    30.667        6    19,15      21.000    28.000
                             7     8,16        21.625    25.333        8    18,15
22.250    28.000

  65       QQ      10        1     20,15       26.000    25.333        2    2,16
24.750    25.333        3    16,16      24.750    20.000
                             4     14,16       26.000    20.000        5    1,16
25.375    25.333        6    10,16      24.750    22.667
                             7     15,16       25.375    20.000        8    9,16
26.000    22.667
```

projectile

ELEMENT DATA

ELEMENT NO.	TYPE	MAT NO.	NODE NO.	NODE I,J	R	Z
66	QQ	10	1	2,16	24.750	25.333
			2	4,16	23.500	25.333
			3	18,16	23.500	20.000
			4	16,16	24.750	20.000
			5	3,16	24.125	25.333
			6	11,16	23.500	22.667
			7	17,16	24.125	20.000
			8	10,16	24.750	22.667
67	QQ	10	1	4,16	23.500	25.333
			2	6,16	22.250	25.333
			3	20,16	22.250	20.000
			4	18,16	23.500	20.000
			5	5,16	22.875	25.333
			6	12,16	22.250	22.667
			7	19,16	22.875	20.000
			8	11,16	23.500	22.667
68	QQ	10	1	6,16	22.250	25.333
			2	7,16	21.000	25.333
			3	1,17	21.000	20.000
			4	20,16	22.250	20.000
			5	8,16	21.625	25.333
			6	13,16	21.000	22.667
			7	2,17	21.625	20.000
			8	12,16	22.250	22.667
69	QQ	10	1	14,16	26.000	20.000
			2	16,16	24.750	20.000
			3	1,18	24.750	14.667
			4	19,17	26.000	14.667
			5	15,16	25.375	20.000
			6	4,17	24.750	17.333
			7	20,17	25.375	14.667
			8	3,17	26.000	17.333
70	QQ	10	1	16,16	24.750	20.000
			2	18,16	23.500	20.000
			3	3,18	23.500	14.667
			4	1,18	24.750	14.667
			5	17,16	24.125	20.000
			6	5,17	23.500	17.333
			7	2,18	24.125	14.667
			8	4,17	24.750	17.333
71	QQ	10	1	18,16	23.500	20.000
			2	20,16	22.250	20.000
			3	5,18	22.250	14.667
			4	3,18	23.500	14.667
			5	19,16	22.875	20.000
			6	6,17	22.250	17.333
			7	4,18	22.875	14.667
			8	5,17	23.500	17.333
72	QQ	10	1	20,16	22.250	20.000
			2	1,17	21.000	20.000
			3	6,18	21.000	14.667
			4	5,18	22.250	14.667
			5	2,17	21.625	20.000
			6	7,17	21.000	17.333
			7	7,18	21.625	14.667
			8	6,17	22.250	17.333
73	QQ	10	1	19,17	26.000	14.667
			2	1,18	24.750	14.667
			3	6,19	24.750	9.333
			4	4,19	26.000	9.333
			5	20,17		

25.375 14.667 6 16,18 24.750 12.000
7 5,19 25.375 9.333 8 15,18
26.000 12.000

74 QQ 10 1 1,18 24.750 14.667 2 3,18
23.500 14.667 3 8,19 23.500 9.333
4 6,19 24.750 9.333 5 2,18
24.125 14.667 6 17,18 23.500 12.000
7 7,19 24.125 9.333 8 16,18
24.750 12.000

75 QQ 10 1 3,18 23.500 14.667 2 5,18
22.250 14.667 3 10,19 22.250 9.333
4 8,19 23.500 9.333 5 4,18
22.875 14.667 6 18,18 22.250 12.000
7 9,19 22.875 9.333 8 17,18
23.500 12.000

76 QQ 10 1 5,18 22.250 14.667 2 6,18
21.000 14.667 3 11,19 21.000 9.333
4 10,19 22.250 9.333 5 7,18
21.625 14.667 6 19,18 21.000 12.000
7 12,19 21.625 9.333 8 18,18
22.250 12.000

77 QQ 10 1 4,19 26.000 9.333 2 6,19
24.750 9.333 3 11,20 24.750 4.000
4 10,20 26.000 4.000 5 5,19
25.375 9.333 6 1,20 24.750 6.667
7 9,20 25.375 4.000 8 20,19
26.000 6.667

78 QQ 10 1 6,19 24.750 9.333 2 8,19
23.500 9.333 3 13,20 23.500 4.000
4 11,20 24.750 4.000 5 7,19
24.125 9.333 6 2,20 23.500 6.667
7 12,20 24.125 4.000 8 1,20
24.750 6.667

```
                                                                       ELEMENT DATA

        ELEMENT                               NODE                                              NODE
                                          NODE
    NO.     TYPE      MAT           NO.    I,J           R            Z              NO.     I,J
  R         Z              NO.       I,J          R          Z

    79      QQ        10             1    8,19        23.500      9.333           2     10,19
 22.250     9.333          3        15,20        22.250      4.000
                                     4    13,20       23.500      4.000           5     9,19
 22.875     9.333          6        3,20         22.250      6.667
                                     7    14,20       22.875      4.000           8     2,20
 23.500     6.667

    80      QQ        10             1    10,19       22.250      9.333           2     11,19
 21.000     9.333          3        16,20        21.000      4.000
                                     4    15,20       22.250      4.000           5     12,19
 21.625     9.333          6        4,20         21.000      6.667
                                     7    17,20       21.625      4.000           8     3,20
 22.250     6.667

    81      QQ        10             1    10,20       26.000      4.000           2     11,20
 24.750     4.000          3        11,21        24.750      2.667
                                     4    19,20       26.000      2.667           5     9,20
 25.375     4.000          6        4,21         24.750      3.333
                                     7    5,21        25.375      2.667           8     18,20
 26.000     3.333

    82      QQ        10             1    11,20       24.750      4.000           2     13,20
 23.500     4.000          3        13,21        23.500      2.667
                                     4    11,21       24.750      2.667           5     12,20
 24.125     4.000          6        6,21         23.500      3.333
                                     7    12,21       24.125      2.667           8     4,21
 24.750     3.333

    83      QQ        10             1    13,20       23.500      4.000           2     15,20
 22.250     4.000          3        15,21        22.250      2.667
                                     4    13,21       23.500      2.667           5     14,20
 22.875     4.000          6        7,21         22.250      3.333
                                     7    14,21       22.875      2.667           8     6,21
 23.500     3.333

    84      QQ        10             1    15,20       22.250      4.000           2     16,20
 21.000     4.000          3        16,21        21.000      2.667
                                     4    15,21       22.250      2.667           5     17,20
 21.625     4.000          6        8,21         21.000      3.333
                                     7    17,21       21.625      2.667           8     7,21
 22.250     3.333

    85      QQ        10             1    19,20       26.000      2.667           2     11,21
 24.750     2.667          3        19,21        24.750      1.333
                                     4    1,21        26.000      1.333           5     5,21
 25.375     2.667          6        18,21        24.750      2.000
                                     7    9,21        25.375      1.333           8     20,20
 26.000     2.000

    86      QQ        10             1    11,21       24.750      2.667           2     13,21
 23.500     2.667          3        12,22        23.500      1.333
                                     4    19,21       24.750      1.333           5     12,21
```

24.125 2.667 6 2,22 23.500 2.000
7 3,22 24.125 1.333 8 18,21

24.750 2.000

87 QQ 10 1 13,21 23.500 2.667 2 15,21
22.250 2.667 3 14,22 22.250 1.333
4 12,22 23.500 1.333 5 14,21
22.875 2.667 6 4,22 22.250 2.000
7 13,22 22.875 1.333 8 2,22

23.500 2.000

88 QQ 10 1 15,21 22.250 2.667 2 16,21
21.000 2.667 3 6,22 21.000 1.333
4 14,22 22.250 1.333 5 17,21
21.625 2.667 6 5,22 21.000 2.000
7 7,22 21.625 1.333 8 4,22

22.250 2.000

89 QQ 10 1 1,21 26.000 1.333 2 19,21
24.750 1.333 3 20,21 24.750 0.000
4 2,21 26.000 0.000 5 9,21
25.375 1.333 6 1,22 24.750 0.667
7 10,21 25.375 0.000 8 3,21

26.000 0.667

90 QQ 10 1 19,21 24.750 1.333 2 12,22
23.500 1.333 3 15,22 23.500 0.000
4 20,21 24.750 0.000 5 3,22
24.125 1.333 6 16,22 23.500 0.667
7 8,22 24.125 0.000 8 1,22

24.750 0.667

91 QQ 10 1 12,22 23.500 1.333 2 14,22
22.250 1.333 3 17,22 22.250 0.000
4 15,22 23.500 0.000 5 13,22
22.875 1.333 6 18,22 22.250 0.667
7 19,22 22.875 0.000 8 16,22

23.500 0.667

ELEMENT DATA

ELEMENT NO.	TYPE	MAT	NODE NO.	NODE I,J	R	Z
92	QQ	10	1	14,22	22.250	1.333
			2	6,22	21.000	1.333
			3	9,22	21.000	0.000
			4	17,22	22.250	0.000
			5	7,22	21.625	1.333
			6	10,22	21.000	0.667
			7	11,22	21.625	0.000
			8	18,22	22.250	0.667
93	QQ	10	1	16,8	26.000	56.000
			2	17,8	24.750	56.000
			3	7,10	24.750	54.667
			4	8,10	26.000	54.667
			5	15,8	25.375	56.000
			6	4,9	24.750	55.333
			7	6,10	25.375	54.667
			8	5,9	26.000	55.333
94	QQ	10	1	17,8	24.750	56.000
			2	19,8	23.500	56.000
			3	12,10	23.500	54.667
			4	7,10	24.750	54.667
			5	18,8	24.125	56.000
			6	9,9	23.500	55.333
			7	11,10	24.125	54.667
			8	4,9	24.750	55.333
95	QQ	10	1	19,8	23.500	56.000
			2	1,9	22.250	56.000
			3	14,10	22.250	54.667
			4	12,10	23.500	54.667
			5	20,8	22.875	56.000
			6	10,9	22.250	55.333
			7	13,10	22.875	54.667
			8	9,9	23.500	55.333
96	QQ	10	1	1,9	22.250	56.000
			2	2,9	21.000	56.000
			3	15,10	21.000	54.667
			4	14,10	22.250	54.667
			5	3,9	21.625	56.000
			6	11,9	21.000	55.333
			7	16,10	21.625	54.667
			8	10,9	22.250	55.333
97	QQ	10	1	8,10	26.000	54.667
			2	7,10	24.750	54.667
			3	12,11	24.750	53.333
			4	13,11	26.000	53.333
			5	6,10	25.375	54.667
			6	3,11	24.750	54.000
			7	11,11	25.375	53.333
			8	4,11	26.000	54.000
98	QQ	10	1	7,10	24.750	54.667
			2	12,10	23.500	54.667
			3	15,11	23.500	53.333
			4	12,11	24.750	53.333
			5	11,10	24.125	54.667
			6	5,11	23.500	54.000
			7	14,11	24.125	53.333
			8	3,11	24.750	54.000
99	QQ	10	1	12,10	23.500	54.667
			2	14,10	22.250	54.667
			3	19,11	22.250	53.333
			4	15,11	23.500	53.333
			5	13,10		

22.875	54.667		6	8,11	22.250	54.000			
				7	18,11	22.875	53.333	8	5,11
23.500	54.000								
100	QQ	10		1	14,10	22.250	54.667	2	15,10
21.000	54.667		3	20,11	21.000	53.333			
				4	19,11	22.250	53.333	5	16,10
21.625	54.667		6	9,11	21.000	54.000			
				7	1,12	21.625	53.333	8	8,11
22.250	54.000								
101	QQ	10		1	13,11	26.000	53.333	2	12,11
24.750	53.333		3	12,12	24.750	52.000			
				4	11,12	26.000	52.000	5	11,11
25.375	53.333		6	4,12	24.750	52.667			
				7	10,12	25.375	52.000	8	5,12
26.000	52.667								
102	QQ	10		1	12,11	24.750	53.333	2	15,11
23.500	53.333		3	14,12	23.500	52.000			
				4	12,12	24.750	52.000	5	14,11
24.125	53.333		6	6,12	23.500	52.667			
				7	13,12	24.125	52.000	8	4,12
24.750	52.667								
103	QQ	10		1	15,11	23.500	53.333	2	19,11
22.250	53.333		3	16,12	22.250	52.000			
				4	14,12	23.500	52.000	5	18,11
22.875	53.333		6	8,12	22.250	52.667			
				7	15,12	22.875	52.000	8	6,12
23.500	52.667								
104	QQ	10		1	19,11	22.250	53.333	2	20,11
21.000	53.333		3	17,12	21.000	52.000			
				4	16,12	22.250	52.000	5	1,12
21.625	53.333		6	9,12	21.000	52.667			
				7	18,12	21.625	52.000	8	8,12
22.250	52.667								

projectile

ELEMENT DATA

ELEMENT NO.	TYPE	MAT	NODE NO.	NODE I,J	R	Z
105	QQ	10	1	15,9	28.000	56.000
			2	13,9	27.333	56.000
			3	18,10	27.333	54.667
			4	18,9	28.000	54.667
			5	16,9	27.667	56.000
			6	14,9	27.333	55.333
			7	19,9	27.667	54.667
			8	17,9	28.000	55.333
106	QQ	10	1	13,9	27.333	56.000
			2	7,9	26.667	56.000
			3	10,10	26.667	54.667
			4	18,10	27.333	54.667
			5	12,9	27.000	56.000
			6	8,9	26.667	55.333
			7	17,10	27.000	54.667
			8	14,9	27.333	55.333
107	QQ	10	1	7,9	26.667	56.000
			2	16,8	26.000	56.000
			3	8,10	26.000	54.667
			4	10,10	26.667	54.667
			5	6,9	26.333	56.000
			6	5,9	26.000	55.333
			7	9,10	26.333	54.667
			8	8,9	26.667	55.333
108	QQ	10	1	18,9	28.000	54.667
			2	18,10	27.333	54.667
			3	20,10	27.333	53.333
			4	1,10	28.000	53.333
			5	19,9	27.667	54.667
			6	19,10	27.333	54.000
			7	2,10	27.667	53.333
			8	20,9	28.000	54.000
109	QQ	10	1	18,10	27.333	54.667
			2	10,10	26.667	54.667
			3	17,11	26.667	53.333
			4	20,10	27.333	53.333
			5	17,10	27.000	54.667
			6	6,11	26.667	54.000
			7	7,11	27.000	53.333
			8	19,10	27.333	54.000
110	QQ	10	1	10,10	26.667	54.667
			2	8,10	26.000	54.667
			3	13,11	26.000	53.333
			4	17,11	26.667	53.333
			5	9,10	26.333	54.667
			6	4,11	26.000	54.000
			7	16,11	26.333	53.333
			8	6,11	26.667	54.000
111	QQ	10	1	1,10	28.000	53.333
			2	20,10	27.333	53.333
			3	1,11	27.333	52.000
			4	3,10	28.000	52.000
			5	2,10	27.667	53.333
			6	2,11	27.333	52.667
			7	4,10	27.667	52.000
			8	5,10	28.000	52.667
112	QQ	10	1	20,10	27.333	53.333
			2	17,11	26.667	53.333
			3	2,12	26.667	52.000
			4	1,11	27.333	52.000
			5	7,11	[illegible]	[illegible]

```
27.000    53.333         6     3,12        26.667    52.667
                                  7      10,11        27.000    52.000          8       2,11
27.333    52.667

 113      QQ       10          1      17,11        26.667    53.333          2       13,11
26.000    53.333         3     11,12       26.000    52.000
                                  4      2,12         26.667    52.000          5       16,11
26.333    53.333         6     5,12        26.000    52.667
                                  7      7,12         26.333    52.000          8       3,12
26.667    52.667

 114      QQ       10          1      10,20        26.000     4.000          2       19,20
26.000     2.667         3     15,19       26.667     2.667
                                  4      13,19        26.667     4.000          5       18,20
26.000     3.333         6     6,20        26.333     2.667
                                  7      14,19        26.667     3.333          8       5,20
26.333     4.000

 115      QQ       10          1      19,20        26.000     2.667          2       1,21
26.000     1.333         3     17,19       26.667     1.333
                                  4      15,19        26.667     2.667          5       20,20
26.000     2.000         6     7,20        26.333     1.333
                                  7      16,19        26.667     2.000          8       6,20
26.333     2.667

 116      QQ       10          1      1,21         26.000     1.333          2       2,21
26.000     0.000         3     18,19       26.667     0.000
                                  4      17,19        26.667     1.333          5       3,21
26.000     0.667         6     8,20        26.333     0.000
                                  7      19,19        26.667     0.667          8       7,20
26.333     1.333

 117      QQ       10          1      13,19        26.667     4.000          2       15,19
26.667     2.667         3     10,18       27.333     2.667
                                  4      8,18         27.333     4.000          5       14,19
26.667     3.333         6     1,19        27.000     2.667
                                  7      9,18         27.333     3.333          8       20,18
27.000     4.000
```

projectile

ELEMENT DATA

ELEMENT NO.	TYPE	MAT NO.	NODE NO.	I,J	R	Z	NODE NO.	I,J	R	Z	NODE NO.	I,J	R	Z
118	QQ	10	1	15,19	26.667	2.667	2	17,19	26.667	1.333	3	12,18	27.333	1.333
			4	10,18	27.333	2.667	5	16,19	26.667	2.000	6	2,19	27.000	1.333
			7	11,18	27.333	2.000	8	1,19	27.000	2.667				
119	QQ	10	1	17,19	26.667	1.333	2	18,19	26.667	0.000	3	13,18	27.333	0.000
			4	12,18	27.333	1.333	5	19,19	26.667	0.667	6	3,19	27.000	0.000
			7	14,18	27.333	0.667	8	2,19	27.000	1.333				
120	QQ	10	1	8,18	27.333	4.000	2	10,18	27.333	2.667	3	11,17	28.000	2.667
			4	8,17	28.000	4.000	5	9,18	27.333	3.333	6	12,17	27.667	2.667
			7	9,17	28.000	3.333	8	10,17	27.667	4.000				
121	QQ	10	1	10,18	27.333	2.667	2	12,18	27.333	1.333	3	14,17	28.000	1.333
			4	11,17	28.000	2.667	5	11,18	27.333	2.000	6	15,17	27.667	1.333
			7	13,17	28.000	2.000	8	12,17	27.667	2.667				
122	QQ	10	1	12,18	27.333	1.333	2	13,18	27.333	0.000	3	16,17	28.000	0.000
			4	14,17	28.000	1.333	5	14,18	27.333	0.667	6	17,17	27.667	0.000
			7	18,17	28.000	0.667	8	15,17	27.667	1.333				

BOUNDARY CONDITIONS

ELEMENT I	J	TYPE	SIDE/NODE	VALUE1	VALUE2	VALUE3
1	1	SLOPE	1	0.0000E+00	0.0000E+00	0.0000E+00
4	1	SLOPE	1	0.0000E+00	0.0000E+00	0.0000E+00
7	1	SLOPE	1	0.0000E+00	0.0000E+00	0.0000E+00
10	1	SLOPE	1	0.0000E+00	0.0000E+00	0.0000E+00
		PRESSURE	2	0.2500E+02	0.2500E+02	0.0000E+00
1	2	PRESSURE	2	0.2500E+02	0.2500E+02	0.0000E+00
15	2	PRESSURE	2	0.2500E+02	0.2500E+02	0.0000E+00
9	3	PRESSURE	2	0.2500E+02	0.2500E+02	0.0000E+00
3	4	PRESSURE	2	0.2500E+02	0.2500E+02	0.0000E+00
17	4	PRESSURE	2	0.2500E+02	0.2500E+02	0.0000E+00
11	5	PRESSURE	2	0.2500E+02	0.2500E+02	0.0000E+00
5	6	PRESSURE	2	0.2500E+02	0.2500E+02	0.0000E+00
19	6	PRESSURE	2	0.2500E+02	0.2500E+02	0.0000E+00
13	7	PRESSURE	2	0.2500E+02	0.2500E+02	0.0000E+00
7	8	PRESSURE	2	0.2500E+02	0.2500E+02	0.0000E+00
16	12	PRESSURE	2	0.2500E+02	0.2500E+02	0.0000E+00
10	13	PRESSURE	2	0.2500E+02	0.2500E+02	0.0000E+00
4	14	PRESSURE	2	0.2500E+02	0.2500E+02	0.0000E+00
18	14	PRESSURE	2	0.2500E+02	0.2500E+02	0.0000E+00
12	15	PRESSURE	2	0.2500E+02	0.2500E+02	0.0000E+00
6	16	PRESSURE	2	0.2500E+02	0.2500E+02	0.0000E+00
20	16	PRESSURE	2	0.2500E+02	0.2500E+02	0.0000E+00
5	18	PRESSURE	2	0.2500E+02	0.2500E+02	0.0000E+00
10	19	PRESSURE	2	0.2500E+02	0.2500E+02	0.0000E+00
15	20	PRESSURE	2	0.2500E+02	0.2500E+02	0.0000E+00
15	21	PRESSURE	2	0.2500E+02	0.2500E+02	0.0000E+00
1	21	SLOPE	3	0.0000E+00	0.0000E+00	0.0000E+00
		SLOPE	2	0.0000E+00	0.0000E+00	0.0000E+00
		PRESSURE	2	0.2500E+02	0.2500E+02	0.0000E+00
		SHEAR	3	0.2500E+02	0.2500E+02	

```
    0.0000E+00
                   19   21   SLOPE        3          0.0000E+00     0.0000E+00
    0.0000E+00
                             SHEAR        3          0.2500E+02     0.2500E+02
    0.0000E+00
                   12   22   SLOPE        3          0.0000E+00     0.0000E+00
    0.0000E+00
                             SHEAR        3          0.2500E+02     0.2500E+02
    0.0000E+00
                   14   22   SLOPE        3          0.0000E+00     0.0000E+00
    0.0000E+00
                             SHEAR        3          0.2500E+02     0.2500E+02
    0.0000E+00
                             PRESSURE     2          0.2500E+02     0.2500E+02
    0.0000E+00
                    1    9   PRESSURE     2          0.2500E+02     0.2500E+02
    0.0000E+00
                   14   10   PRESSURE     2          0.2500E+02     0.2500E+02
    0.0000E+00
                   19   11   PRESSURE     2          0.2500E+02     0.2500E+02
    0.0000E+00
                   17   19   SLOPE        2          0.0000E+00     0.0000E+00
    0.0000E+00
                             PRESSURE     2          0.2500E+02     0.2500E+02
    0.0000E+00
                   12   18   SLOPE        2          0.0000E+00     0.0000E+00
    0.0000E+00
                             PRESSURE     2          0.2500E+02     0.2500E+02
    0.0000E+00

RANGE OF I AN J VALUES AND COORDINATES FOUND DURING ELEMENT DEFINITION

 IMIN =    1          JMIN =    1          IMAX =   20          JMAX =   22

 RMIN =    0.0000E+00 ZMIN =    0.0000E+00 RMAX =    2.8000E+01 ZMAX =    7.9600E
+01

TIME IN SETUP          =   1.980E+00 SECONDS

BODY FORCES:
ACELR =    0.000E+00  ACELZ =    1.610E+04  ACELT =    0.000E+00  OMEGA =    0.000E+
00

FORMKF:  JPRINT =    3  INCT =      0  TREF =  -1.000E+00

TIME IN FORMKF         =   2.280E+00 SECONDS

TIME IN ZIPP           =   4.240E+00 SECONDS
```

projectile

LARGEST AND SMALLEST STRESSES AND STRAINS BY MATERIAL

MATERIAL = 10

QUANTITY	R	Z	ELEM	MAXIMUM	R	Z	ELEM	MINIMUM
SIGR	0.000E+00	7.960E+01	1	1.281E+02	2.475E+01	0.000E+00	90	-8.946E+01
SIGZ	2.100E+01	1.333E+00	92	3.028E+02	2.667E+01	4.000E+00	114	-4.474E+01
SIGT	0.000E+00	7.960E+01	1	1.279E+02	2.800E+01	2.667E+00	121	-8.596E+00
TAURZ	2.600E+01	0.000E+00	116	5.802E+01	2.600E+01	4.000E+00	114	-1.372E+02
TAURT	2.767E+01	1.333E+00	122	0.000E+00	2.767E+01	1.333E+00	122	0.000E+00
TAUZT	2.767E+01	1.333E+00	122	0.000E+00	2.767E+01	1.333E+00	122	0.000E+00
SIG1	2.600E+01	4.000E+00	77	3.036E+02	2.667E+01	4.000E+00	117	-1.275E+01
SIG2	2.475E+01	4.000E+00	81	3.498E+01	2.475E+01	0.000E+00	90	-8.946E+01
SIG3	0.000E+00	7.960E+01	1	1.279E+02	2.800E+01	2.667E+00	121	-8.596E+00
TAUMAX	2.100E+01	1.333E+00	92	1.637E+02	2.460E+01	6.234E+01	29	5.563E-01
EPSR	0.000E+00	7.765E+01	4	3.707E-06	2.350E+01	0.000E+00	90	-6.111E-06
EPSZ	2.100E+01	1.333E+00	92	1.111E-05	0.000E+00	7.700E+01	4	-3.968E-06
EPST	0.000E+00	7.765E+01	4	3.687E-06	2.800E+01	0.000E+00	122	-2.234E-07
GAMRZ	2.600E+01	0.000E+00	116	6.035E-06	2.600E+01	4.000E+00	114	-1.427E-05
GAMRT	2.767E+01	1.333E+00	122	0.000E+00	2.767E+01	1.333E+00	122	0.000E+00
GAMZT	2.767E+01	1.333E+00	122	0.000E+00	2.767E+01	1.333E+00	122	0.000E+00
EPS1	2.100E+01	1.333E+00	92	1.111E-05	2.667E+01	5.200E+01	112	-4.920E-07
EPS2	2.733E+01	2.667E+00	120	3.253E-08	2.350E+01	0.000E+00	90	-6.280E-06
EPS3	0.000E+00	7.765E+01	4	3.687E-06	2.800E+01	0.000E+00	122	-2.234E-07
GAMMAX	2.100E+01	1.333E+00	92	1.703E-05	2.460E+01	6.234E+01	29	5.786E-08

TIME IN STRESS = 5.410E+00 SECONDS

TEXGAP2D TO PATRAN TRANSLATION (RESULTS FROM STRESS OPTION)
GENERATED PATRAN STRESS/STRAIN NEUTRAL FILE
GENERATED PATRAN DISPLACEMENT NEUTRAL FILE

TIME IN TRANSLATE = 8.700E-01 SECONDS

TIME IN STOP = 1.831E+01 SECONDS

GLOSSARY and SYMBOLS

Axial Load (F): Applied load (Impact Force) in MN or kip.

Baseline: Reference temp and moisture content, and micro mechanical data, back calculated from experimentally determined ply data.

CFRP: Graphite fiber reinforced plastic.

C_{moist}: Moisture concentration in absolute value.

Delamination: Debonding process primarily resulting from unfavorable Interlaminar stresses.

Degradation: Loss of property due to aging, corrosion, and repeated or sustained stress.

<ep>: In-plane strain (Geometric measurement of deformation).

E_{fx}: Fiber longitudinal Young's modulus in msi.

E_m: Matrix Young's modulus in GPa or msi.

E_m/E^o_m: Matrix degradation factor required for the last-ply-failure prediction.

$\{E^o\}$ Lim: Effective in-plane engineering constants.

E^u/E^1: Ratio of the effective engineering constant at design ultimate over limit. These ratios indicate laminate stiffness degradation due to matrix/interface cracking.

FPF: first ply failure.

GFRP: Glass fiber reinforced plastic.

h#: Total thickness including core in number of plies.

h, E-3: Total thickness in mm or inches.

Isotropy: Property that is not directionally dependent. Strength and stiffness remain the same for all orientations of the coordinate axis.

Laminate: Plate consisting of layers of uni or multidirectional plies of one or more composite materials.

Layup (ß): Ply stacking sequence or ply orientations of laminate.

Length: Length of pressure vessel. This length affects only the angle of twist under torque.

LFP: Last ply failure.

Limit: The lower ply failure divided by safety margins.

Limit*: Ultimate divided by safety margin.

Mandrel: Male mold used for filament winding.

Macromechanics: Structural behavior of composite laminates using the laminated plate theory. The fiber and matrix within each ply are smeared and no longer identifiable.

Micromechanics: Calculation of the effective ply properties as functions of the fiber and matrix properties.

[Modified]: User defined modification.

Ply Angle: The first group is the outermost; i.e, the ply angles run from the outer surface toward the mid-plane.

Ply #: Number of plies for each ply angle or ply group.

Pressure (P): Internal or external pressure in ksi.

Q: Reduced stiffness matrix.

R/Degraded: Strength/Stress ratio of each ply group using degraded matrix.

Railgun: Electromagnectic launcher.

R/FPF: Lowest strength ratio for intact matrix is first-ply-failure.

R/Intact: Strength/Stress ratio for each ply group using an intact matrix (no matrix/interface cracks).

R/Lim: Strength ratio at limit = Min (FPF,Lim*).

R/lim*: Strength ratio based on ultimate = Ult/Safety.

R/LPF: Lowest strength ratio for degraded matrix is last-ply-failure.

R/Ult: Strength ratio at ultimate = Max (FPF,LPF).

Repeat: Repeated sublaminates.

Rotate: Rigid body rotation of entire laminate (degree).

Safety: Factor of safety.

<sg>: In-plane membrane stress, based on strength of materials.

<sg> Lim: In-plane stress at design limit based on a chosen safety margin.

<sg> Lim*: In-plane stress at ultimate-based limit based on a chosen safety margin.

<sg> Ult: In-plane stress at ultimate.

Stiffness: Ratio between the applied stress and the resulting strain.

T_{opr}: Operating temperature in degree C or F.

Vol/f: Fiber volume fraction in absolute value.

X_m: Matrix strength in ksi or MPa.

X_{fx}: Fiber longitudinal strength in ksi.

Young's Modulus: The slope of a stress-strain curve under uniaxial test.

γ: Poission's ratio

BIBLIOGRAPHY

Tsai, Stephen W. Composite Design. 3rd ed. Dayton: Think Composites, 1987.

Egeland, Alv. "Birkeland's Electromagnetic Gun: A historical Review." IEEE Transactions on Plasma Science. Vol. 17, No. 2 (April 1989): 73-82.

Rashleigh, S. C. and Marshall, R. A. "Electromagnetic acceleration of macro particles to high velocities," Journal of Applied Physics. Vol. 49, (April 1978): 2540-2542.

Thornhill, L. D., Batteh, J. H., and Littrell, D. M. "Scaling Study for the Performance of Railgun Armatures." IEEE Transactions on Plasma Science. Vol. 17, No. 3 (April 1989): 409-421.

Zukas, Jonas A. and Greszczuk, Longin B. Impact Dynamics. New York: John Wiley and Sons, Inc., 1982.

Shigley, Josesph E. Mechanical Engineering Design. New York: McGraw-Hill Book Company, 1977.

Davies, G. A. Structural Impact and Crashworthiness. New York: Elsevier Applied Science Publishers, 1984.

Zucrow, Maurice and Hoffman, Joe Gas Dynamics. New York: John Wiley and Sons, Inc., 1976.

Fung, Y. C. Continuum Mechanics. New Jersey: Prentice-Hall, Inc., 1977.

Patran Plus User's Manual, Version 2.4, PDA Engineering, Costa Mesa, CA, 1989.

TEXGAP2D User's Manual, ANATECH International Corp, La Jolla, CA, 1987.

TASK II

DIALECTICS FOR GRAPHITE/EPOXIES

ABSTRACT

The purpose of this task of the study was to determine the feasibility of dialectics to monitor cure of graphite/epoxies. Several panels were fabricated, cured and tested. Dialectics were used to monitor the results. Encouraging results of monitoring the care of graphite/epoxies were obtained.

RESULTS AND CONCLUSIONS

A separate report was submitted to the Astronautics Lab (Mr. Jim Koury). No copy available.

TASK III

STUDY FOR THE OPTIMUM CURE PROCESS FOR LARGE STRUCTURES

INTRODUCTION

The field of composite materials is growing at a rapid rate. Research into the subject always discovers something new and exciting. Engineering majors coming into the workforce will encounter composite structures on at least one occasion. Therefore, an engineering degree would not be complete without at least touching on the subject of composite materials. This is the purpose of Aero 410-Structural Analysis, even further and in-depth analysis is done in Aero 412-Composite Structural Analysis.

A composite is a material composed of two or more different types of material fused together or bonded together to create a material that has the better property of both materials. Another definition of a composite is a material made up of the same basic material, but in different forms. Such as Carbon-Carbon plies, which consist of carbon fibers imbedded into a matrix of carbon.

Another type of composite is the laminate. A laminate consists of layers of material, lamina, bonded together to combine the best aspects of the constituent layers to create a material superior to the lamina by itself. An example is laminated glass. Glass is brittle, but resistant to surface scratches, plexiglass is flexible and strong yet scratches very easily. Thus if we sheathed a layer of plexiglass between two layers of glass, we have a material which is resistant to scratches yet still stronger than brittle glass. The laminate in this experiment is a carbon-carbon build-up with each layer oriented into different directions.

TEST DESCRIPTION

To begin this experiment, specimens were needed. It was then up to the student to build their own layers of composite material. The material used in this experiment was donated by the Astronautics Laboratory at Edwards Air Force Base, Edwards, Ca. The Carbon-Carbon material was readily available on a spool. Using a straight-edge and a sharp knife, pieces were cut from the roll of material to used in stacking out laminate. Many different orientations were used, 0°, 30°, 45°, 60°, 90°. After the plies were cut, they were stacked together in a symmetric fashion about the center plane. Stacking symmetrically reduced the tendancy for the laminate to flex when cured. After the plies were stacked, the composite was cured with one of three cycles. Cycle I was curing at 300°F under 80lbs of force for 4 hours, then cooling to 85°F. Cycle II cured the composite at 350°F under 85lbs of force for 3.5 hours then cooling to 90°F. Cycle III had a curing cycle at 400°F under 90lbs of force for 3 hours then coolin to 85°F. After curing, the laminates were sent to the lab for cutting and strain gage installation.

After the specimens were cut, the strain gages installed, and tabs epoxied on, we were ready to test. An Instron loading machine was used to apply a tensile load to the specimens. An IBM PC was used in conjuction with several strain indicators to collect data. The IBM was able to take the signal from the strain indicators and convert the signal into a digital form so that the computer could interpret what was goin on. The PC however, only collected strain versus time values. To obtain load, the strip chart on the Instron Controller was used. The strip chart would graph load versus time. With these two plots, it was possible to obtain stress vs. strain correlations by using the time factor as a basis for both tests.

SAMPLE CALCULATIONS

Calculation of stress versus strain

Step 1:

Take maximum load and divide by number of squares to obtain load per increment.

2810 / 56.5 = 49.73
Assume 50 lbs / increment

Step 2:

Determine time unit per increment. If paper rate = 5in/min, then 1.2 seconds per increment. If 10in/min, then 0.6 seconds per increment.

Paper rate was 5 in/min, thus 1.2 seconds per increment.

Step 3:

Determine total time from start to failure of specimen.

(N# of increments)x(1.2s/inc)
= 24.1 x 1.2 = 28.92 seconds

Step 4:

Compare this time to strain versus time graph from the IBM PC. Check for correlation.

Time from Strain vs. Time was about 27 seconds. Thus the Strain vs. Time started taking data after loading had begun. In this case, data will be correlated based on t=27 sec on strain vs. time and t = 29 sec on load vs. time. These two times can be used as reference points in correlation of the data.

Step 5:

Break the time span into several segments and take strain and load at these times. (Strain must be converted from mV to in/in)

At time = 12 seconds,
Load = 1455 lbs,
Strain = 0.00671 in/in

Step 6:

Determine Stress based on Load

Load/Area = Stress
1455 lbs/(1.42")(0.024")=42.6ksi

Step 7:

Plot Stress vs Strain, then use a best fit line to determine 'E'

Using CricketGRAPH, points were plotted and equation of line made. See Figures 1 thru 9.

SAMPLE CALCULATIONS

Calculation of Theoretical Values:

Note:

Because of the large number of test cases with laminates of so many layers, a fortran program was developed to expedite the process of obtaining the A, B, and D matrices. A listing is provided in the appendix. Also there is no 'E' for the laminate, only the 'A' matrix. With the 'A' matrix, N_x, N_y, N_{xy} can be found as a function of strain by the relation:

$$\begin{vmatrix} N_x \\ N_y \\ N_{xy} \end{vmatrix} = \begin{vmatrix} A_{11} & A_{12} & A_{13} \\ A_{21} & A_{22} & A_{23} \\ A_{31} & A_{32} & A_{33} \end{vmatrix} \begin{vmatrix} \varepsilon_x^o \\ \varepsilon_y^o \\ \gamma_{xy}^o \end{vmatrix}$$

For symmetrical laminates, as in this experiment, A_{13} and A_{23} are zero, thus shear strain is not taken into account.

Step 1:

Since N_y is zero, solve for ε_y in terms of ε_x.

$$0 = A_{21}\varepsilon_x + A_{22}\varepsilon_y$$

$$\varepsilon_y = -(A_{21}/A_{22})\varepsilon_x$$

Step 2:

Solve for N_x in terms of ε_x.

$$N_x = A_{11}\varepsilon_x + A_{21}(-(A_{21}/A_{22})\varepsilon_x)$$

$$N_x = A_{11}\varepsilon_x - A_{21}(A_{21}/A_{22})\varepsilon_x$$

$$N_x = (A_{11} - A_{21}^2/A_{22})\varepsilon_x$$

Step 3:

Since N_x/t is essentially stress of the structure, a plot is made of N_x/t vs. ε_x and compared to Stress vs. Strain.

Since several of the load cases were the same, only 6 comparisons were made. See Figures 10 thru 15.

SAMPLE CALCULATIONS

Error Analysis

Step 1:

Using step 3 above, N_x was calculated. By dividing N_x by t, the thickness of the specimen, the 'stress' is obtained.

σ-theoretical = N_x/t

Step 2:

If we use correlating values of ex from the experimental calculations and the theoretical calculations, we can compare the experimental and theoretical values of stress.

σ-theoretical compares with σ-experimental as determined from the graphs.

Step 3:

To obtain a percent error, a standard equation is used.

$$\% \text{ Error} = \frac{|\text{actual - theoretical}|}{\text{theoretical}}(100)$$

RESULTS

Load Case 1

# Layers =	4
Orientation =	[0.90]s
Cycle =	II
Ultimate Load =	2810 lbs

Strain Reading (in/in)	Stress Reading (lbs/in^2)	Theoretical 'Stress' (Nx/t)	% Error
0.00073	7354.23	8912.16	17.48%
0.00257	29416.9	31541.9	6.74%
0.00380	42631.1	46620.3	8.56%
0.00671	70583.1	82268.9	14.20%
0.00783	82332.3	95986.5	14.23%

Load Case 2

# Layers =	6
Orientation =	[0.90,0]s
Cycle =	II
Ultimate Load =	2675 lbs

Strain Reading (in/in)	Stress Reading (lbs/in^2)	Theoretical 'Stress' (Nx/t)	% Error
0	0	0	0.00%
0.00179	12925.2	23477	44.95%
0.00246	21768.7	32264.5	32.53%
0.00336	29932	44068.6	32.08%
0.00425	38775.5	55741.5	30.44%
0.00582	58503.4	76333.1	23.36%
0.00716	70748.3	93908.1	24.66%

Load Case 3

# Layers =	48
Orientation =	[0.90,0,90]s
Cycle =	II
Ultimate Load =	4500 lbs

Strain Reading (in/in)	Stress Reading (lbs/in^2)	Theoretical 'Stress' (Nx/t)	% Error
0.00179	21602.9	21943.3	1.55%
0.00224	35104.8	27459.7	27.84%
0.00334	48606.6	40944.4	18.71%
0.00447	64268.7	54796.9	17.29%
0.00604	94512.9	74043.2	27.65%

Load Case 4

# Layers =	6
Orientation =	[-45,45,-45]s
Cycle =	II
Ultimate Load =	945 lbs Horizontal

Strain Reading (in/in)	Stress Reading (lbs/in^2)	Theoretical 'Stress' (Nx/t)	% Error
0.00268	6650.9	-2887.3	130.35%
0.00358	10109.4	-3856.9	218.86%
0.00515	12917.5	-5548.4	132.82%
0.00783	17292.3	-8435.7	104.99%

Load Case 5

# Layers =	4
Orientation =	[45,-45]s
Cycle =	II
Ultimate Load =	675 lbs Vertical

Strain Reading (in/in)	Stress Reading (lbs/in^2)	Theoretical 'Stress' (Nx/t)	% Error
0.00034	940.242	-1E+06	100.08%
0.00134	4701.21	-5E+06	100.10%
0.00291	10342.7	-1E+07	100.10%
0.00447	14291.7	-2E+07	100.09%
0.00615	17864.6	-2E+07	100.08%
0.00750	19745.1	-3E+07	100.07%

Load Case 6

# Layers =	4
Orientation =	[-45,45]s
Cycle =	II
Ultimate Load =	360 lbs Horizontal

Strain Reading (in/in)	Stress Reading (lbs/in^2)	Theoretical 'Stress' (Nx/t)	% Error
0	0	0	0.00%
0.00224	6944.44	-2413.3	187.76%
0.00492	9548.61	-5300.6	80.14%
0.00738	13020.8	-7951	63.76%
0.01	13888.9	-10774	28.92%
0.0104	13888.9	-11205	23.96%
0.0104	13020.8	-11205	16.21%

Load Case 7

# Layers =	4
Orientation =	[0.90]s
Cycle =	II
Ultimate Load =	3150 lbs

Strain Reading (in/in)	Stress Reading (lbs/in^2)	Theoretical 'Stress' (N_x/t)	% Error
0.00201	0	24682.9	100.00%
0.00280	9861.93	34281.8	71.23%
0.00392	28599.6	47994.5	40.41%
0.00481	45364.9	58964.6	23.06%
0.00582	58185.4	71306.1	18.40%
0.00873	74950.7	106959	29.93%
0.01130	89743.6	138498	35.20%

Load Case 8

# Layers =	6
Orientation =	[0.90,0]s
Cycle =	II
Ultimate Load =	2875 lbs

Strain Reading (in/in)	Stress Reading (lbs/in^2)	Theoretical 'Stress' (N_x/t)	% Error
0.00213	0	27875.2	100.00%
0.00246	7022.87	32276.6	78.24%
0.00280	18435	36677.9	49.74%
0.00291	27213.6	38145.1	28.66%
0.00347	36870	45480.6	18.93%
0.00470	58816.2	61618.9	4.55%

Load Case 10

# Layers =	8
Orientation =	[0.90,0,90]s
Cycle =	II
Ultimate Load =	6650 lbs

Strain Reading (in/in)	Stress Reading (lbs/in^2)	Theoretical 'Stress' (N_x/t)	% Error
0.00195	0	23904.7	100.00%
0.00252	6666.67	30853.6	78.39%
0.00392	18750	47994.5	60.93%
0.00475	30208.3	58279	48.17%
0.00531	42708.3	65135.4	34.43%
0.00643	59375	78848.1	24.70%

CONCLUSION

The experiment proved that composite materials definitely have value and are worth looking into for high strength/low weight applications.

For composites made with fibers and resin, the best performance is when the fibers are aligned parallel with the load direction and increasing strength is gained from increasing layer thickness.

Also cooking method II, which has a slightly lower temperature and pressure, but longer cook time, seems to give better performance than either of the other cooking methods and is the most reliable.

Overall, the experiment was very educational, constructive, and well worth the time.

APPENDIX: TABLES AND FIGURES

Matrices for Load Case # 1

A =	311690.75	73811.44	20.85
	73811.44	311690.75	-19.69
	20.85	-19.69	1366153.87
B =	.00	.00	.00
	.00	.00	.00
	.00	.00	.00
D =	17.37	3.54	.00
	3.54	12.60	.00
	.00	.00	65.58

****

Matrices for Load Case # 2

A =	500362.44	110717.14	20.85
	110717.14	434709.81	-19.61
	20.85	-19.61	2049230.75
B =	.00	.00	.00
	.00	.00	.00
	.00	.00	.00
D =	55.61	11.96	.00
	11.96	45.37	.00
	.00	.00	221.32

****

Matrices for Load Case # 3

A =	623381.50	147622.86	41.70
	147622.86	623381.56	-39.39
	41.70	-39.39	2732307.50
B =	.00	.00	.00
	.00	.00	.00
	.00	.00	.00
D =	129.14	28.34	.01
	28.34	110.24	.00
	.01	.00	524.60

****

Matrices for Load Case # 4

A =	1286082.75	-1760130.50	-16407.86
	-1760130.50	2338391.50	303598.81
	-16407.86	303598.81	178412.17
B =	.00	.00	.00
	.00	.00	.00
	.00	.00	.00
D =	135.80	-150.09	-2.56
	[illegible]	[illegible]	[illegible]
	-2.56	47.36	19.27

****

Matrices for Load Case # 5

ORIGINAL PAGE IS
OF POOR QUALITY

A =	857388.56	-1173420.50	.00
	-1173420.50	1558927.75	.00
	.00	.00	118941.46

B =	.00	.00	.00
	.00	.00	.00
	.00	.00	.00

D =	41.15	-56.32	1.18
	-56.32	74.83	-21.86
	1.18	-21.86	5.71

****

Matrices for Load Case # 6

A =	857388.56	-1173420.50	.00
	-1173420.50	1558927.75	.09
	.00	.09	118941.46

B =	.00	.00	.00
	.00	.00	.00
	.00	.00	.00

D =	41.15	-56.32	-1.18
	-56.32	74.83	21.86
	-1.18	21.86	5.71

****

Matrices for Load Case # 7

A =	311690.78	73811.44	20.85
	73811.44	311690.75	-19.69
	20.85	-19.69	1366153.87

B =	.00	.00	.00
	.00	.00	.00
	.00	.00	.00

D =	17.32	3.54	.00
	3.54	12.60	.00
	.00	.00	65.58

****

Matrices for Load Case # 8

A =	500362.44	110717.14	20.85
	110717.14	434709.81	-19.61
	20.85	-19.61	2049230.75

B =	.00	.00	.00
	.00	.00	.00
	.00	.00	.00

D =	55.61	[illegible]	.00
	[illegible]	[illegible]	.00
	.00	.00	221.32

****

Matrices for Load Case # 9

A =	[illegible]	[illegible]	41.70
	[illegible]	[illegible]	[illegible]

ORIGINAL PAGE IS OF POOR QUALITY

```
      !          41.70             -39.39        2732307.50!

B  =  !            .00                .00               .00!
      !            .00                .00               .00!
      !            .00                .00               .00!

D  =  !         129.14              28.34               .01!
      !          28.34             110.24               .00!
      !            .01                .00            524.60!
 ***************************************
Matrices   for Load Case #   10
A  =  !      311690.78           73811.44             20.85!
      !       73811.44          311690.75            -19.69!
      !          20.85             -19.69        1366153.87!

B  =  !            .00                .00               .00!
      !            .00                .00               .00!
      !            .00                .00               .00!

D  =  !          17.32               3.54               .00!
      !           3.54              12.60               .00!
      !            .00                .00             65.58!
 ***************************************
```

Figure 1

Stress vs. Strain - Load Case 1

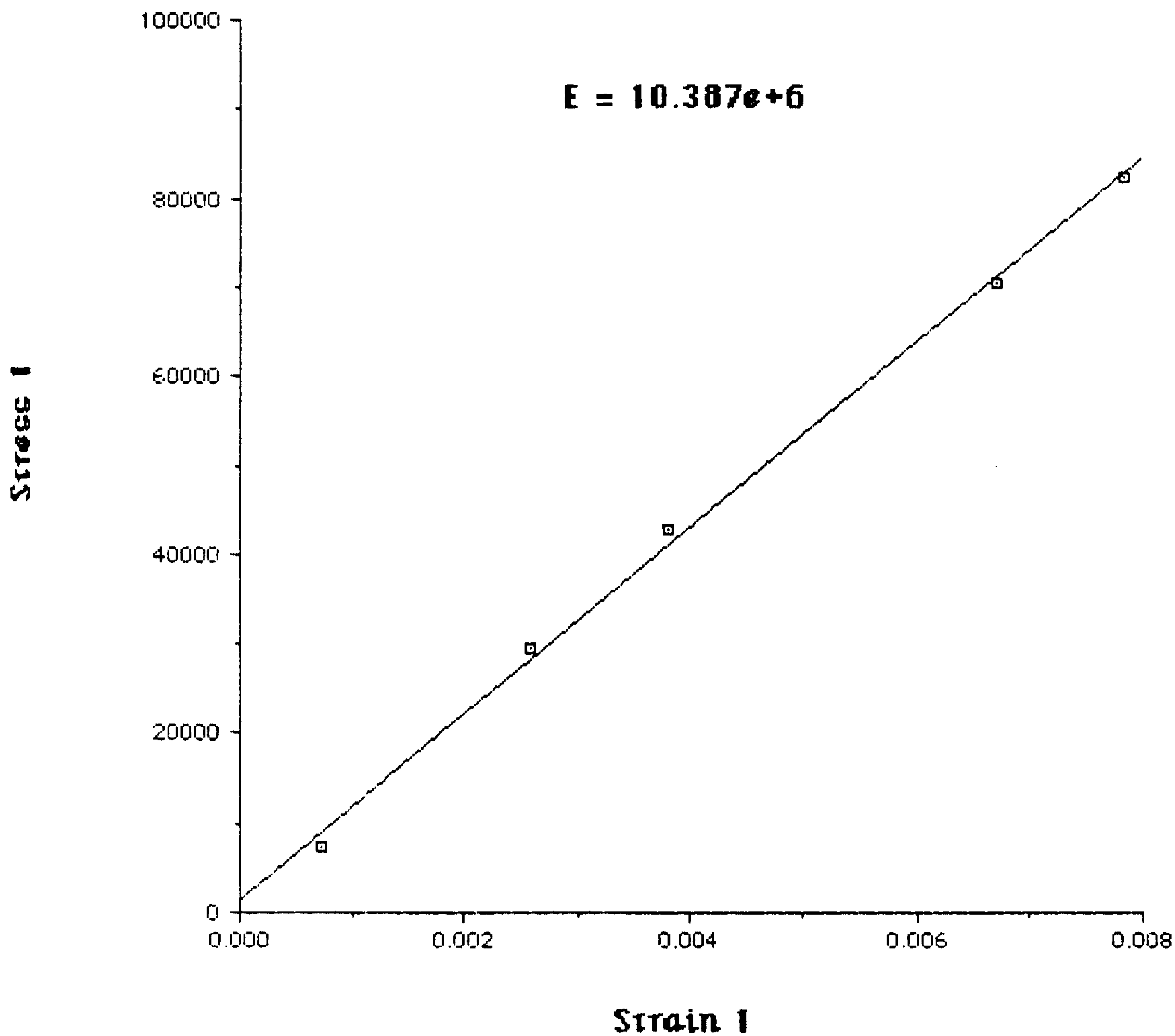

Figure 2

Stress vs. Strain - Load Case 2

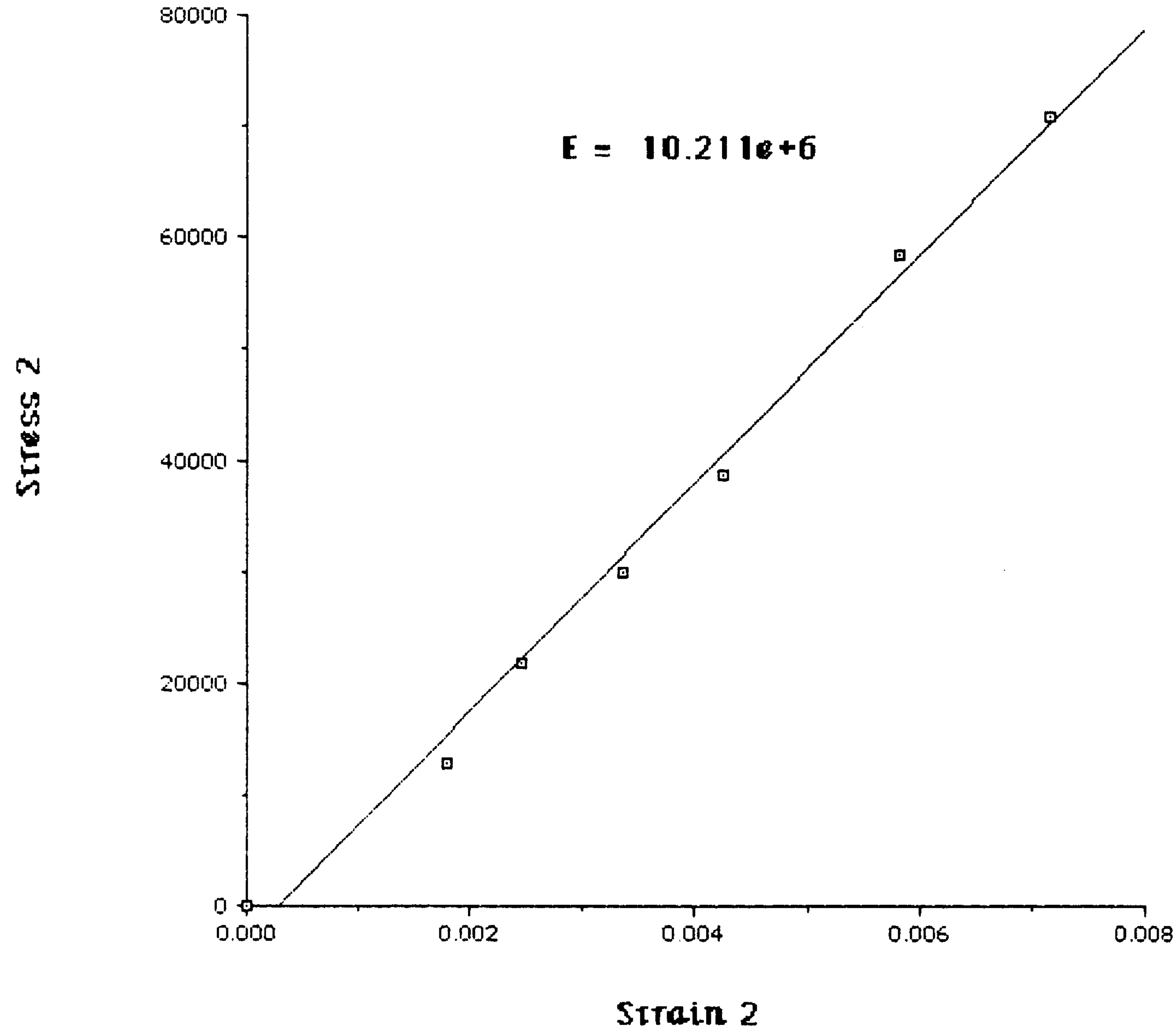

Figure 3

Stress vs. Strain - Load Case 3

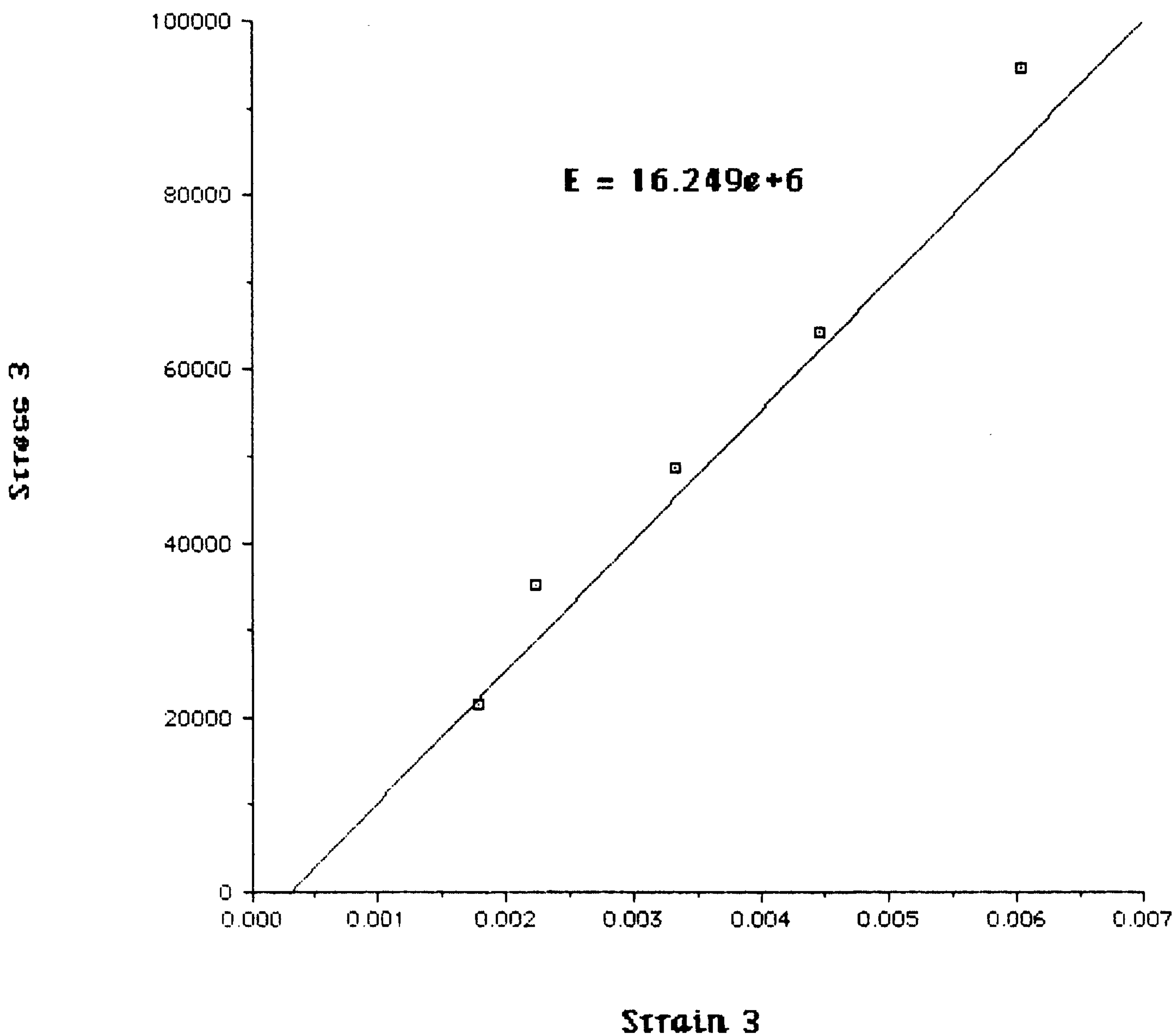

Figure 4

Stress vs. Strain - Load Case 4

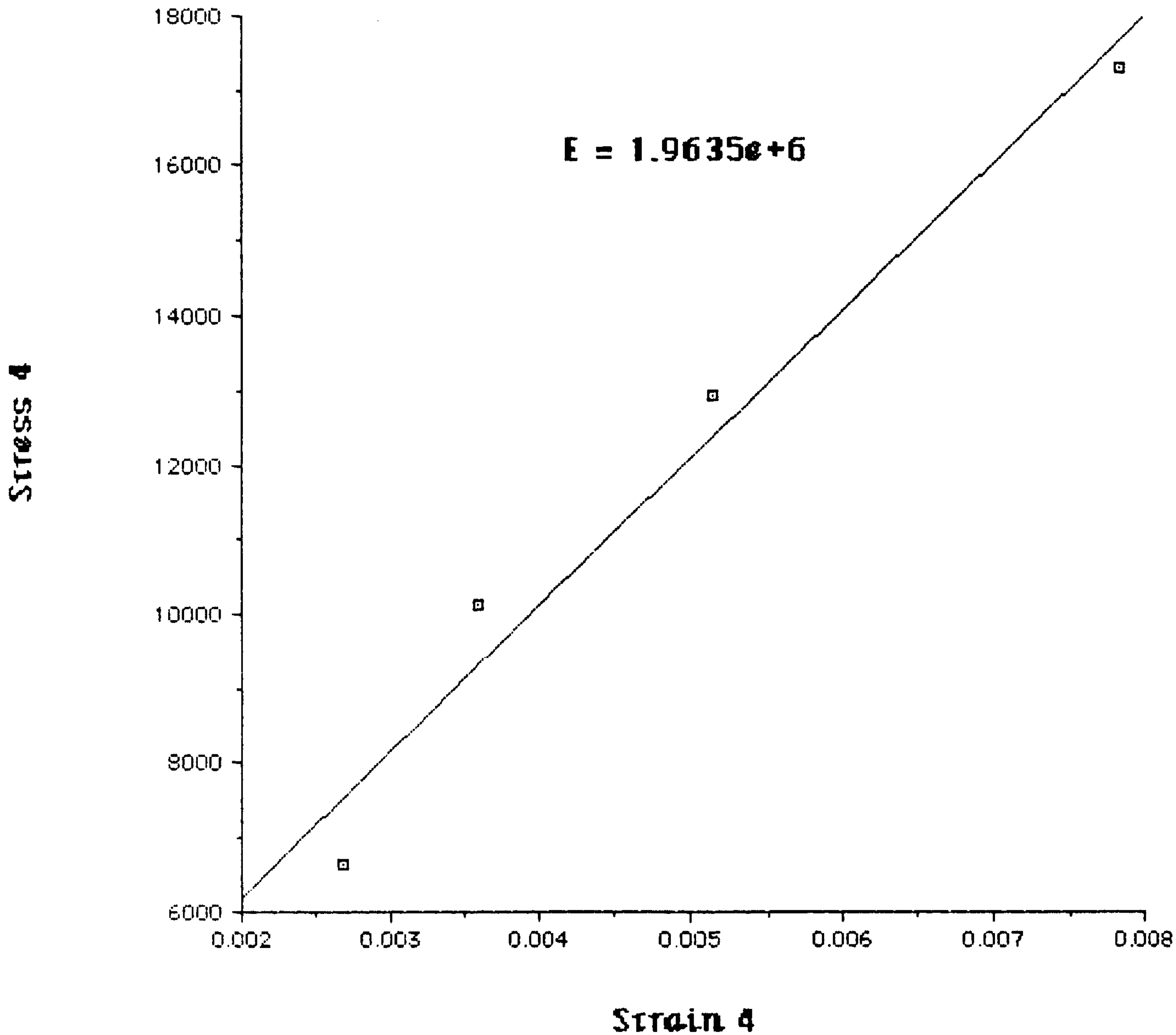

Figure 5

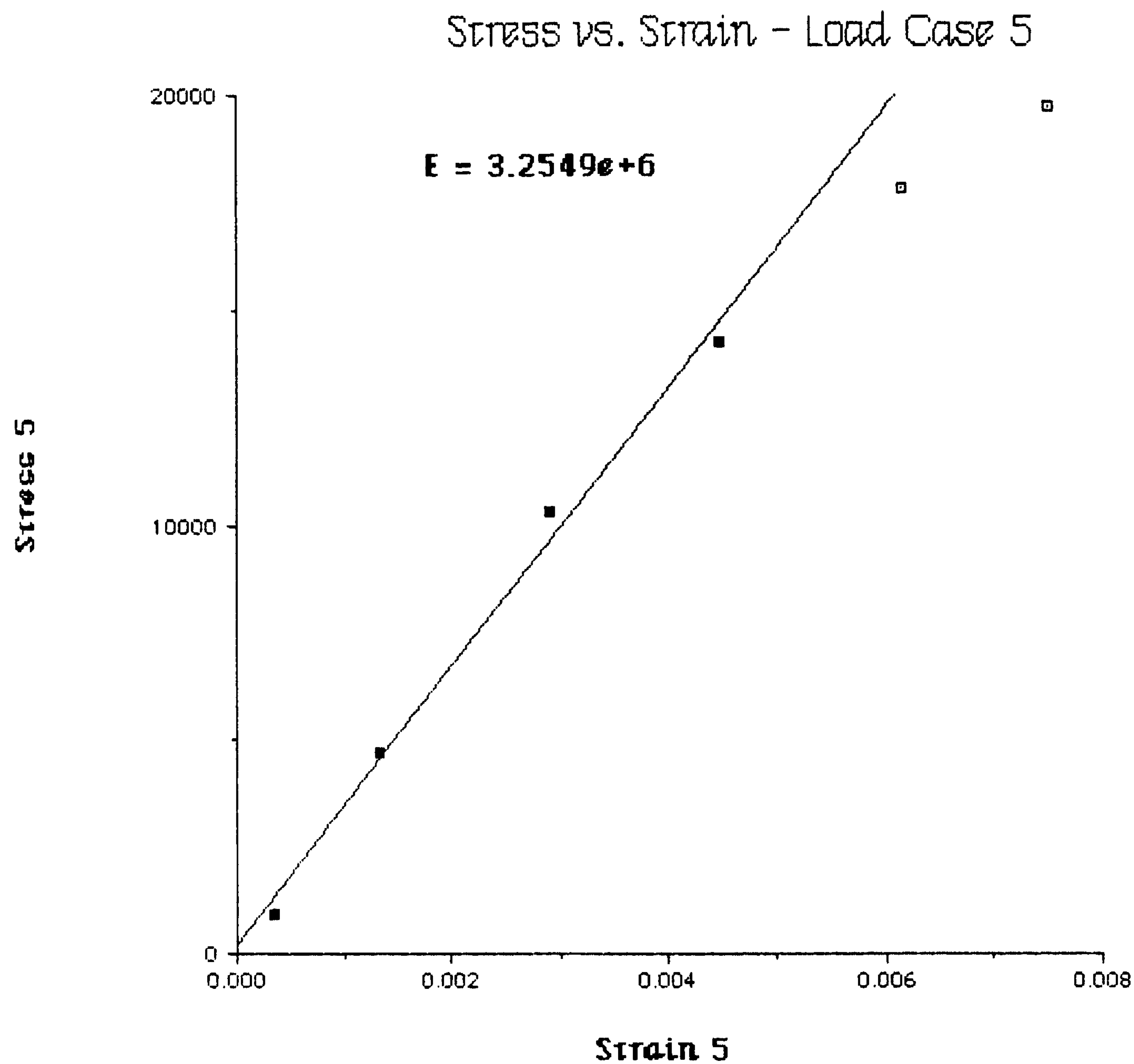

Stress vs. Strain - Load Case 5
E = 3.2549e+6
20000
10000
0
0.000
0.002
0.004
0.006
0.008
Strain 5
Stress 5

Figure 6

Stress vs. Strain - Load Case 6

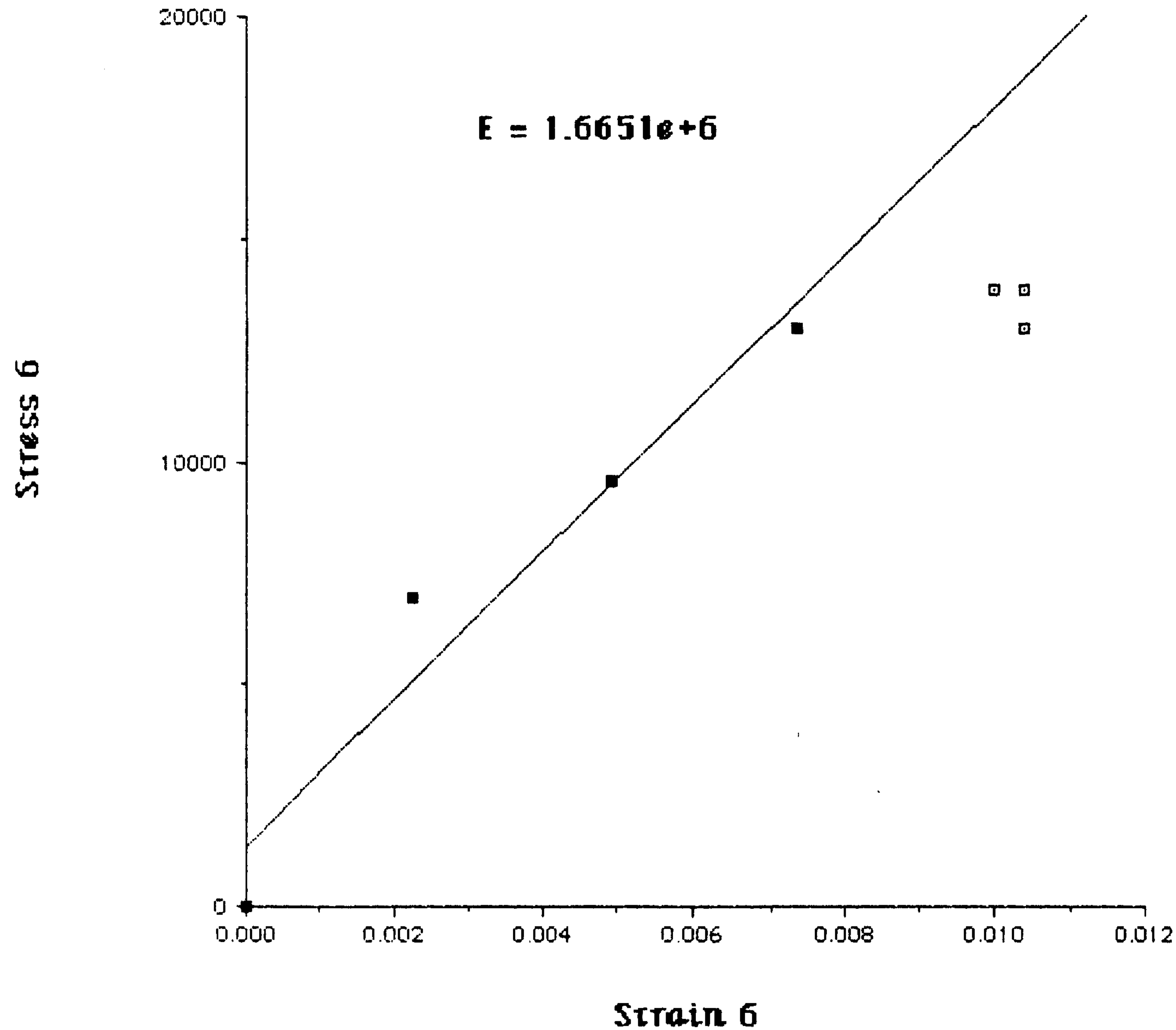

Figure 7

Stress vs. Strain - Load Case 7

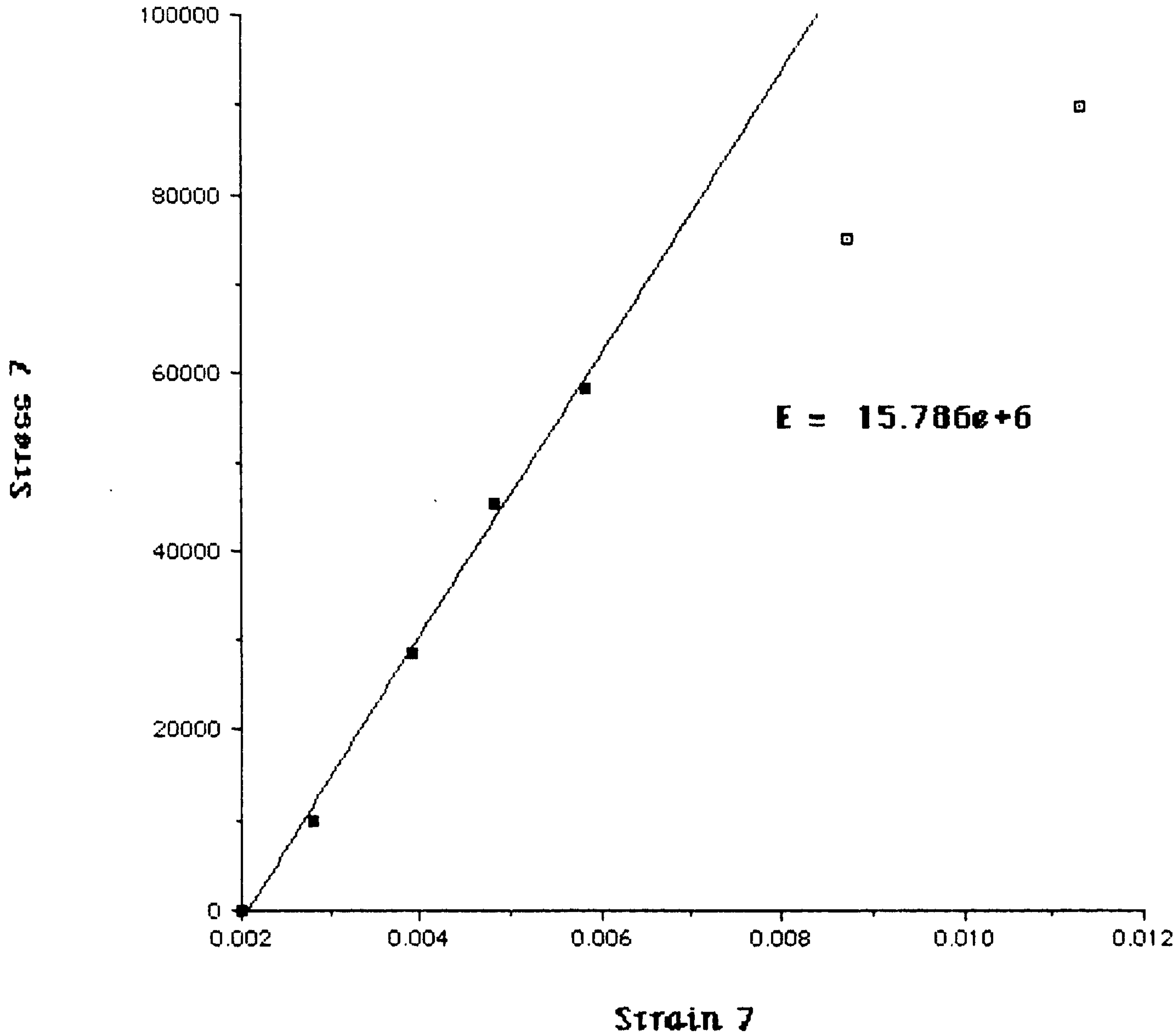

Figure 8

Stress vs. Strain - Load Case 8

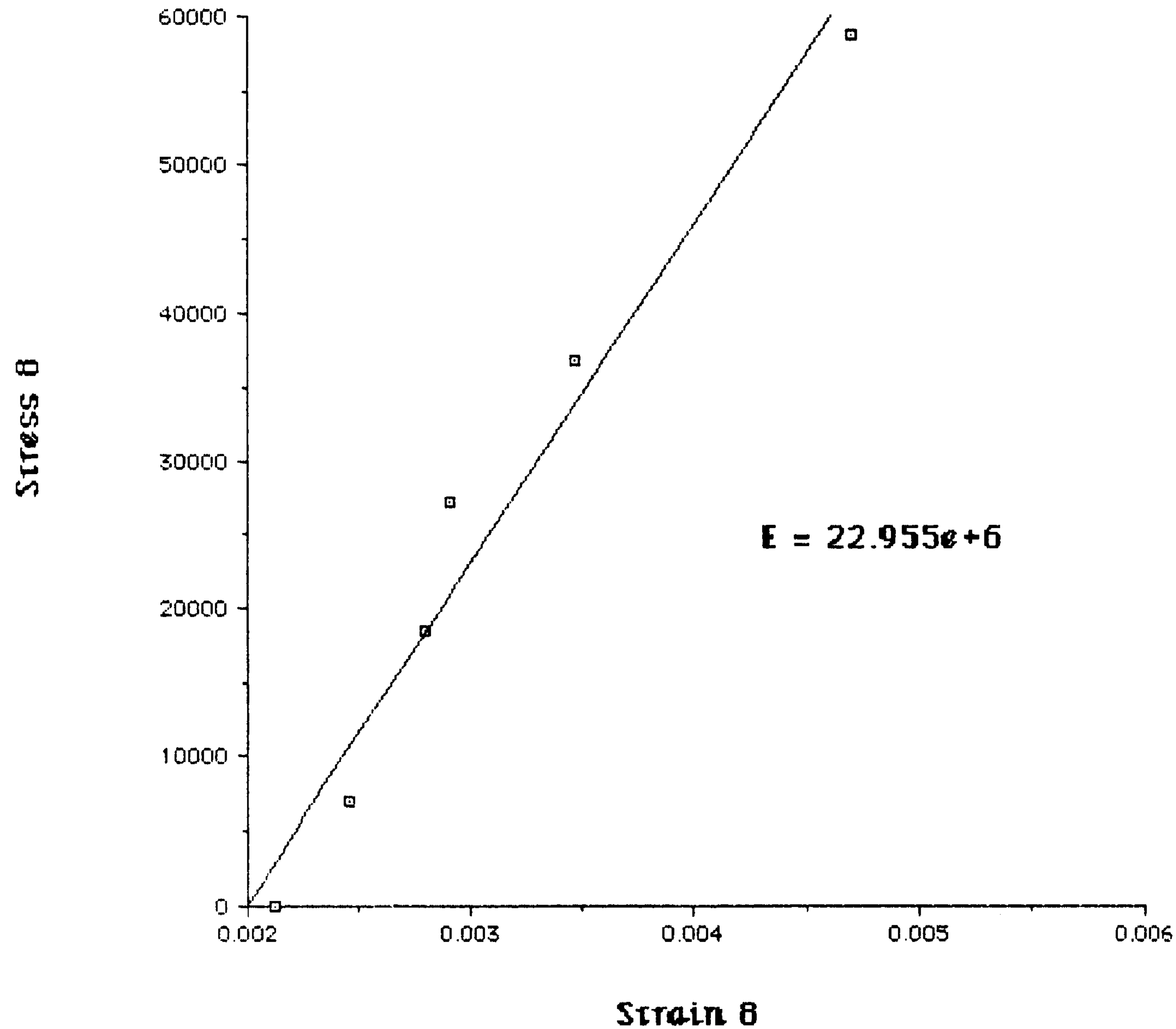

Figure 9

Stress vs. Strain - Load Case 10

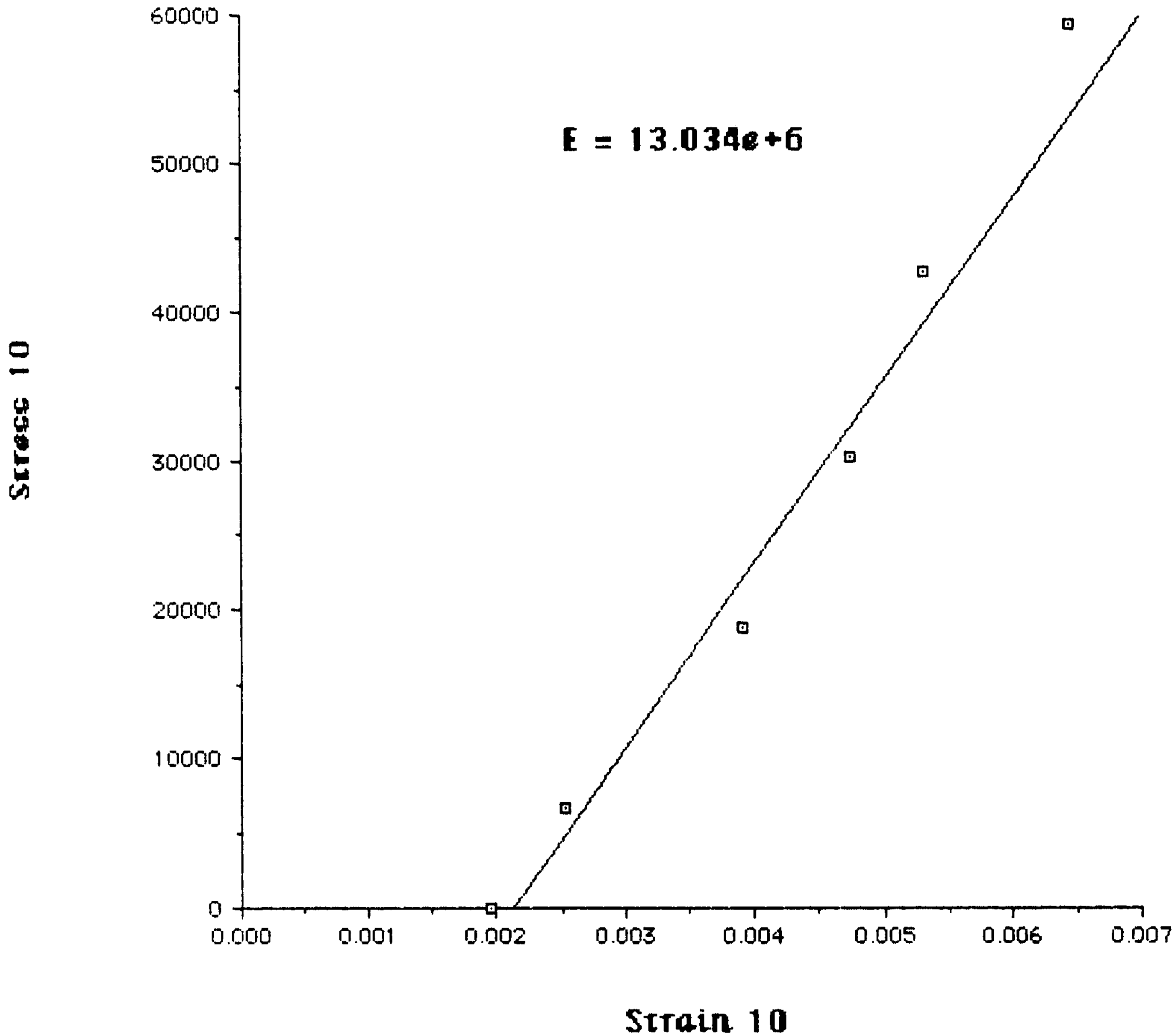

Figure 10

Stress vs. Strain - Load Case 1

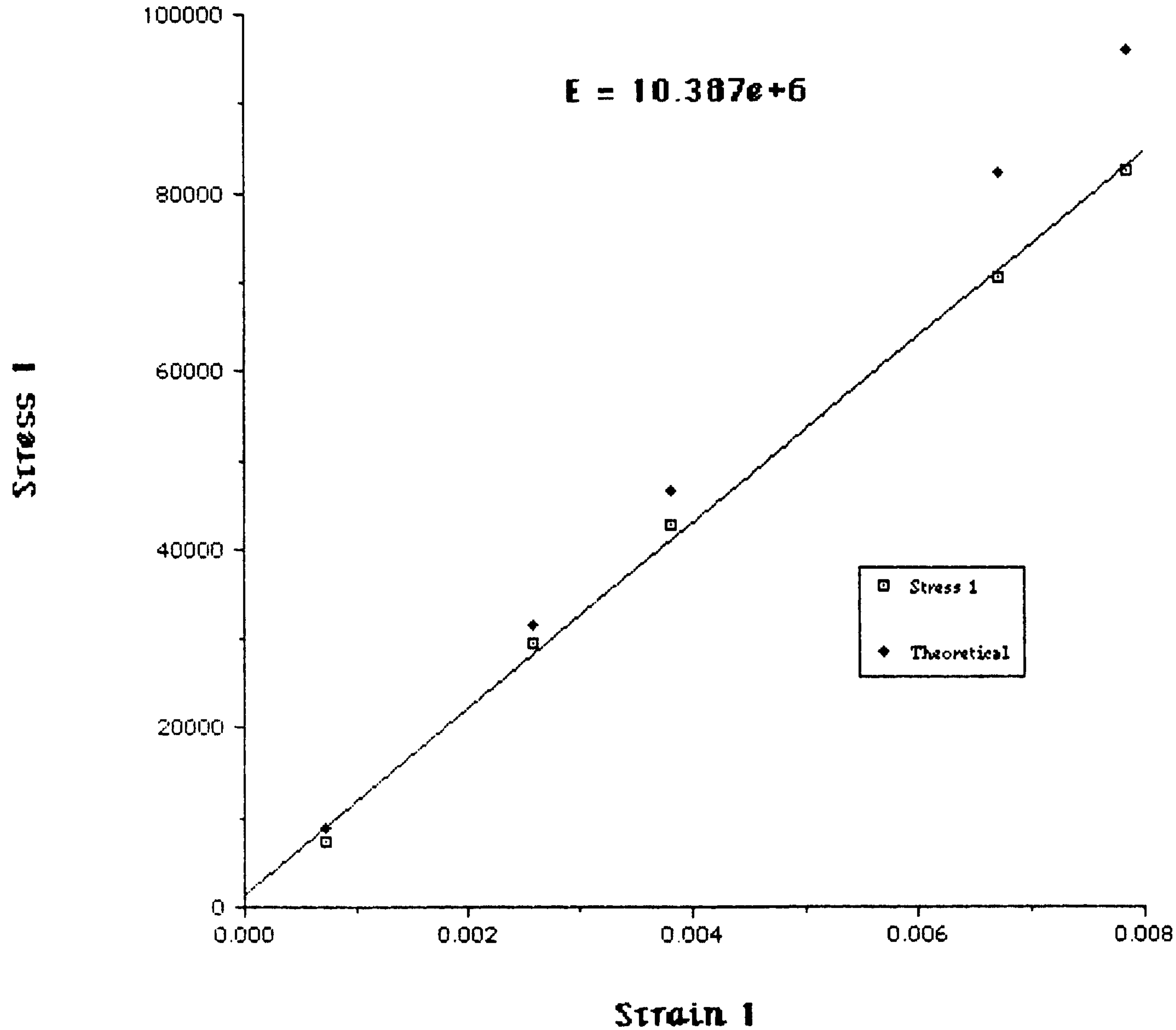

Figure 11

Stress vs. Strain - Load Case 2

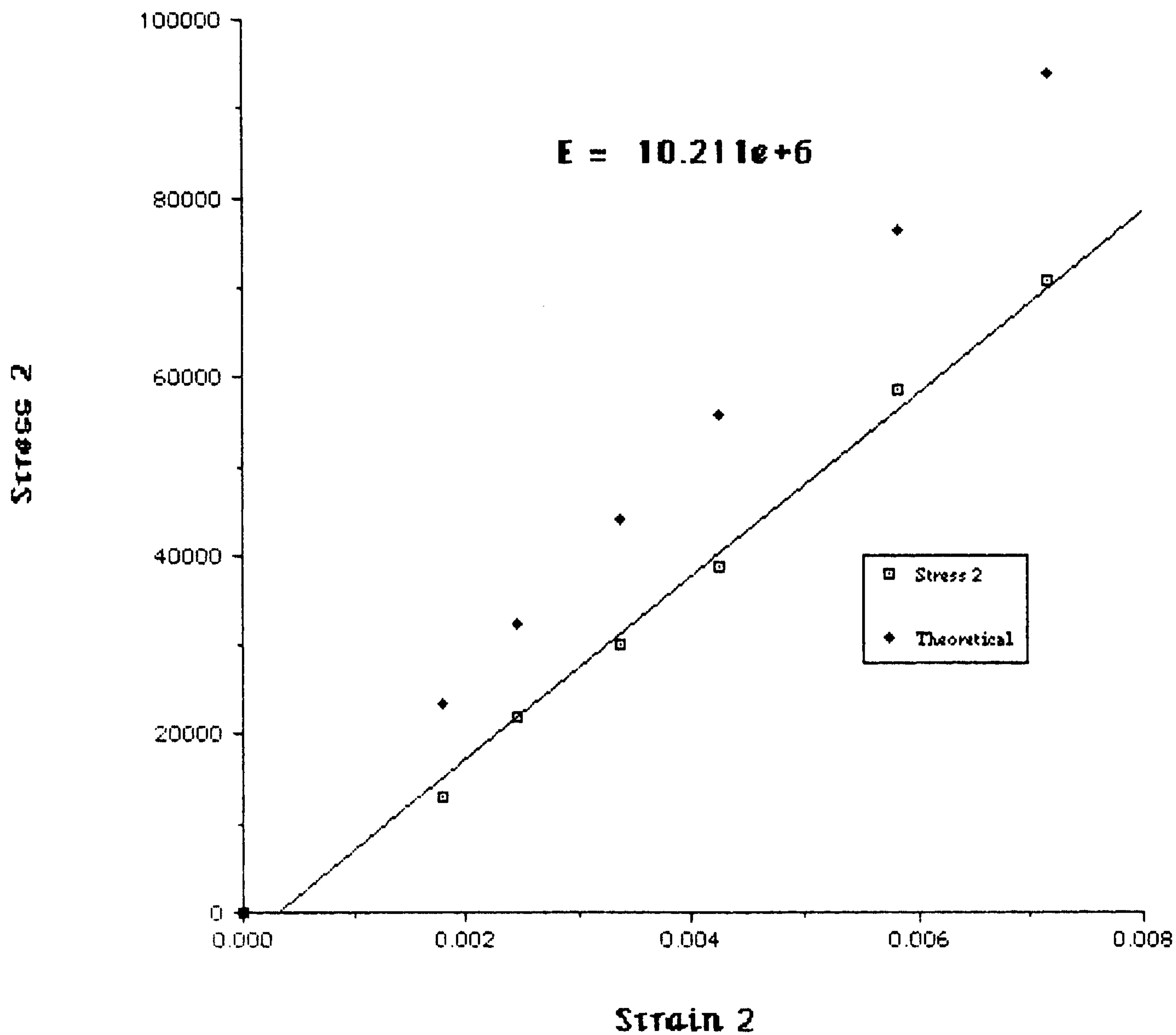

Figure 12

Stress vs. Strain - Load Case 3

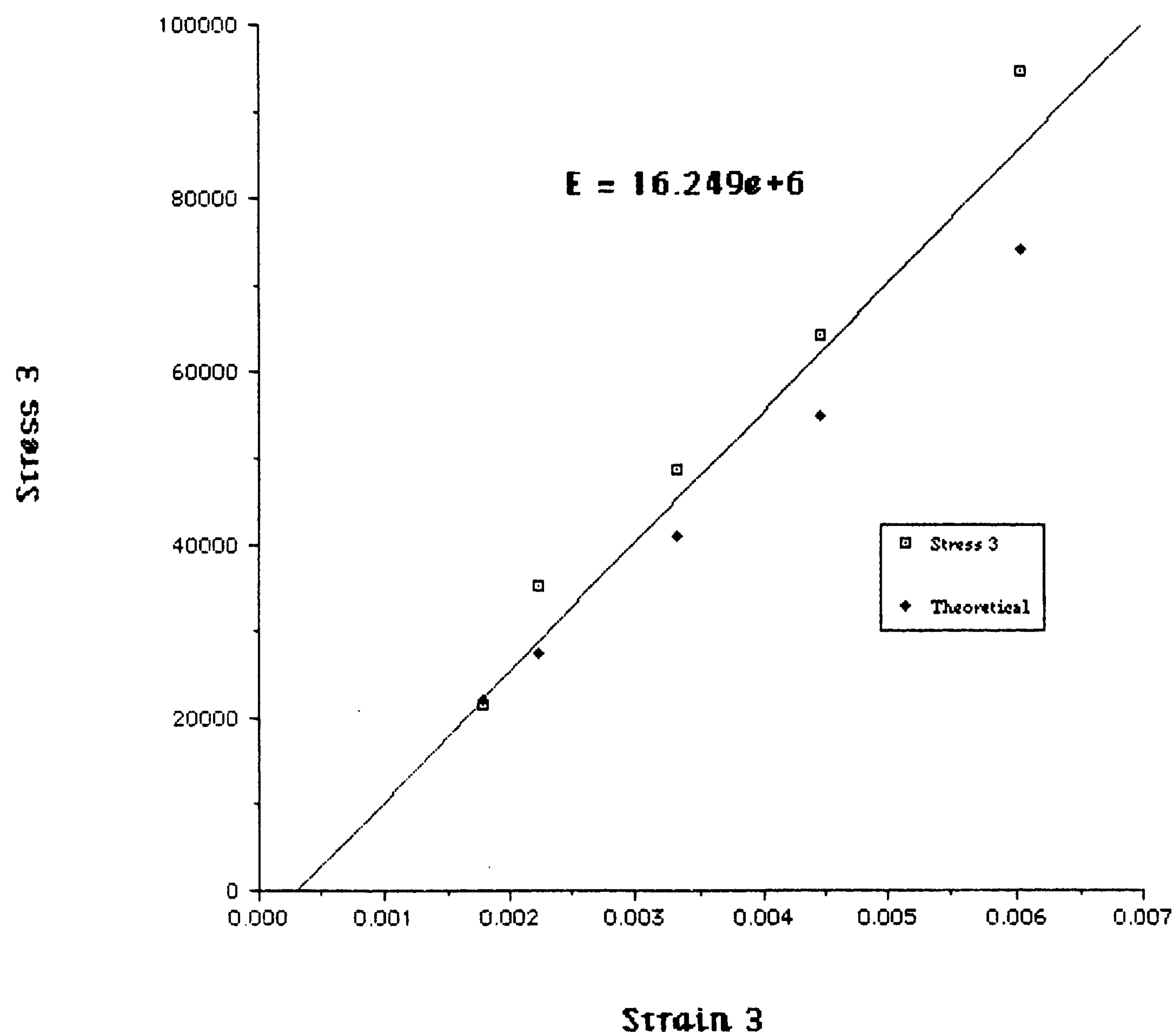

Figure 13

Stress vs. Strain - Load Case 7

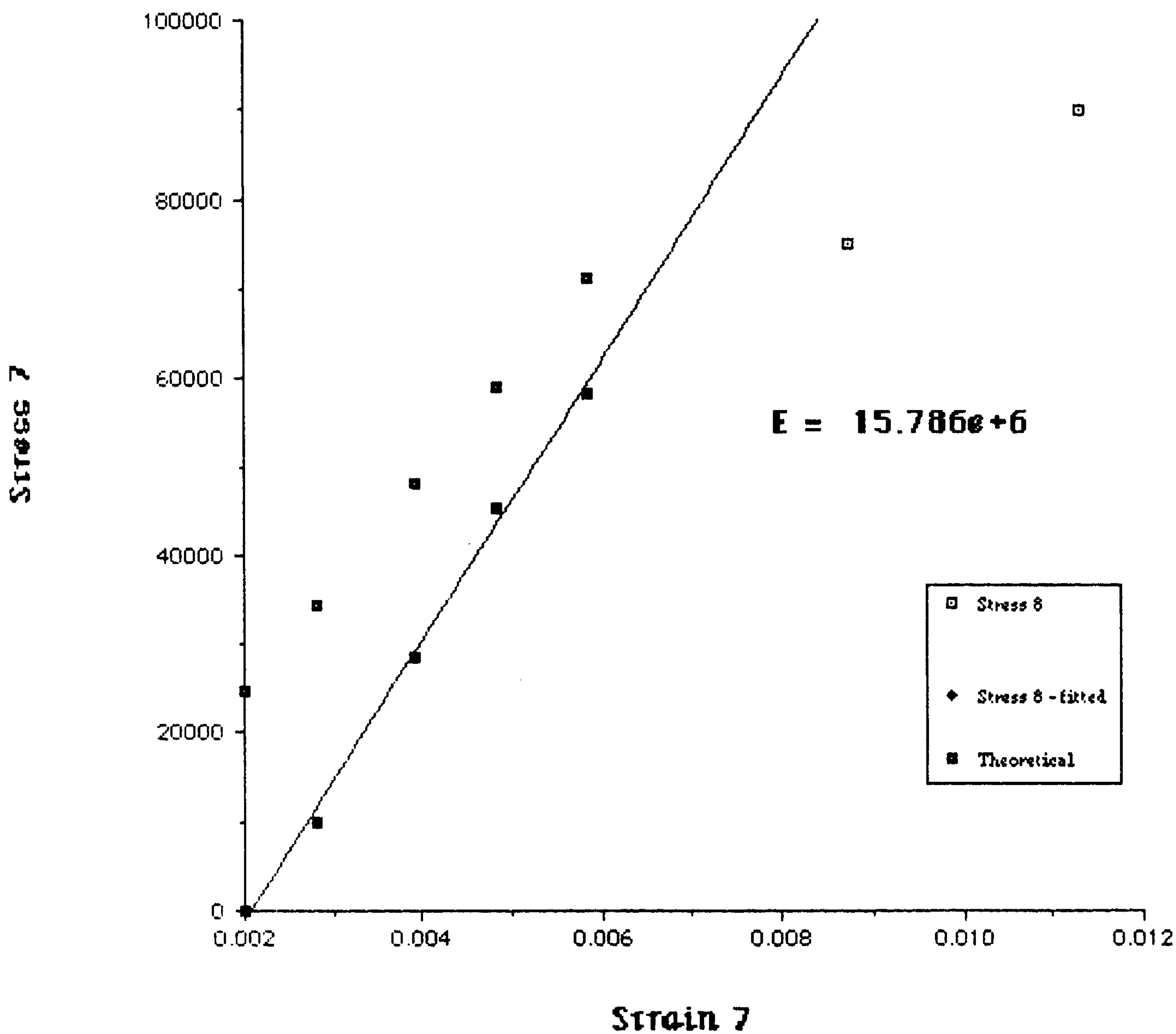

Figure 14

Stress vs. Strain - Load Case 8

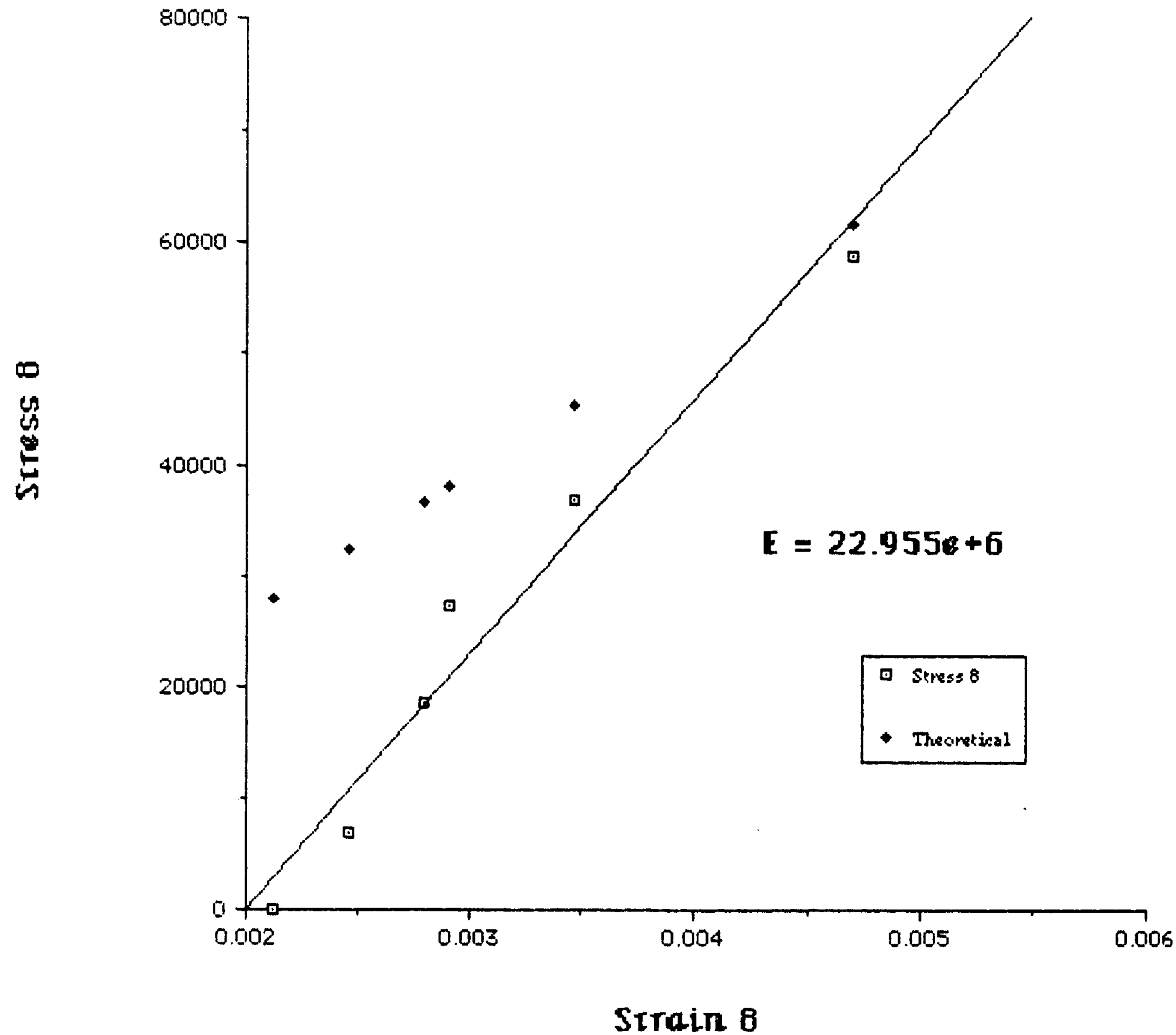

Figure 15

Stress vs. Strain - Load Case 10

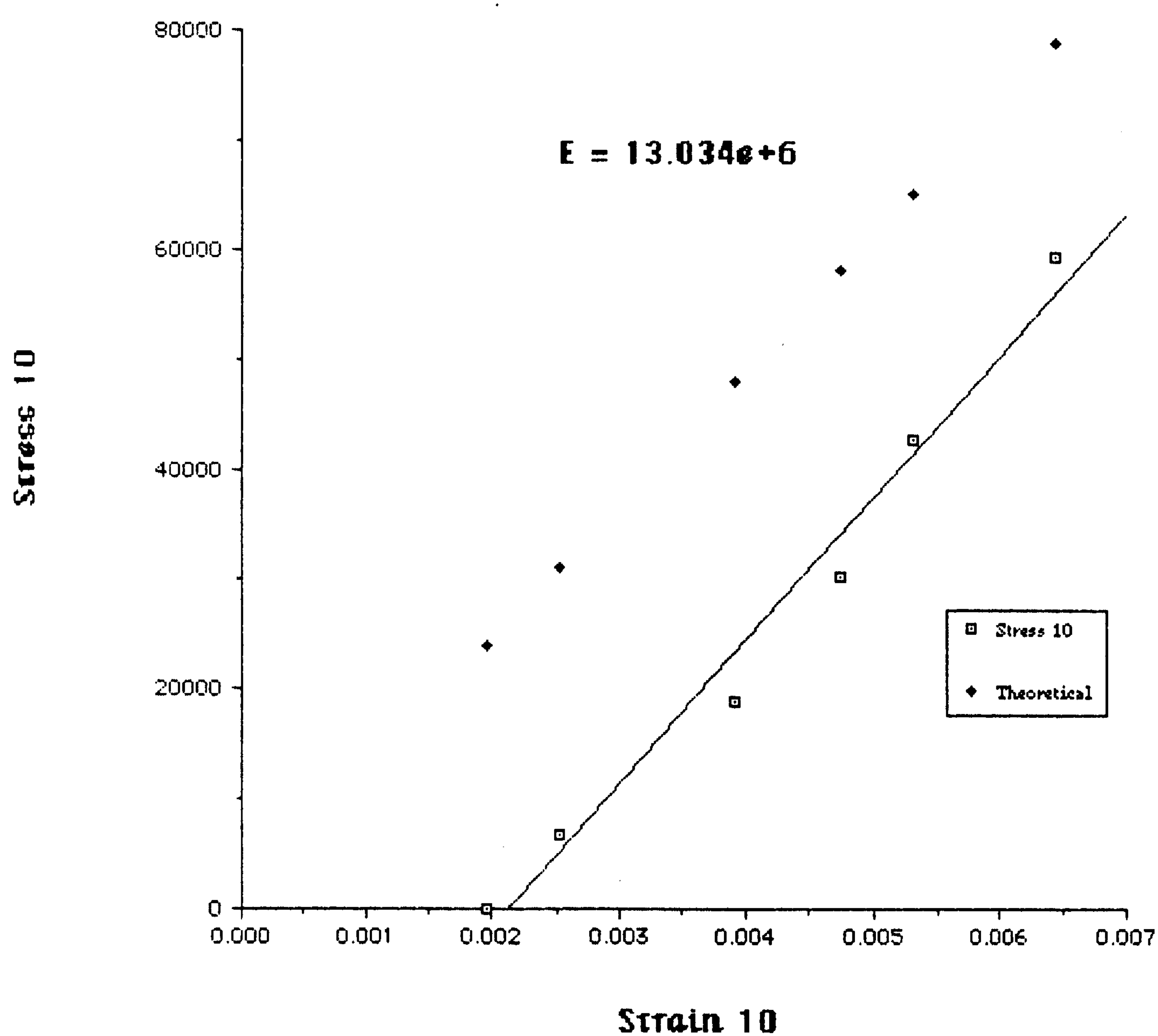

Test #1	Area =	0.03413		Info		
t	Load	Stress	Strain	Layers	4	Strain
2.4	251	7354.23	0.00073	Dir	[0,90]s	0.00073
7.2	1004	29416.9	0.00257	Cycle	2	0.00257
12	1455	42631.1	0.00380	Ult. Load	2810	0.00380
24	2409	70583.1	0.00671			0.00671
28.8	2810	82332.3	0.00783			0.00783

Test#2	Area =	0.03675		Info		
t	Load	Stress	Strain	Layers	6	Strain
0	0	0	0	Dir	[0,90]s	0
5	475	12925.2	0.00179	Cycle	2	0.00179
10	800	21768.7	0.00246	Ult. Load	2675	0.00246
15	1100	29932	0.00336			0.00336
20	1425	38775.5	0.00425			0.00425
30	2150	58503.4	0.00582			0.00582
35	2600	70748.3	0.00716			0.00716

Test#3	Area =	0.04629		Info		
t	Load	Stress	Strain	Layers	8	Strain
6	1000	21602.9	0.00179	Dir	[0,90]s	0.00179
12	1625	35104.8	0.00224	Cycle	2	0.00224
18	2250	48606.6	0.00334	Ult. Load	4500	0.00334
24	2975	64268.7	0.00447			0.00447
36	4375	94512.9	0.00604			0.00604

Test#4	Area =	0.03383		Info		
t	Load	Stress	Strain	Layers	6	Strain
4	225	6650.9	0.00268	Dir	[-45,45]	0.00268
6	342	10109.4	0.00358	Cycle	2	0.00358
8	437	12917.5	0.00515	Ult. Load	945	0.00515
12	585	17292.3	0.00783	Horizontal		0.00783

Test*5	Area =	0.02393		Info		
t	Load	Stress	Strain	Layers	4	Strain
1	22.5	940.242	0.00034	Dir	[45,-45]	0.00034
3	112.5	4701.21	0.00134	Cycle	2	0.00134
6	247.5	10342.7	0.00291	Ult. Load	675	0.00291
9	342	14291.7	0.00447	Vertical		0.00447
12	427.5	17864.6	0.00615			0.00615
14	472.5	19745.1	0.00750			0.00750

Test*6	Area =	0.02592		Info		
t	Load	Stress	Strain	Layers	4	Strain
0	0	0	0	Dir	[45,-45]	0
4	180	6944.44	0.00224	Cycle	2	0.00224
6	247.5	9548.61	0.00492	Ult. Load	360	0.00492
10	337.5	13020.8	0.00738	Horizontal		0.00738
14	360	13888.9	0.01			0.01
16	360	13888.9	0.0104			0.0104
24	337.5	13020.8	0.0104			0.0104

Test*7	Area =	0.02535		Info		
t	Load	Stress	Strain	Layers	4	Strain
0	0	0	0.00201	Dir	[45,-45]	0.00201
2	250	9861.93	0.00280	Cycle	2	0.00280
6	725	28599.6	0.00392	Ult. Load	3150	0.00392
10	1150	45364.9	0.00481			0.00481
14	1475	58185.4	0.00582			0.00582
18	1900	74950.7	0.00873			0.00873
22	2275	89743.6	0.01130			0.01130

Test*8	Area =	0.0356		Info		
t	Load	Stress	Strain	Layers	6	Strain
0	0	0	0.00213	Dir	[0,90,0]	0.00213
2	250	7022.87	0.00246	Cycle	2	0.00246
6	656.25	18435	0.00280	Ult. Load	2875	0.00280
10	968.75	27213.6	0.00291			0.00291
14	1312.5	36870	0.00347			0.00347
20	2093.7	58816.2	0.00470			0.00470

Test#1C	Area =	0.024	
t	Load	Stress	Strain
0	0	0	0.00195
2	160	6666.67	0.00252
6	450	18750	0.00392
10	725	30208.3	0.00475
14	1025	42708.3	0.00531
20	1425	59375	0.00643

Info	
Layers	4
Dir	[0,90]s
Cycle	2
Ult. Load	2980

Strain
0.00195
0.00252
0.00392
0.00475
0.00531
0.00643